DOE/NASA/0191-1
NASA CR-174804

ELECTRIC UTILITY ACID FUEL CELL STACK TECHNOLOGY ADVANCEMENT FINAL REPORT

W.H. Johnson
Program Manager
United Technologies Corporation
Power Systems Division
Fuel Cell Operations
South Windsor, CT.

November 1984

Prepared for
NATIONAL AERONAUTICS AND SPACE ADMINISTRATION
Lewis Research Center
Under Contract DEN3-191

for

U.S. DEPARTMENT OF ENERGY
OFFICE OF FOSSIL ENERGY
MORGANTOWN ENERGY TECHNOLOGY CENTER

DISCLAIMER

Printed in the United States of America

Available from
National Technical Information Service
U.S. Department of Commerce
5285 Port Royal Road
Springfield, VA 22161

NTIS price codes[1]
Printed copy: A08
Microfiche copy: A01

[1]Codes are used for pricing all publications. The code is determined by the number of pages in the publication. Information pertaining to the pricing codes can be found in the current issues of the following publications, which are generally available in most libraries: Energy Research Abstracts (ERA); Government Reports Announcements and Index (GRA and I); Scientific and Technical Abstract Reports (STAR); and publication, NTIS-PR-360 available from NTIS at the above address.

DOE/NASA/0191-1
NASA CR-174804

ELECTRIC UTILITY ACID FUEL CELL STACK TECHNOLOGY ADVANCEMENT FINAL REPORT

Program Manager
W.H. Johnson

Project Manager
T.G. Schiller

Principal Investigators

J.V. Congdon	G.W. Austin
G.J. Goller	S. Bose
G.J. Greising	R.D. Coykendall
J.J. O'Brien	W.L. Luoma
S.A. Randall	M.W. McCloskey
R.J. Roethlein	R.D. Sawyer
G.J. Sandelli	M. Krasij
R.D. Breault	

November 1984

Prepared for
NATIONAL AERONAUTICS AND SPACE ADMINISTRATION
Lewis Research Center
Under Contract DEN3-191

for

U.S. DEPARTMENT OF ENERGY
OFFICE OF FOSSIL ENERGY
MORGANTOWN ENERGY TECHNOLOGY CENTER

CONTENTS

CONTENTS (Cont'd)

CONTENTS (Cont'd)

LIST OF ILLUSTRATIONS

LIST OF ILLUSTRATIONS (CONT'D)

LIST OF ILLUSTRATIONS (CONT'D)

LIST OF ILLUSTRATIONS (CONT'D)

LIST OF TABLES

INTRODUCTION

In April of 1980 the Department of Energy initiated the program reported herein to advance the electric utility fuel cell power plant technology under the technical management and administration of the National Aeronautics and Space Administration at the Lewis Research Center. The program was conducted by the Fuel Cell Operations of United Technologies Corporation and concentrated on improvements to the cell stack assembly. Previous efforts had identified major areas of technology deserving of further development to improve cell stack performance at lower resultant costs. The principal areas needing improvement were: increased cell stack operating pressures and temperatures (from 50 psia, 375°F to 120 psia, 405°F); increased cell active area (from 3.7 ft^2 to 10 ft^2); incorporation of the "ribbed substate" cell configuration at the above conditions; and the introduction of higher performing electrocatalysts.

The principal effort under this program was directed at the cell stack technology required to accomplish the initial feasibility demonstrations of the above technology improvement goals. A secondary effort was directed at preliminary concepts for power plant palletization of the fuel cell dc module.

The program results were successful with the primary accomplishments being:

- Fabrication of 10-ft^2 cell components
- Assembly of a 10-ft^2 30-cell short stack (shown in Figure 1)
- Initial test of this stack at 120 psia and 405°F

These accomplishments demonstrate the feasibility of fabricating and handling large area cells using materials and processes that are oriented to low cost manufacture.

An additional accomplishment under the program was the testing of two 3.7-ft^2 short stacks at 120 psia/405°F to 5400 and 4500 hours respectively. These tests demonstrate the durability of the components and the cell stack configuration to a nominal 5000 hours at the higher pressure and temperature condition planned for the next electric utility power plant.

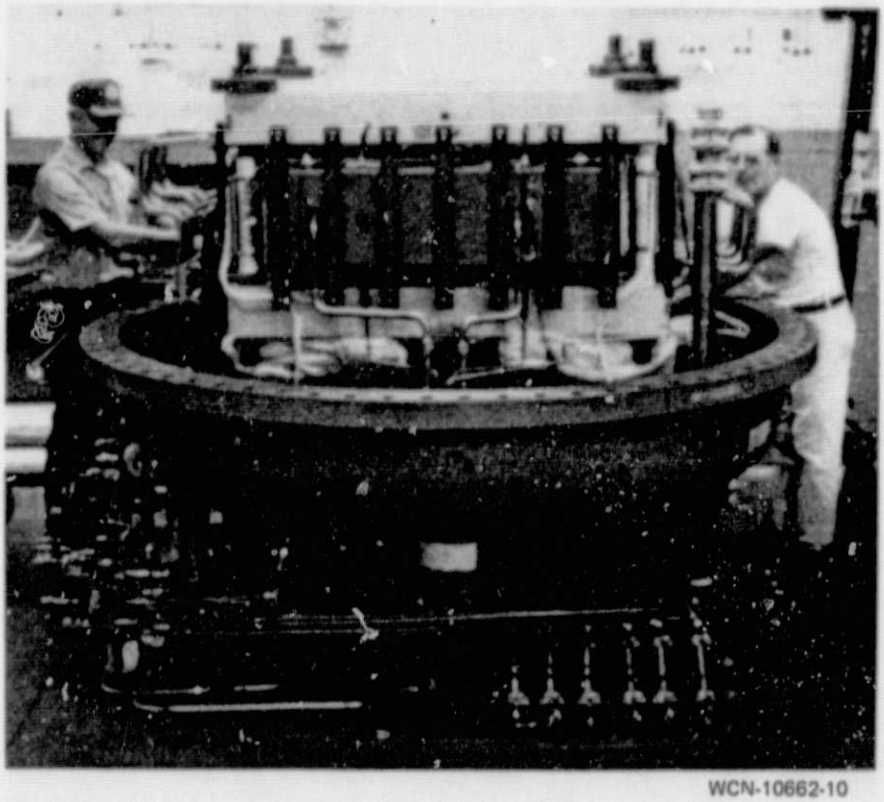

WCN-10662-10

Figure 1. 10-ft^2, 20-Cell Short Stack Mounted in Containment Vessel Base

SECTION 1
CATALYST AND CELL STACK MATERIALS

Task 1 of Contract DEN3-191 was directed at laboratory investigations of graphite materials used in fabricating cell substrates and separator plates, and the performance of cathode catalysts developed for operations at higher temperatures and pressures. Results of the graphite characterization will be utilized in subsequent process development. The catalysts tested resulted in recommendations of electrodes for use in subsequent short stack tests.

1.1 CELL STACK MATERIALS

Objective

The objective of this task was to characterize the corrosion resistance, under higher pressure and temperature conditions, of fuel cell graphitic structures as a function of heat-treat parameters and material content.

Summary

The effects of several heat-treat parameters (temperature, time, rate of heating, gas environment and gas flow rate) on corrosion resistance and mechanical and electrical properties of structures used in phosphoric acid fuel cells were investigated. Heat-treat at higher temperature and for longer times resulted in improved corrosion resistance and electrical conductivity but reduced strength. The rate of heating to the heat-treat temperature had no significant effect. Of the three gas environments -- hydrogen, argon, and helium -- only hydrogen resulted in additional improvement of corrosion resistance. However, the mechanical strength of the structures was reduced drastically, precluding the use of hydrogen from further consideration. Gas flow rate had no appreciable effect on the component properties.

The corrosion resistance and strength of separator plates were found to improve with increasing resin content. However, the associated shrinkage and brittleness impose manufacturing and handling problems when resin content exceeds 50 percent.

Discussion

Structures for acid cell stack components with increased corrosion resistance are required for high pressure and temperature operation. The materials program was aimed at identifying heat-treat conditions which would provide optimum corrosion resistance and mechanical properties for cell stack components. A number of heat-treat variables have been identified that directly or indirectly influence relevant component properties. To permit systematic analysis of the individual effects of these variables a test matrix, shown in Table 1-1, was constructed. It was designed to address a sufficient number of conditions for each variable to allow derivation of a behavior pattern. Both separator and substrate materials were tested. An additional parameter investigated was the resin content of separators and its effect on corrosion resistance and mechanical properties.

Effect of Heating Rate - The effect of rate of heating on the separator and substrate samples was determined by subjecting them to different heat-up rates. The specimen sizes were 7.6 cm x 7.6 cm. The separator samples were ground for flatness. All samples were heated in helium in an Astro furnace (Model 62200-FF) to 2100°C, at three heating rates: 16, 11 and 8°C/minute. After the heat treatment the sample threshold corrosion potential, flexural strength (of separators only) and electrical resistivity were measured.

Test specimens, 3.6 cm x 1.3 cm in size, were cut from the heat-treated samples for ambient pressure potentiodynamic sweep tests run in 99 percent phosphoric acid at 400°F under nitrogen atmosphere. Threshold corrosion potentials were determined from the resulting curves.

Analyses of the test data show that, allowing for measurement errors, the corrosion potential of separators and substrates (Figure 1-1), flexural strength of separa-

TABLE 1-1. HEAT-TREAT TEST MATRIX

Variable	Values	Sample No.	Constant Parameters	Values
1. Heat-up Rate, °C/min. (Separators and Substrates)	16	1	Temperature, °C	2100
	11	2	Time, hours	5
	8	3	Gas	Helium
			Flowrate, ℓ/min	0.500
2. Flowrate, ℓ/min (Separators and Substrates)	0.125	4	Temperature, °C	2100
	0.250	5	Time hours	2
	0.500	Baseline from ¶1.	Gas	Helium
			Heat-up Rate	From ¶1.
3. Type of Gas (Separators and Substrates)	H_2	6	Temperature, °C	2100
	He	Baseline from ¶2.	Time, hours	2
	Ar	7	Flowrate	From ¶2.
			Heat-up Rate	From ¶1.
4. Time, hour/ Temp., °C (Separators and Substrates)	0.25/2100	8	Heat-up Rate	From ¶1.
	0.50/2100	9	Gas	Helium
	1.0/2100	10	Flowrate	From ¶2.
	2.0/2100	Baseline from ¶2.		
	5.0/2100	Baseline from ¶1.		
	10.0/2100	11		
	0.25/2300	12		
	0.50/2300	13		
	1.0/2300	14		
	2.0/2300	15		
	5.0/2300	16		
	10.0/2300	17		
	0.25/2500	18		
	0.50/2500	19		
	1.0/2500	20		
	2.0/2500	21		
	5.0/2500	22		
	10.0/2500	23		
	0.25/2800	24		
	0.50/2800	25		
	1.0/2800	26		
	2.0/2800	27		
	5.0/2800	28		
	10.0/2800	29		
5. Resin Content, % (Separators Only)	30	30	Temperature, °C	2100
	40	31	Time, hours	2
	50	27	Gas	Helium
	60	32	Heat-up Rate	From ¶1.
	70	33	Flowrate	From ¶2.

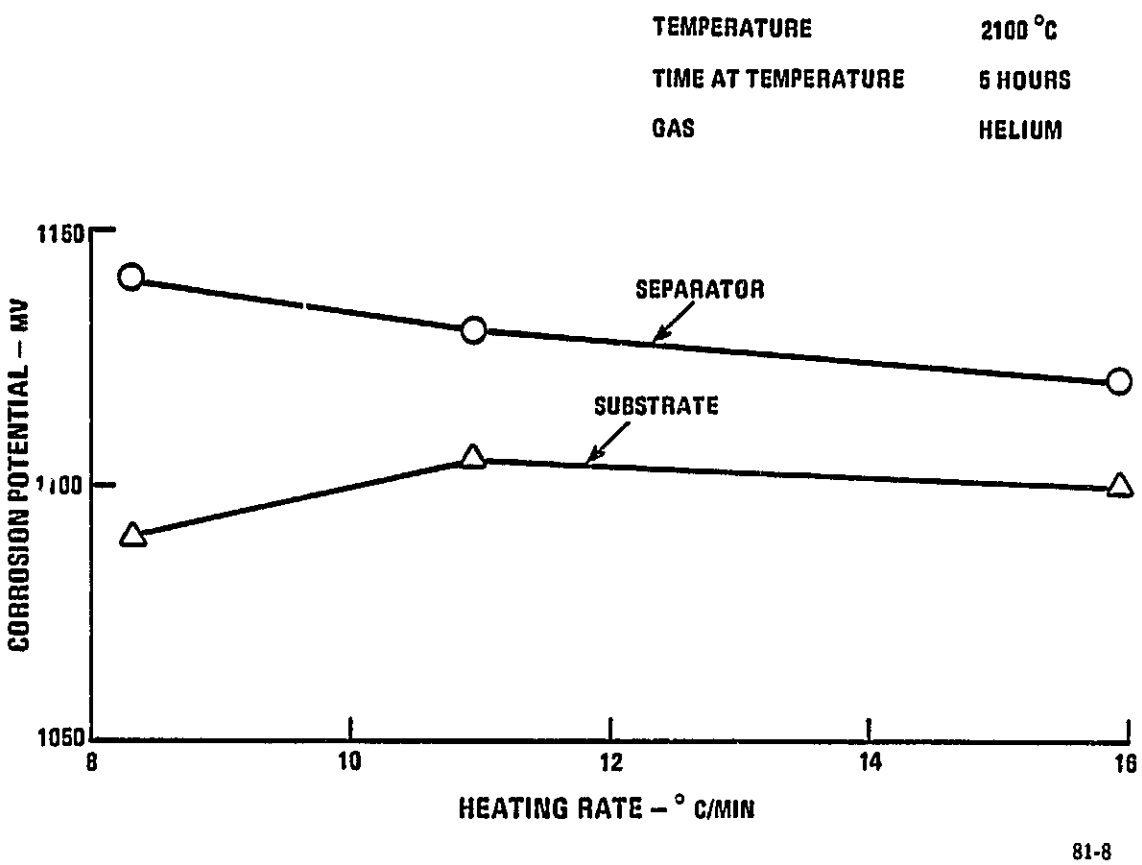

Figure 1-1. Corrosion Potential vs. Heating Rate

tors (Figure 1-2) and in-plane electrical resistivity of both separators and substrates (Figure 1-3) do not vary significantly with increasing heating rate. It is concluded that heating rate has little effect on the properties analyzed. The fastest heating rate (16°C/minute) was therefore selected for subsequent experiments. One advantage of this fast heating rate is a reduction of overall furnace time with attendant cost reduction.

Effect of Gas Atmosphere and Gas Flow Rate - The effects of gas atmosphere and the flow rate of the gases were determined by heat treating samples of stack materials at 2100°C for 2 hours in three gases (H_2, He and Ar) and at three flow rates (0.500, 0.250 and 0.125 liter/minute).

Analysis of corrosion test data indicates that the gas flow rate had no significant effect on the corrosion potential of the samples. For further trials a flow rate of 0.500 liter/minute was selected. Of the gases evaluated, hydrogen was found to increase corrosion potential, as shown in Table 1-2. However, the strength of the test specimens was drastically reduced when they were graphitized in hydrogen. As a result hydrogen was dropped from further consideration. An argon atmosphere was judged inadequate because this gas is known to ionize above 2500°C. Therefore, all subsequent activity, particularly at temperatures exceeding 2500°C, was conducted in helium.

Effect of Resin Content of Separators - Separators molded with varying resin contents (70, 60, 50, 40 and 30 weight percent as resin) were heat-treated at 2800°C for 30 minutes in helium after being carbonized at 1000°C in nitrogen. These separators were then characterized using potentiodynamic sweep tests and flexural strength measurements. The test data show that both corrosion potential and flexural strength increase with increasing binder content, as seen in Figures 1-4 and 1-5. In these plots the carbon yield from the resin binder is assumed to be 50 percent. Although higher resin content produces plates of better corrosion resistance and higher strength, the resulting shrinkage and brittleness imposes practical manufacturing and handling problems. Brittleness, measured by fracture

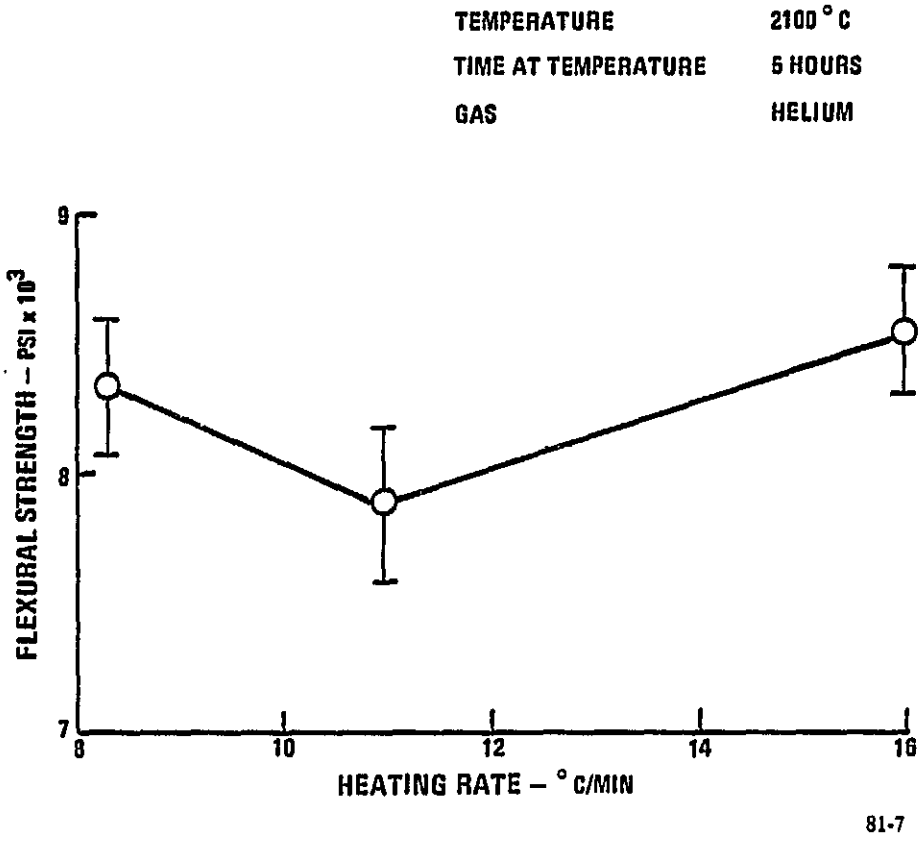

Figure 1-2. Separator Flexural Strength vs. Heating Rate

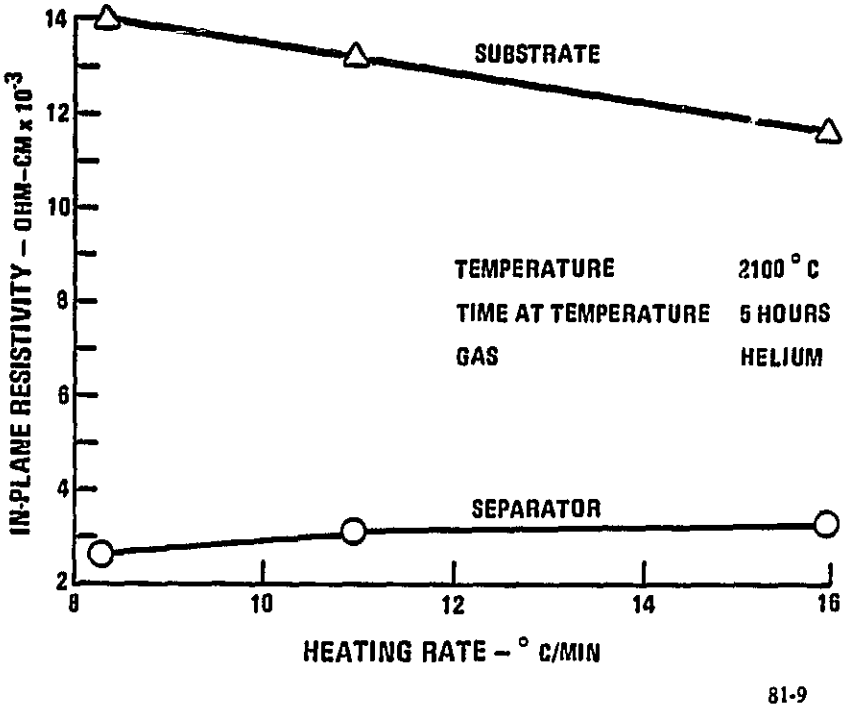

Figure 1-3. Resistivity vs. Heating Rate

resistance (stress at failure multiplied by strain at failure) is found to be minimum for a 50/50 composition separator plate.

TABLE 1-2. EFFECT OF HEAT-TREAT ATMOSPHERE ON CORROSION POTENTIAL

HEAT-TREAT ATMOSPHERE	CORROSION POTENTIAL, mV	
	SEPARATOR	SUBSTRATE
H_2	1175	1160
He	1120	1090
Ar	1125	1090

Effect of Heat-Treat Temperature and Time - To study the effects of heat treatment temperature and time on separator and substrate properties, samples were heat-treated at several temperatures for various lengths of time following the test matrix of Table 1-1. Potentiodynamic corrosion tests indicated that the corrosion potential of both separators and substrates increases with increased hold time at constant temperature and with increased temperature at constant hold time. Compressive strength of the substrates, flexural modulus (or stiffness) of separators, and electrical resistivity all decrease with increased hold time at constant temperature and with increased temperature at constant hold time.

Corrosion potential, compressive strength, flexural modulus and in-plane electrical resistivity data have been analyzed to determine relative rate constants of the processes which occur during heat treatment. The technique of superposition (Reference 1), has been used. One of the advantages of the technique is that it is applicable even when there is a broad distribution of rate constants, if the dis-

(Reference 1: D. B. Fischbach; Technical Report No. 32-532; February 1, 1966 Jet Propulsion Laboratory, CALTECH, Pasadena, California).

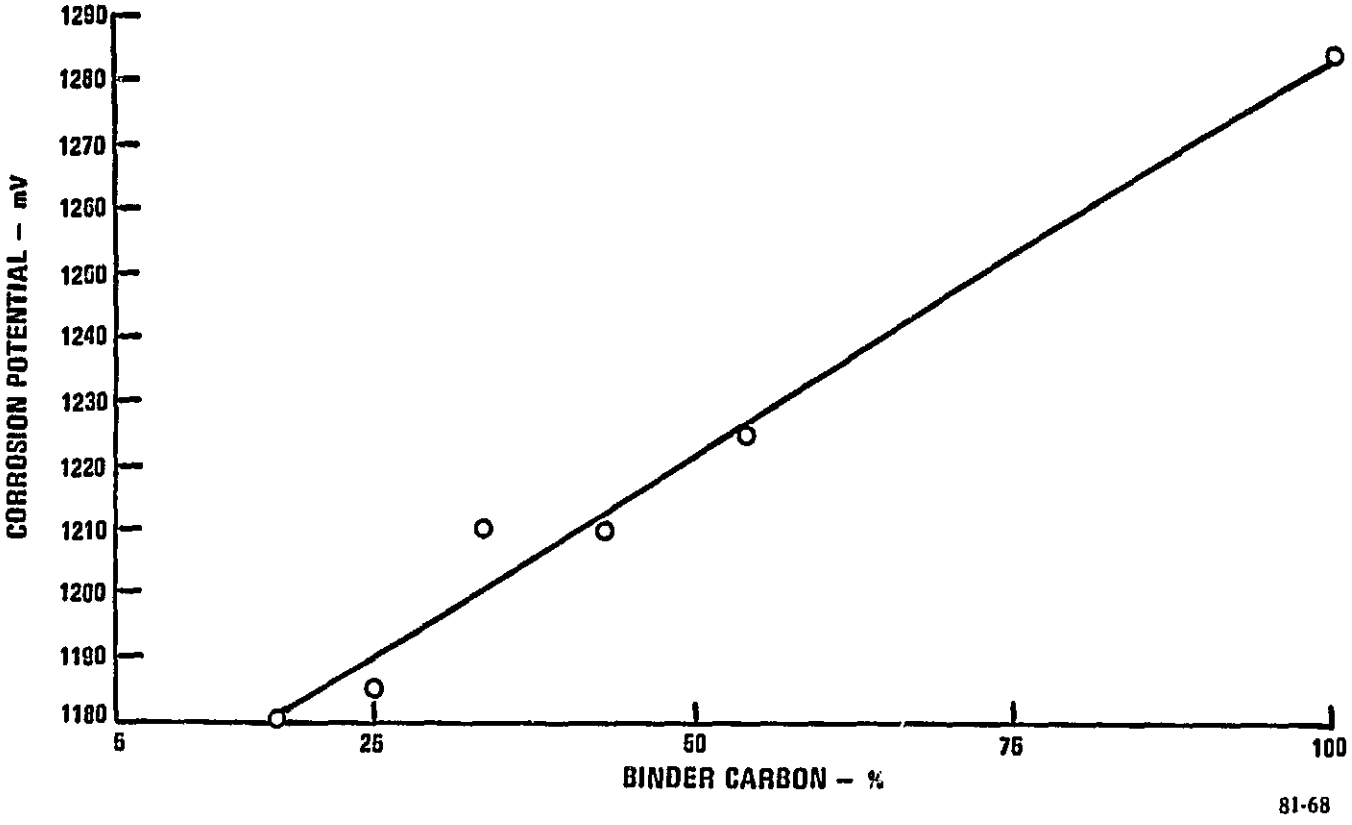

Figure 1-4. Corrosion Potential of Separators vs. Binder Carbon Content

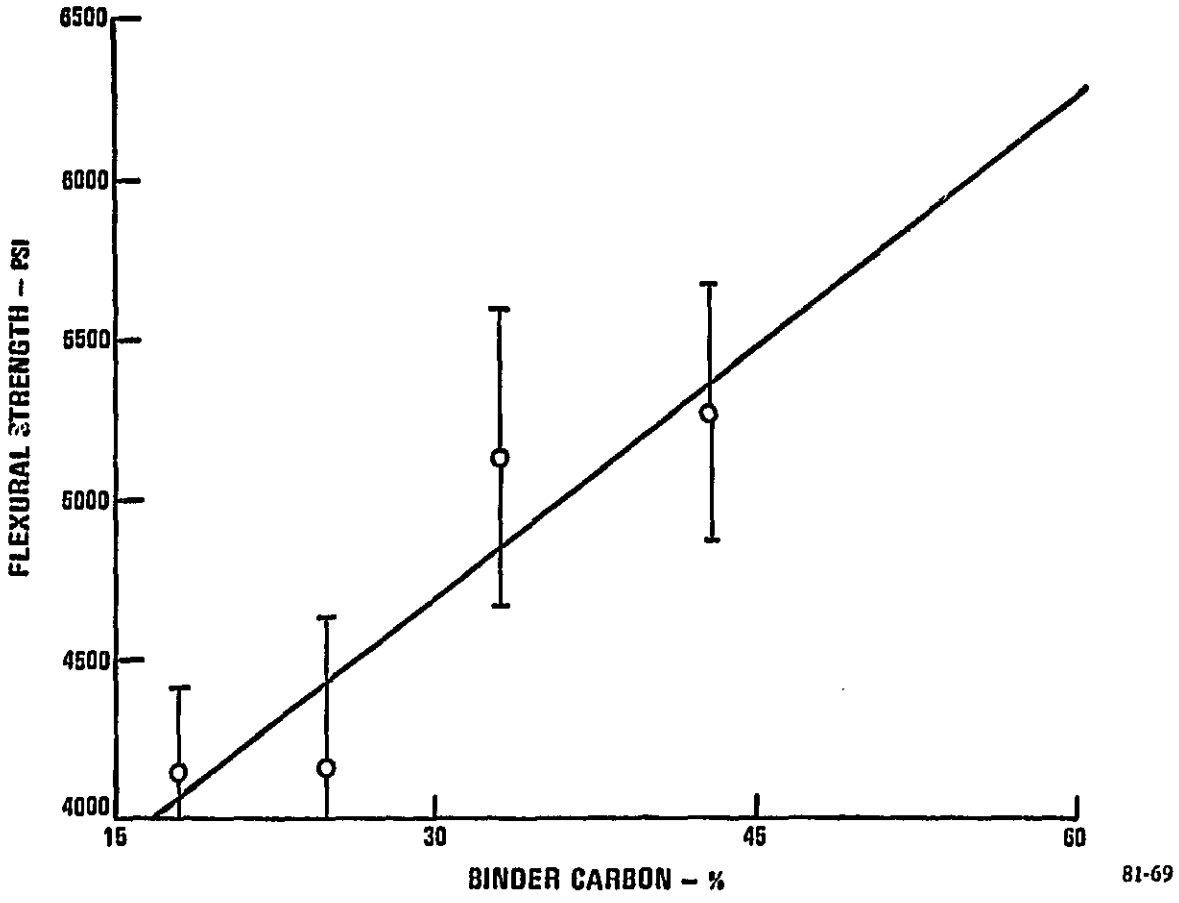

Figure 1-5. Flexural Strength of Separators vs. Binder Carbon Content

tribution is temperature independent. The superposition technique is relatively insensitive to data scatter. Corrections for the finite heat-up time were made, the cooling time correction being negligible.

Figure 1-6 is a plot of the logarithm of the relative rate constants, determined from the corrosion potential versus time data at various temperatures, against the reciprocal of temperature. It follows the Arrhenius relationship giving an activation energy of 5.5 eV/atom. While the significance of the activation energy was not investigated, the plot has been used to determine rate constants at intermediate temperatures and thus chart the corrosion potential, time, temperature diagram for the time and temperature range of interest, Figures 1-7 and 1-8. Similarly charted are plots of resistivity, compressive strength and flexural modulus, Figures 1-9, 1-10 and 1-11. Figure 1-12 is a plot of separator plate resistivity as a function of temperature.

1.2 CELL MATERIALS AND CATALYST LAYER EVALUATION

Objective

The objective of this task was to evaluate UTC developed candidate catalyst layers for operation at higher pressure and temperature conditions, and to recommend catalyst layers for use in short stack demonstrations and endurance tests. An endurance goal of testing one subscale 2-in. by 2-in. cell for 5000 hours was established.

Voltage during the endurance tests was compared to a performance goal designated as "E-line". This goal was analytically and empirically determined as the performance available based on many prior subscale tests. It was established for atmospheric conditions and extrapolated to higher pressure and temperature conditions.

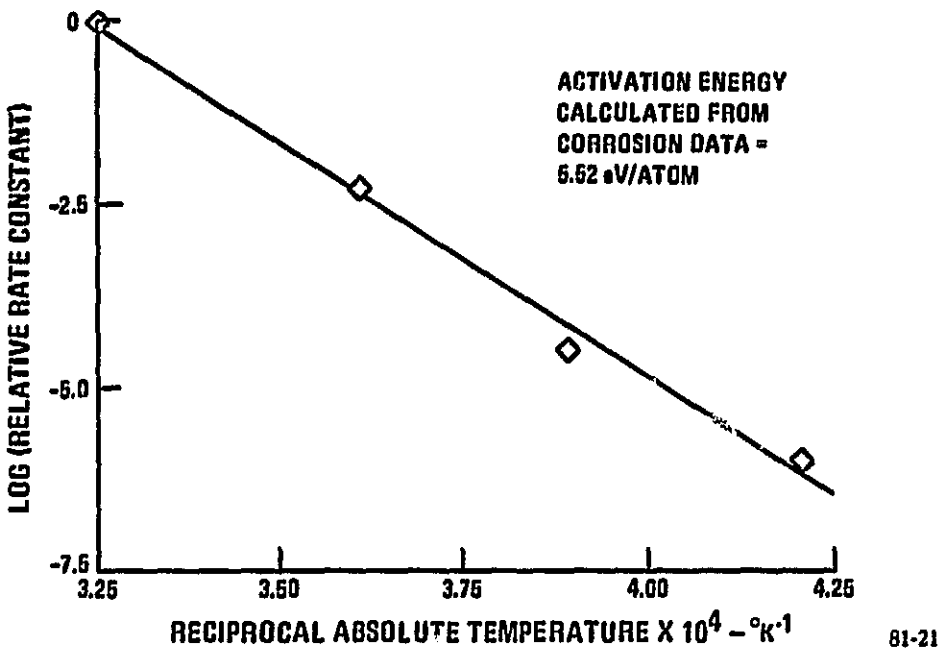

Figure 1-6. Arrhenius Plot for Electrode Substrate Corrosion Resistance as a Function of Graphitizing Time vs. Graphitizing Temperature

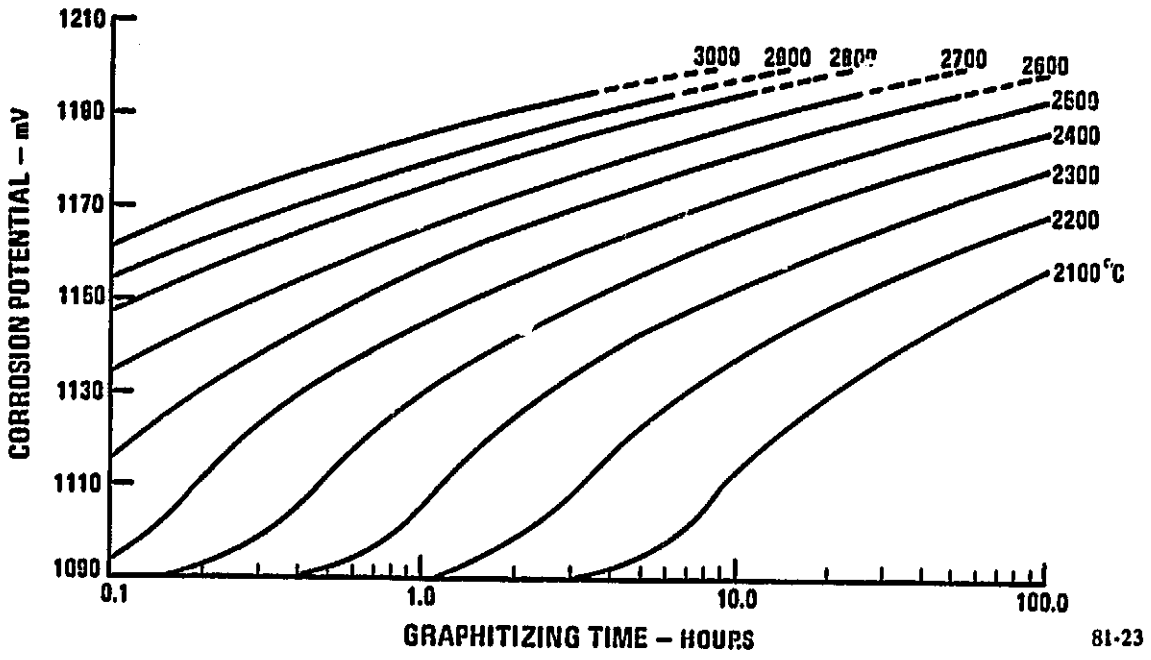

Figure 1-7. Substrate Graphitization Time, Temperature, and Corrosion Potential Relationship

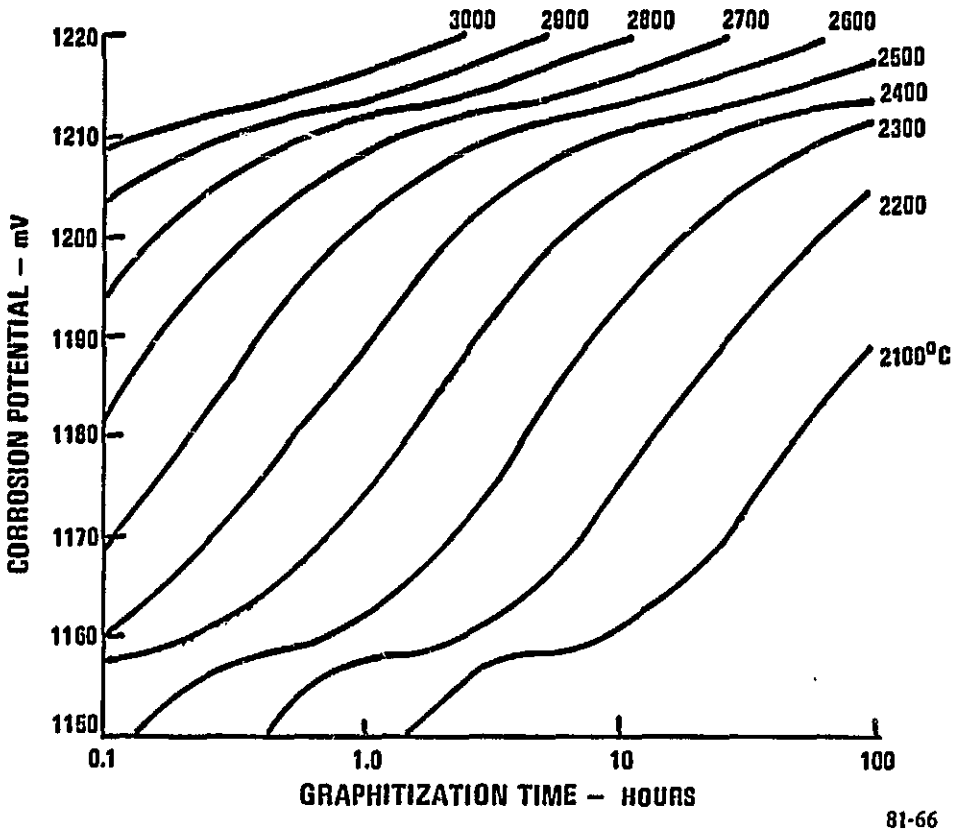

Figure 1-8. Separator Graphitization Time, Temperature, and Corrosion Potential Relationship

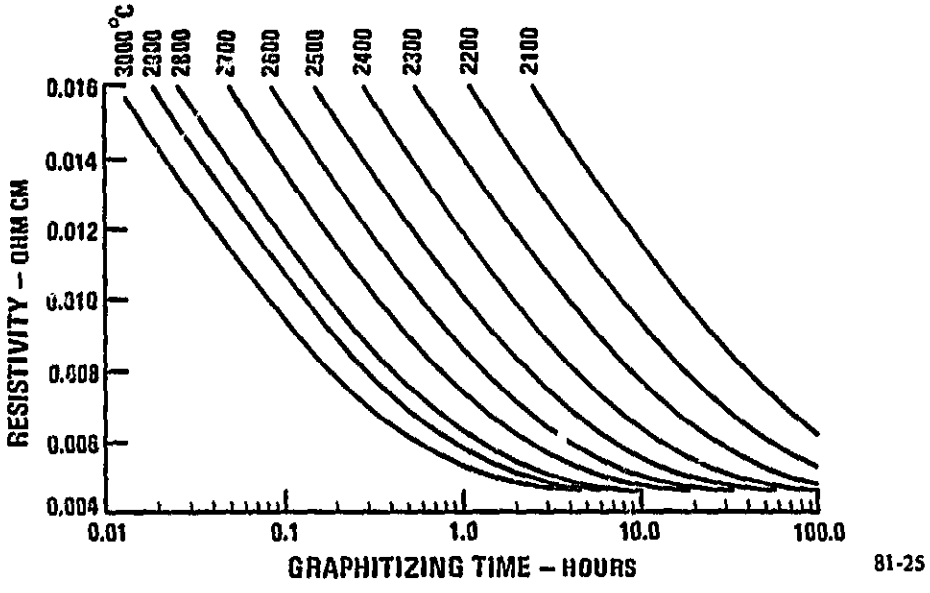

Figure 1-9. Substrate In-Plane Electrical Resistivity

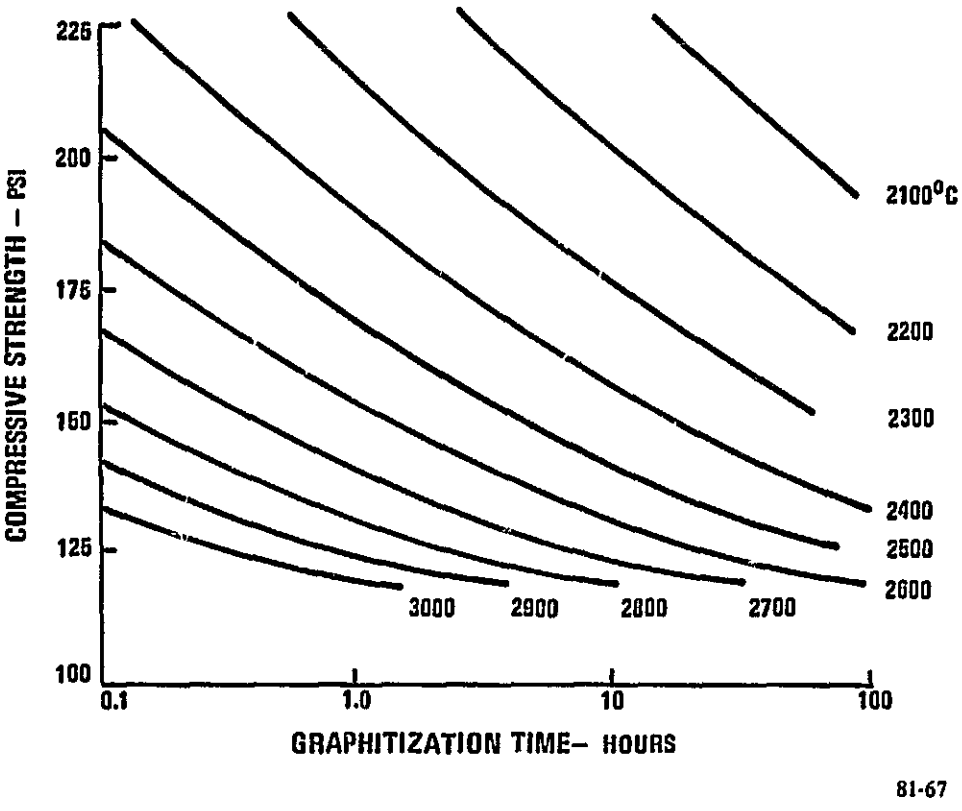

Figure 1-10. Substrate Graphitization Compressive Strength

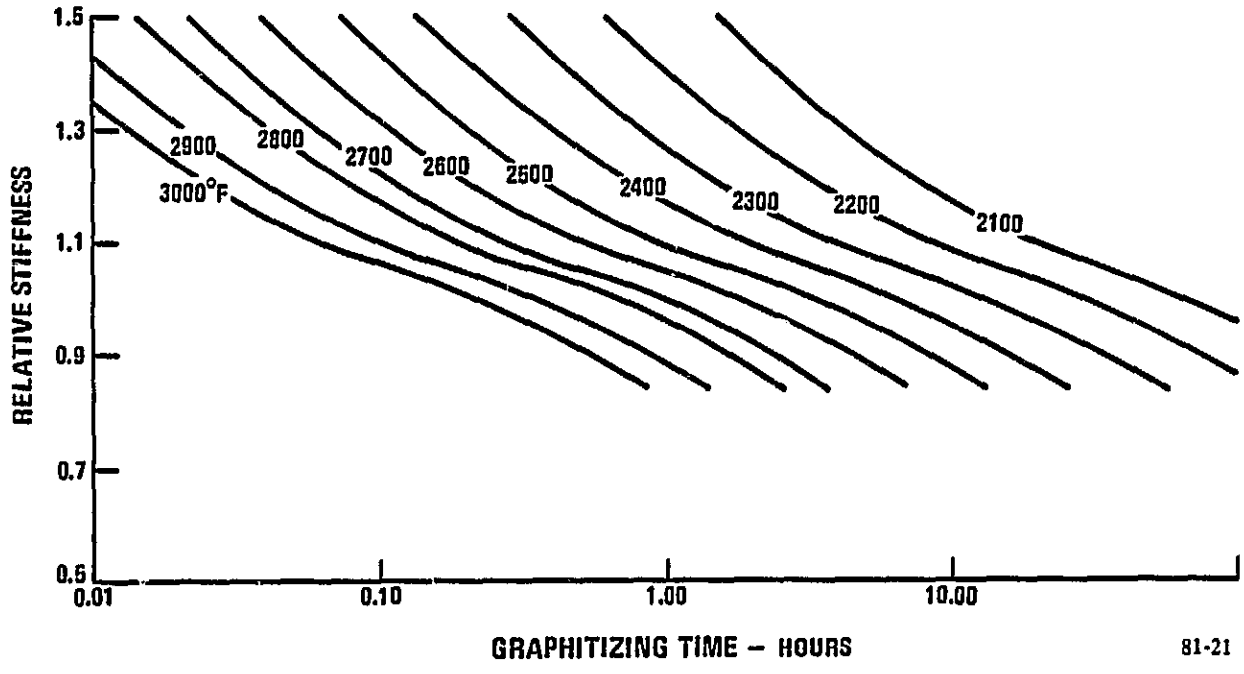

Figure 1-11. Relative Stiffness vs. Time and Temperature Relationship for Separator Graphitization

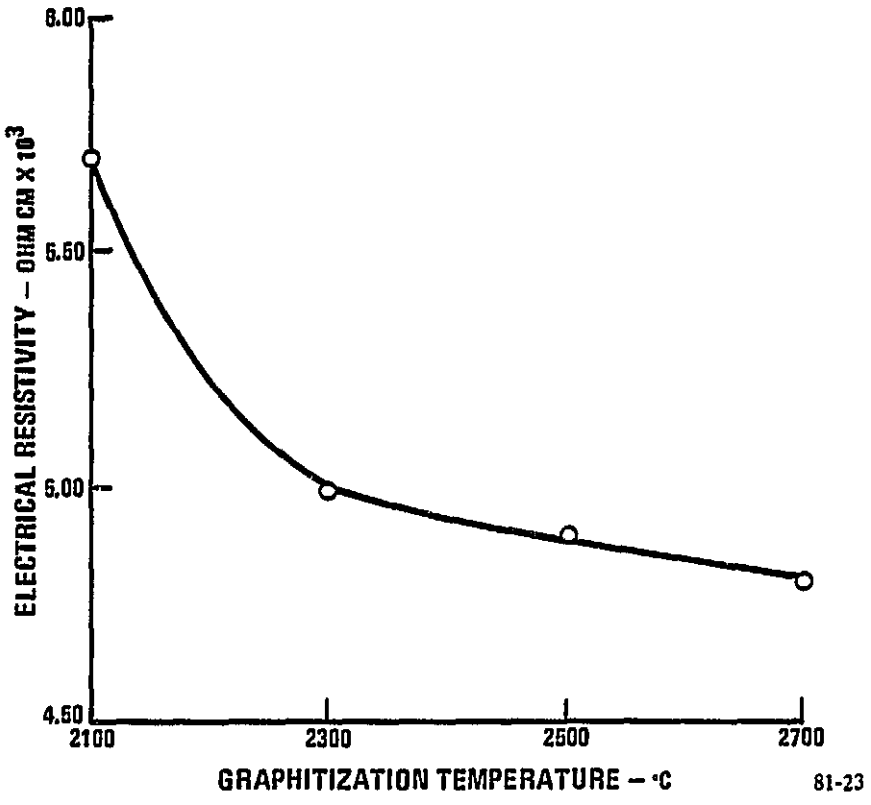

Figure 1-12. Through-Plane Electrical Resistivity vs. Temperature Relationship for Separator Graphitization

Summary

The endurance goal of 5000 hours was met by one subscale cell that ran for over 6500 hours and performance exceeded the 120 psia/400°F goal at 5000 hours by 8 mV. Ten 2-in. by 2-in. subscale cells were tested for terms ranging from 1400 to 6500 hours. Three cathode catalyst layers, GSB-15, GSB-17, and GSB-18, were tested with initial performance well above the E-line goal. Both GSB-15 and GSB-17 were recommended for full-size tests in short stacks.

A secondary accomplishment under the program was the improvement of the reactant gas seal configuration for the subscale 2-in. by 2-in. hardware. The initial solid fluoropolymer seal previously used successfully for 15 and 50 psia testing was marginal at 120 psia. During the course of the above catalyst evaluation several improvements in the solid seal configuration were evolved, thus extending the capability to test these subscale cells to several thousand hours. These solid fluoropolymer seals are used only for the bench testing of the subscale 2-in. by 2-in. cells to enable a fast turnaround and minimize the complexity of the test facility without a containment vessel. This exposes the gas seal to a 105 psi pressure differential but uses only two gases.

Discussion

Hardware and Test Description - The 2-in. by 2-in. cell hardware consists of the test electrodes separated by a porous matrix (silicon carbide) to hold electrolyte, gold plated tantalum plates which hold the electrodes and provide gas chambers and current take-off, a thick steel pressure plate, heater pads, and Teflon® seals (see Figure 1-13).

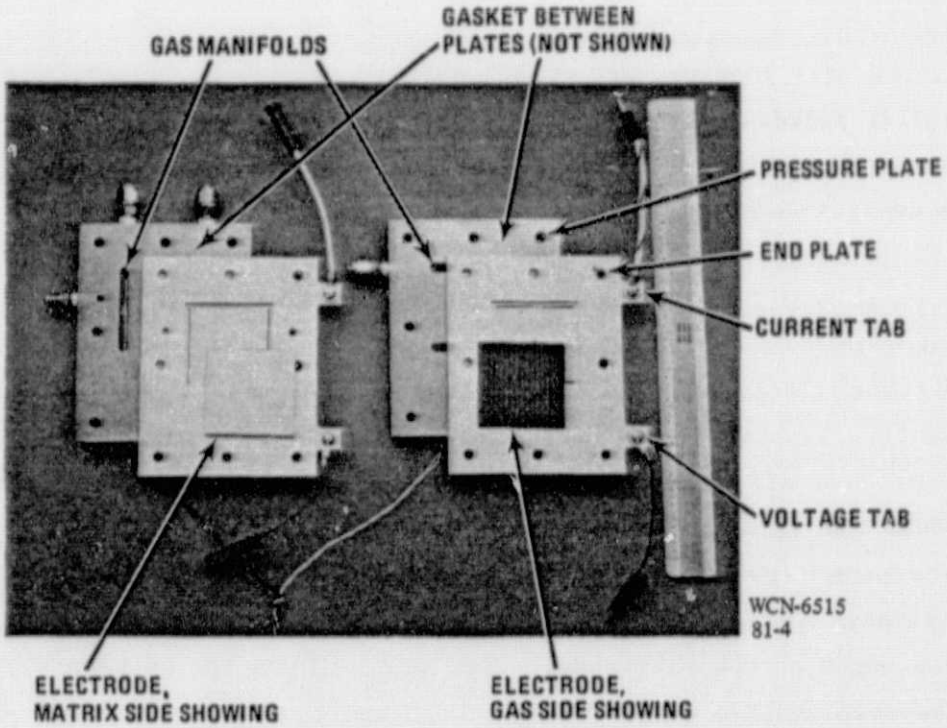

Figure 1-13. Tantalum Subscale Cell Hardware

The cells were operated at the following conditions:

Temperature	400°F
Pressure	120 psia
Fuel, VHP (to March 20, 1981)	72.7% H_2, 4.3% CO, 23% CO_2, dry basis
RL-1 (from March 20, 1981)	70% H_2, 1% CO, 29% CO_2, dry basis
Utilization of H_2	70%
Dewpoint of Fuel	246°F
Air	79% N_2, 21% O_2
Utilization of O_2	70%
Dewpoint of Air	Dry
Current Density	Adjusted to maintain 0.79V cell voltage

There is no measurable difference in performance between the two fuel mixes, the lower H_2 in the latter being compensated by lower CO in the former. The switch was made to conform to the fuel used by full-size stacks.

Once a week, the cell load was set at 372 ASF, to provide a direct comparison with the analytically protected E-line performance goal. These points provide a history of performance versus time. For consistency data from diagnostic tests are quoted at the above conditions at 372 ASF.

Improved Internal Seal Development - Although the seals of the cells prevent external leaks, they do not eliminate the mixing of fuel and air (crossover) around the edges of the electrodes. A thin gasket between the edges of the anode and cathode, the "overlapping gasket", is intended to prevent crossover, but it can deform and lose its effectiveness with time. Several variations of gasketing were tried to reduce the incidence of internal fuel-air mixing - "crossover". The first was the "staggered" overlapping gasket, shown in Figure 1-14. A ¼-in. smaller cathode eliminated the need to pinch the overlapping gasket, reducing shearing forces on the edges of the electrode. This approach was not successful; the gasket which lies between the two electrodes (in both configurations) deforms and the path that the reactants can follow around the edges is too short. Therefore several

cells were started with a wider overlapping gasket (see Figure 1-14). This scheme did not eliminate crossover completely but helped Cell 6167 reach the 5000-hour goal.

Evaluation of GSB-15 Cathodes - The GSB-15 cathode was tested in five cells. In the first, Cell 6132, performance initially was 0.719 V, 21 mV above the goal. Good performance continued for 1200 hours until affected by crossover (see Figure 1-15). The cell was shut down at 2825 hours. Cell 6165 used the wider overlapping gasket. Initial performance was 0.705 V. Before 1000 hours, slight crossover did develop, caused by an accidental imbalance of pressures during a power failure. Performance was 3 mV above the goal at 3000 hours, but increasing diffusion losses led to low voltage thereafter. The cell was shut down at 3173 hours (see Figure 1-16).

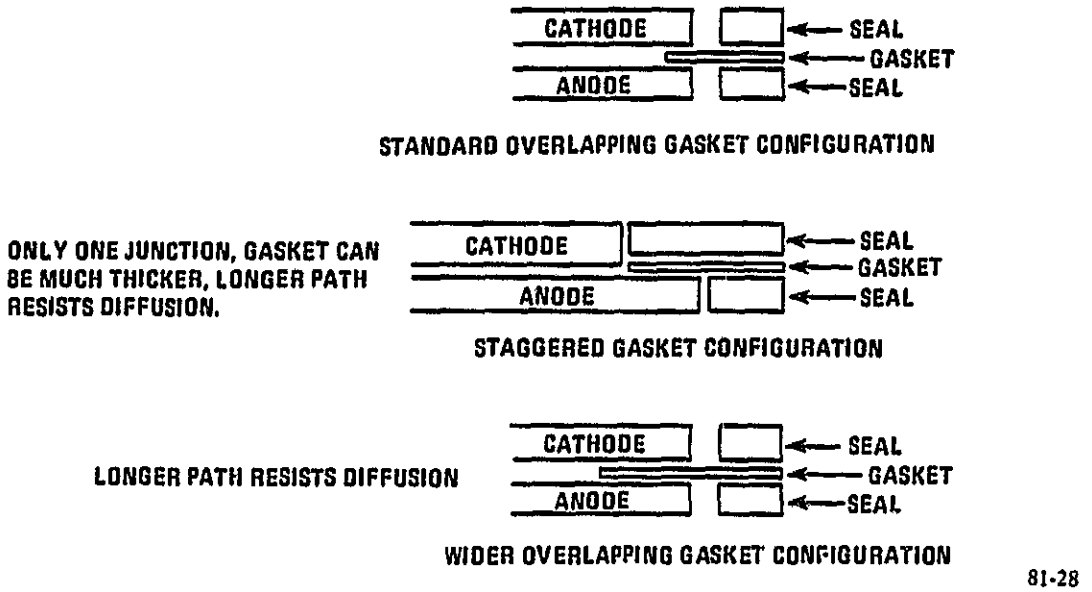

Figure 1-14. Staggered Overlapping Gasket and Wider Overlapping Gasket

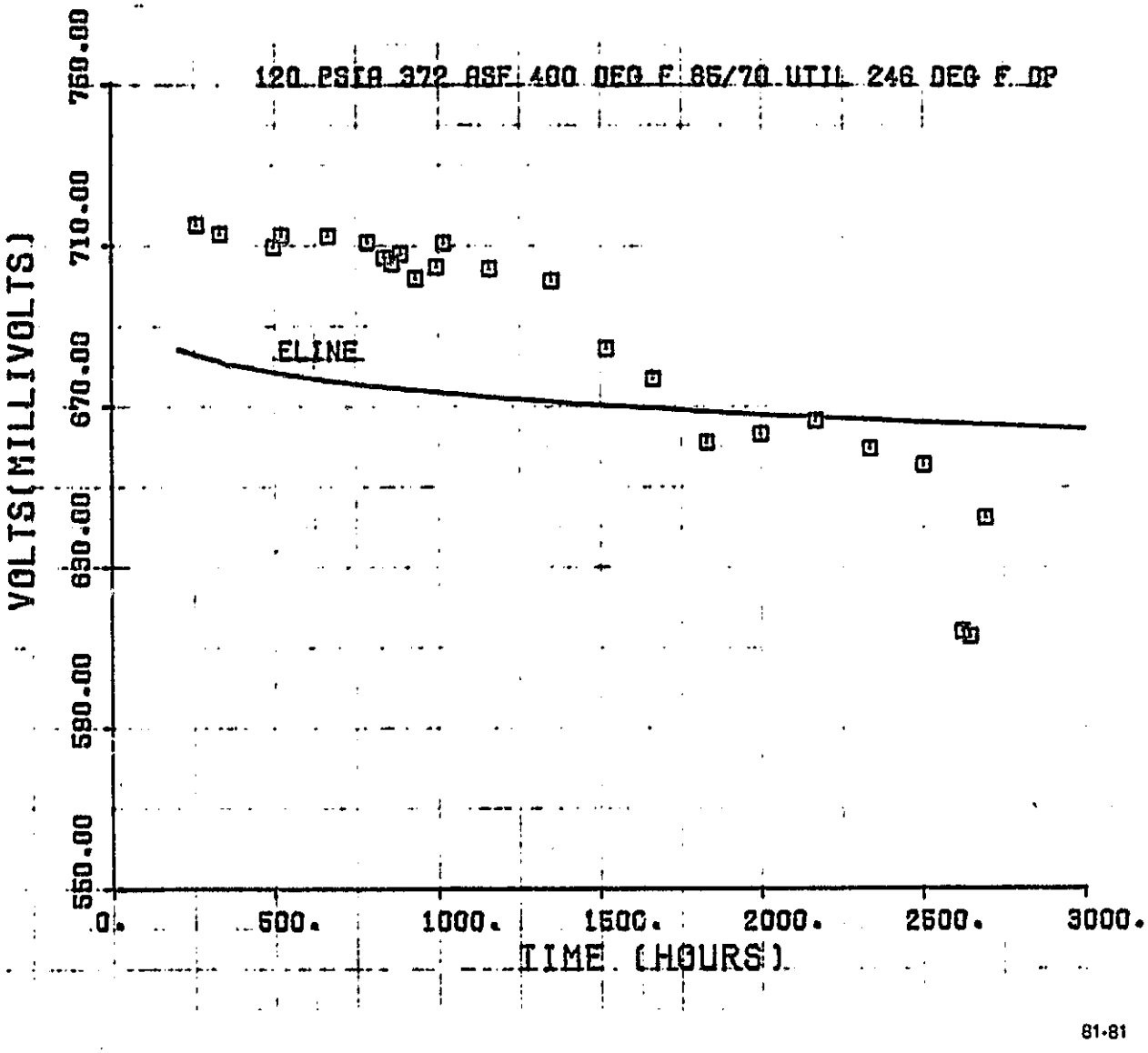

Figure 1-15. Performance of Cell 6132 Testing GSB-15 Catalyst

Cell 6195 initial performance was 0.718 V. Performance continued well above the goal to 2581 hours (see Figure 1-17) when the cell was shut down for the vacation period. There was no loss upon restart. This cell and others at 120 psia then suffered from facility-induced fuel starvation. Both anodes and cathodes rose to high potentials; the anodes because of lack of H_2, the cathodes because no load could be held. This cell lost 28 mV. It was shut down at 3048 hours.

A similar cell, 6198, had to be shut down at 1981 hours due to crossover (see Figure 1-18). Performance until then was meeting the goal.

Cell 6202 performance was excellent until 1412 hours, when it was affected by the same facility-induced fuel starvation noted above. Initial performance was 0.719 V but the fuel starvation lowered performance 27 mV. Testing was continued beyond the end of this contract to evaluate the seals. After 9500 hours, there was no crossover problem, though the cathode had lost catalytic activity and had high diffusion losses. Performance history is shown in Figure 1-19.

Evaluation of GSB-17 Cathodes - There were three tests of the GSB-17 cathode. In the first, Cell 6131, initial performance was 0.750 V, 52 mV above the goal. Performance was above the goal to 3500 hours and was only 4 mV below the 5000-hour goal. The test was stopped at 6039 hours. The performance history is shown in Figure 1-20.

Two cells, 6166 and 6167, were built with the wider overlapping gasket. The first cell, 6166, had crossover by 1000 hours and was terminated. The second cell, 6167, achieved the 5000-hour goal. Initial performance was 0.718 V. Performance continued well above the goal, reaching 5000 h rs at 0.668 V, 8 mV above goal. At 6000 hours, diagnostics indicated a drop in cathode performance since 5000 hours, and the cell was shut down at 6570 hours. The performance history is shown in Figure 1-21.

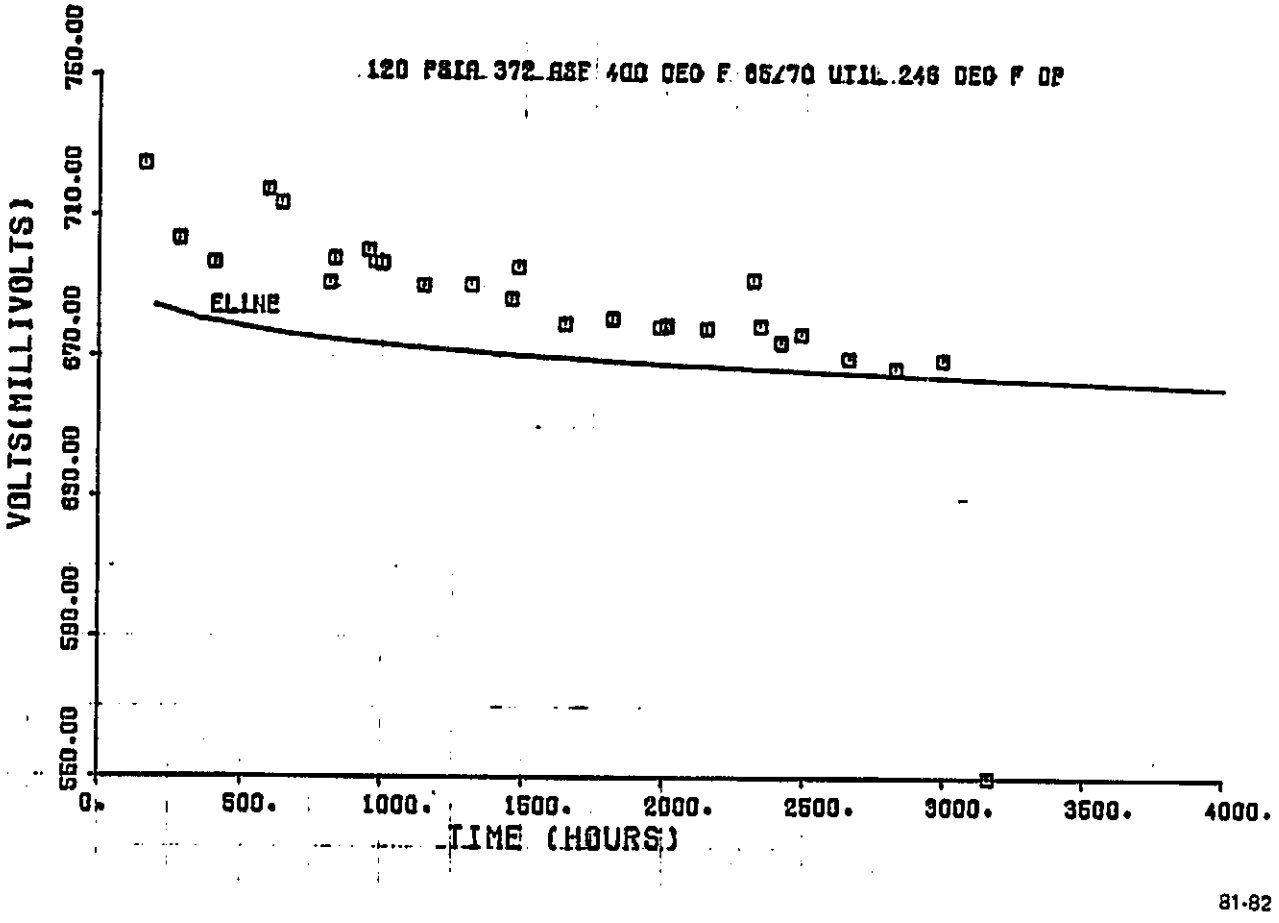

Figure 1-16. Performance of Cell 6165 Testing GSB-15 Catalyst

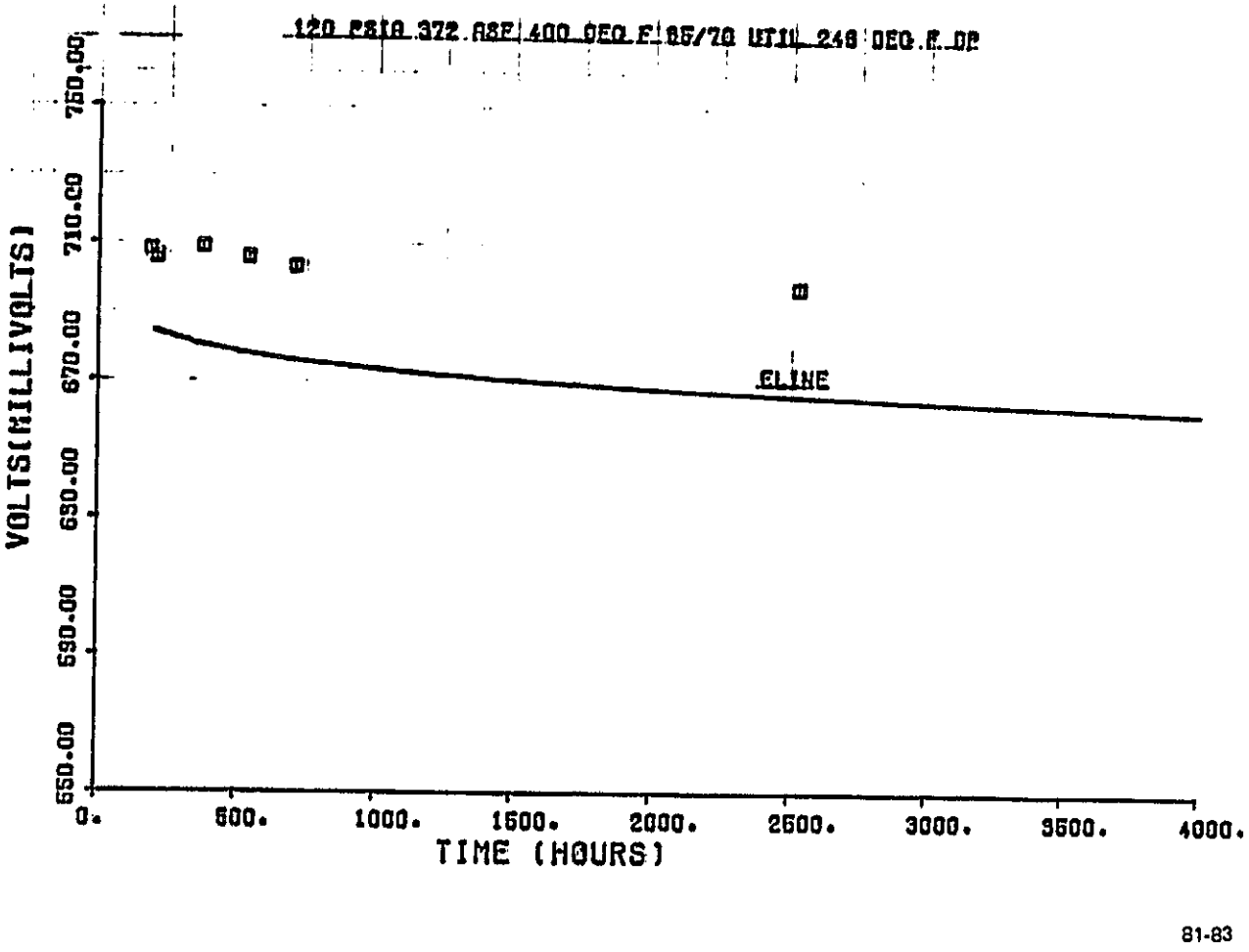

Figure 1-17. Performance of Cell 6195 Testing GSB-15 Catalyst

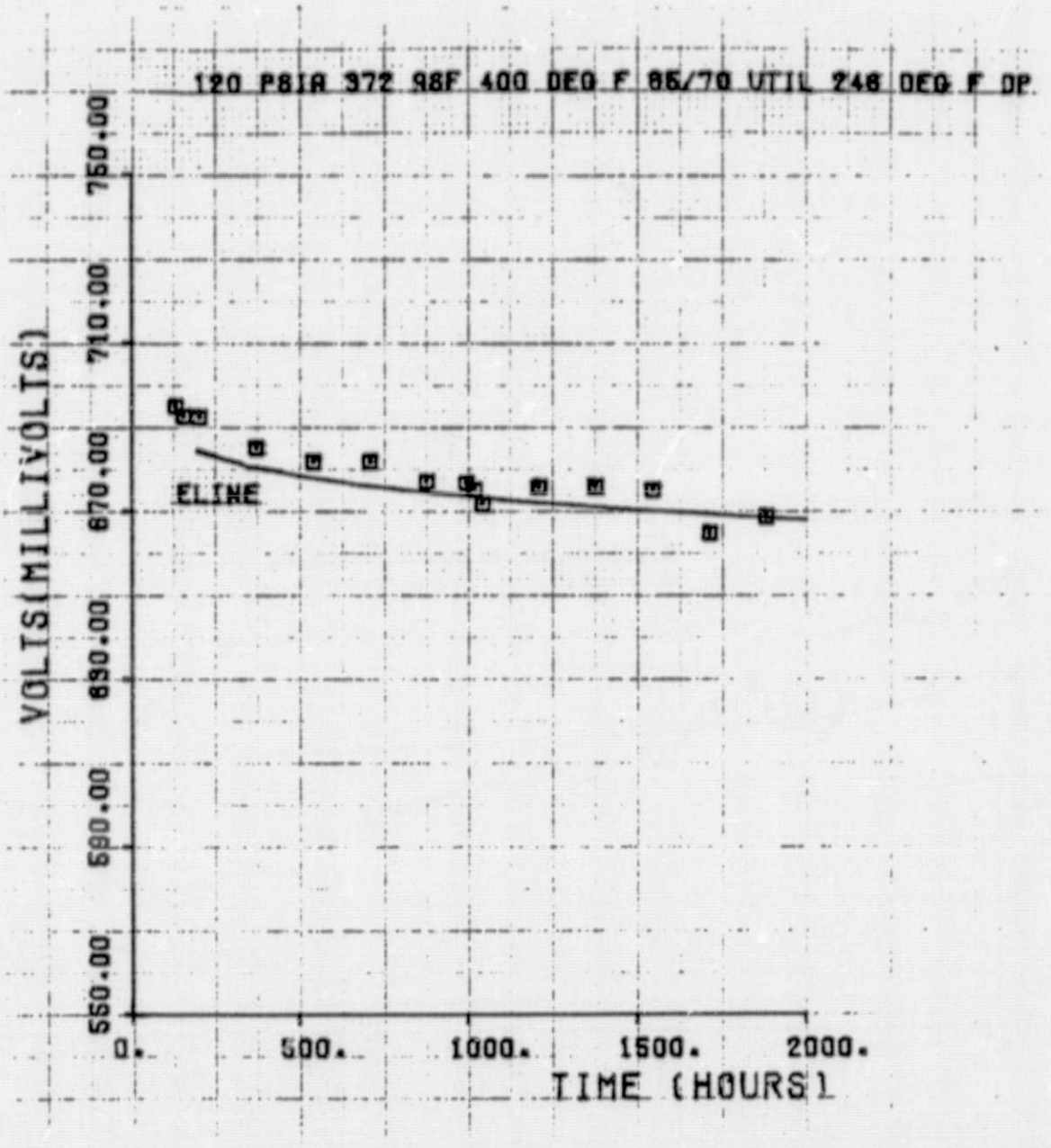

Figure 1-18. Performance of Cell 6198 Testing GSB-15 Catalyst

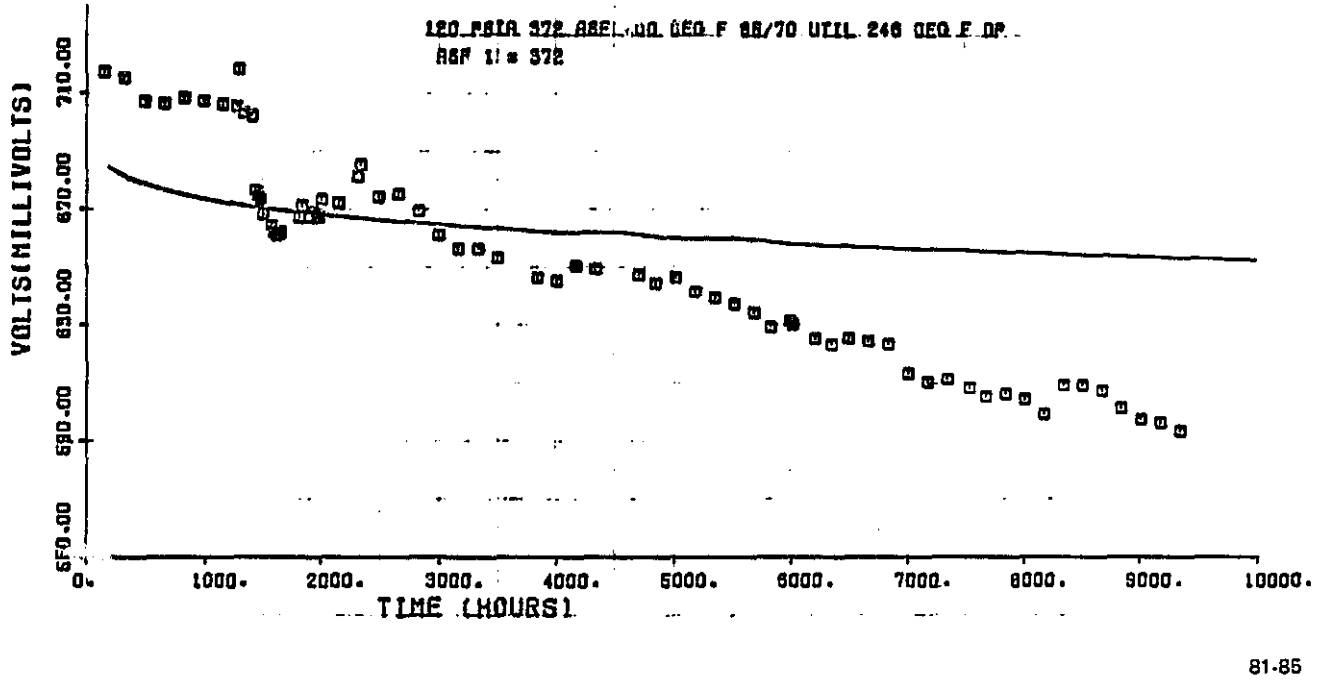

Figure 1-19. Performance of Cell 6202 Testing GSB-15 Catalyst

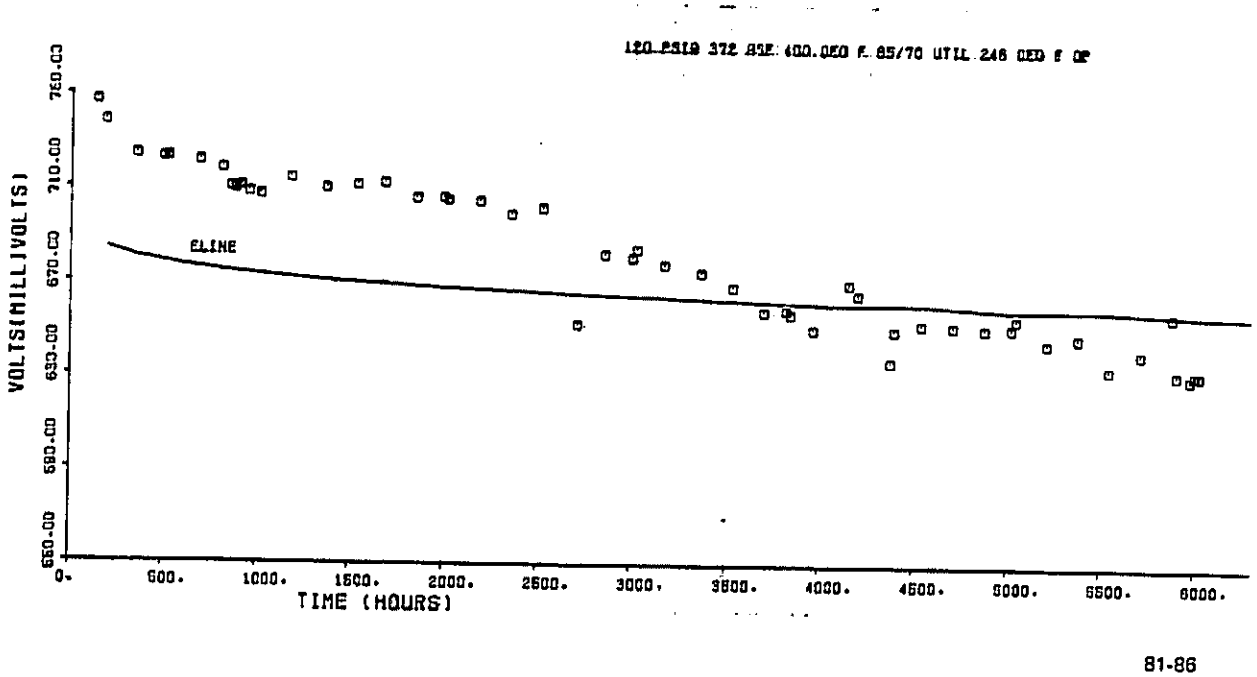

Figure 1-20. Performance of Cell 6131 Testing GSB-17 Catalyst

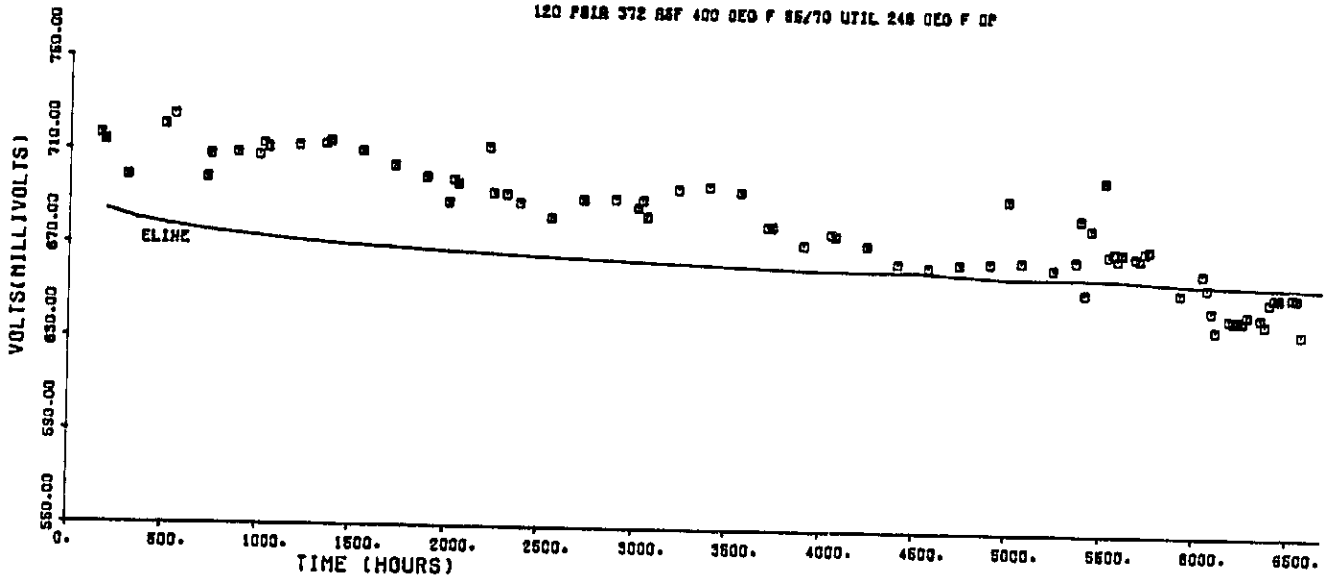

81-87

Figure 1-21. Performance of Cells 6166 and 6167 Testing GSB-17 Catalyst

Evaluation of GSB-18 Cathodes - Cell 6141, the first test of the GSB-18 cathode, was built with the "staggered" gasket. Despite slight crossover, initial performance was above the goal, but then the performance was affected by the same power failure and consequent pressure imbalance suffered by 6165. The cell was shut down at 2700 hours (see Figure 1-22).

In a second test of a GSB-18 cathode with a "staggered" gasket, Cell 6183 had initial performance of 0.708 V, 10 mV above the goal. Performance decayed at a high rate. At 2059 hours, with performance 10 mV below the goal, the cell was shut down (see Figure 1-23).

Electrode Evaluation Results - On the basis of the foregoing evaluation, GSB-15 and GSB-17 cathodes were recommended for use in full-size stacks. Their performance with time is summarized in Figures 1-24, 1-25, and 1-26 using data from the diagnostic tests. The data are averages of the cells which ran that long and were not excessively influenced by crossover. Figure 1-24 shows overall cell voltage at the 372 ASF, 120 psia condition. The data indicate GSB-17 performs better than GSB-15 and both exceed the goal to about 4000 hours, but are losing performance at a rate higher than that projected for the goal.

Figure 1-25 shows that the iR-free performance of GSB-15 and GSB-17 cathodes on pure gases is similar and also decays faster than the goal performance.

Figure 1-26 shows the diffusion loss evidenced by the "O_2 gain" of GSB-15 and GSB-17 cathodes, the difference between performance on air and on pure O_2 at 70% oxygen utilization. The GSB-15 tends to have higher O_2 gains than the GSB-17. In both cases, the gains are increasing faster than projected.

Crossover of reactants also reduces performance, but is difficult to quantify. Only cells with minimal or no crossover are shown on the curves, but crossover influence over time may be a cause of performance decay.

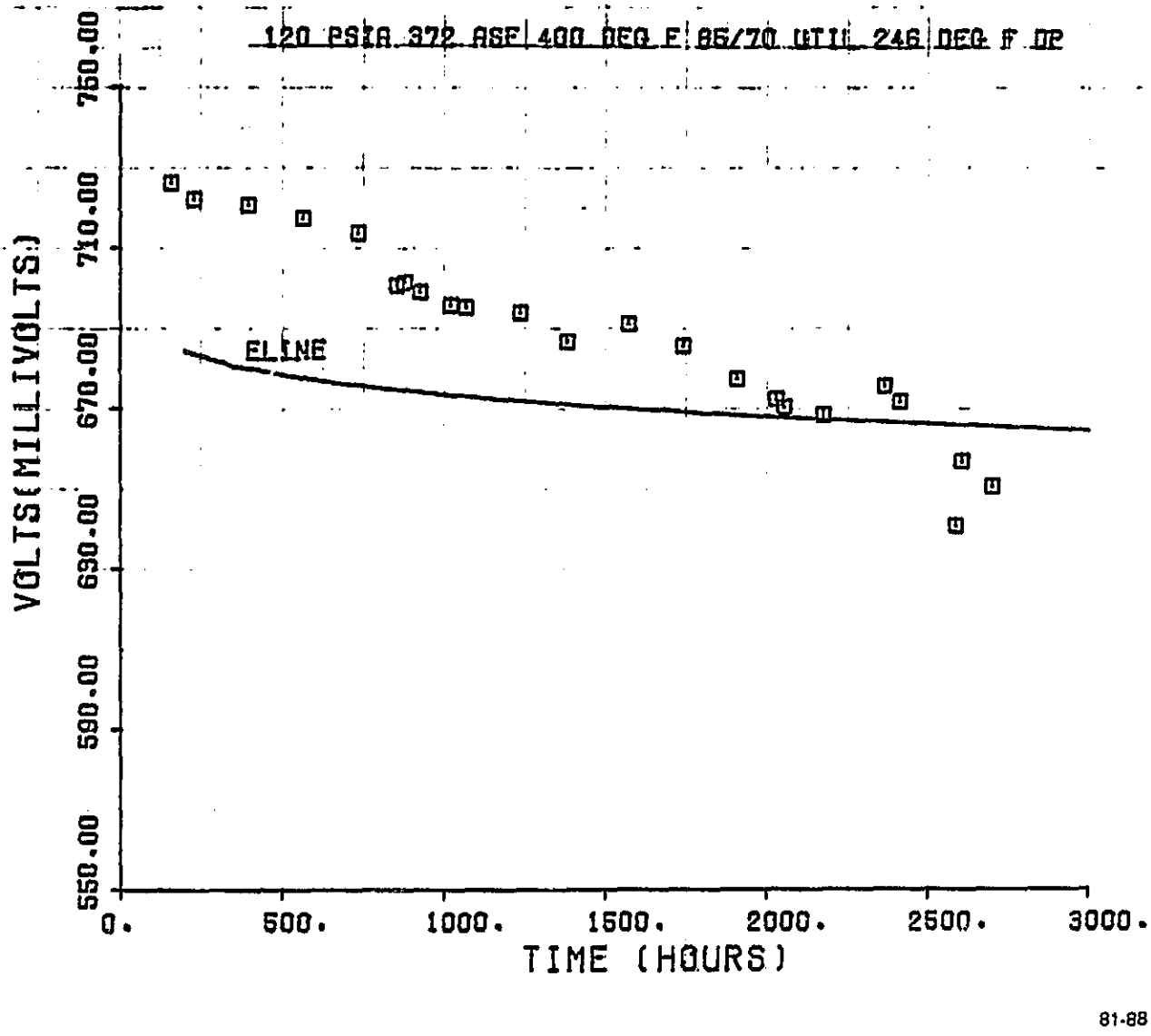

Figure 1-22. Performance of Cell 6141 Testing GSB-18 Catalyst

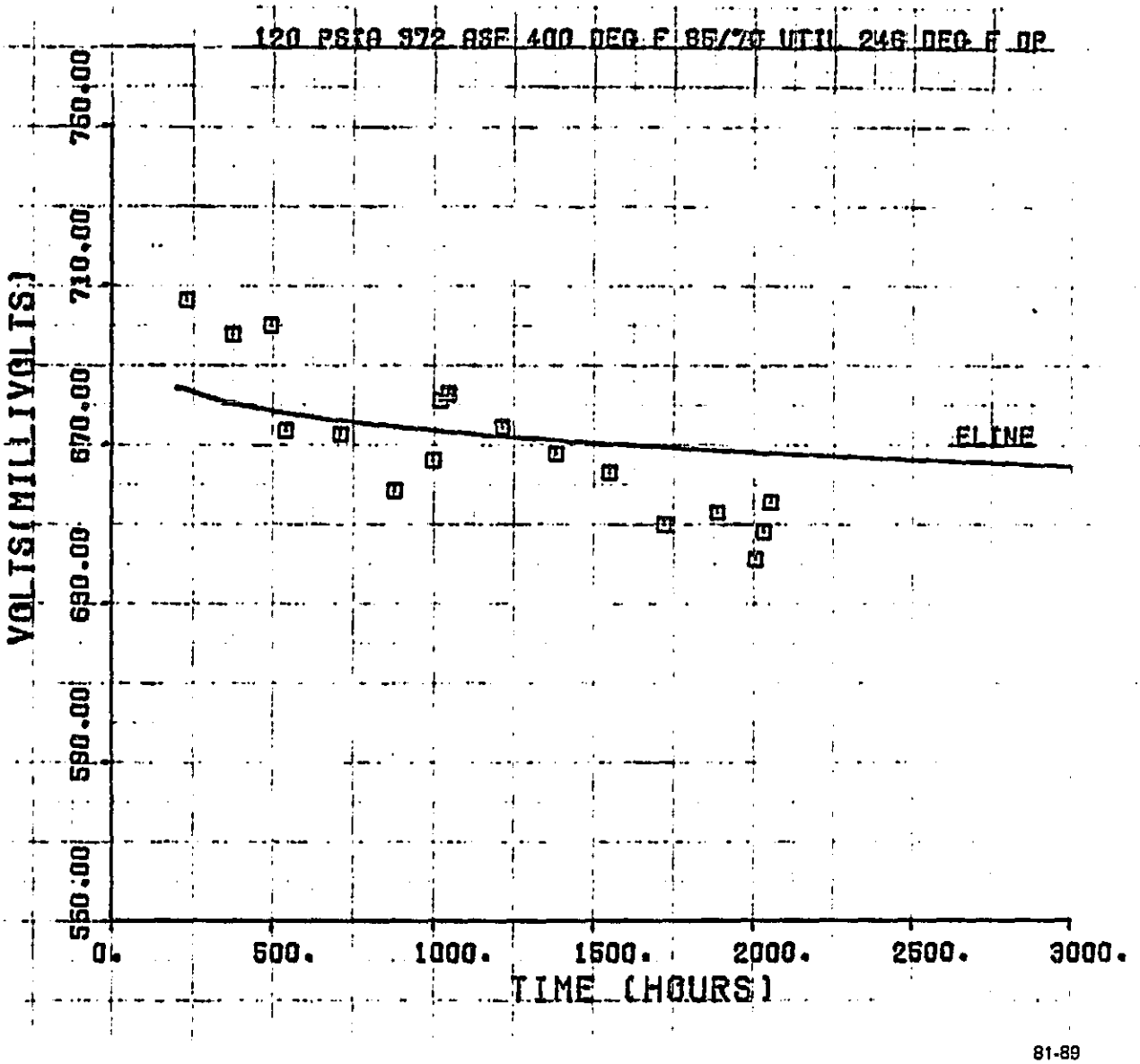

Figure 1-23. Performance of Cell 6183 Testing GSB-18 Catalyst

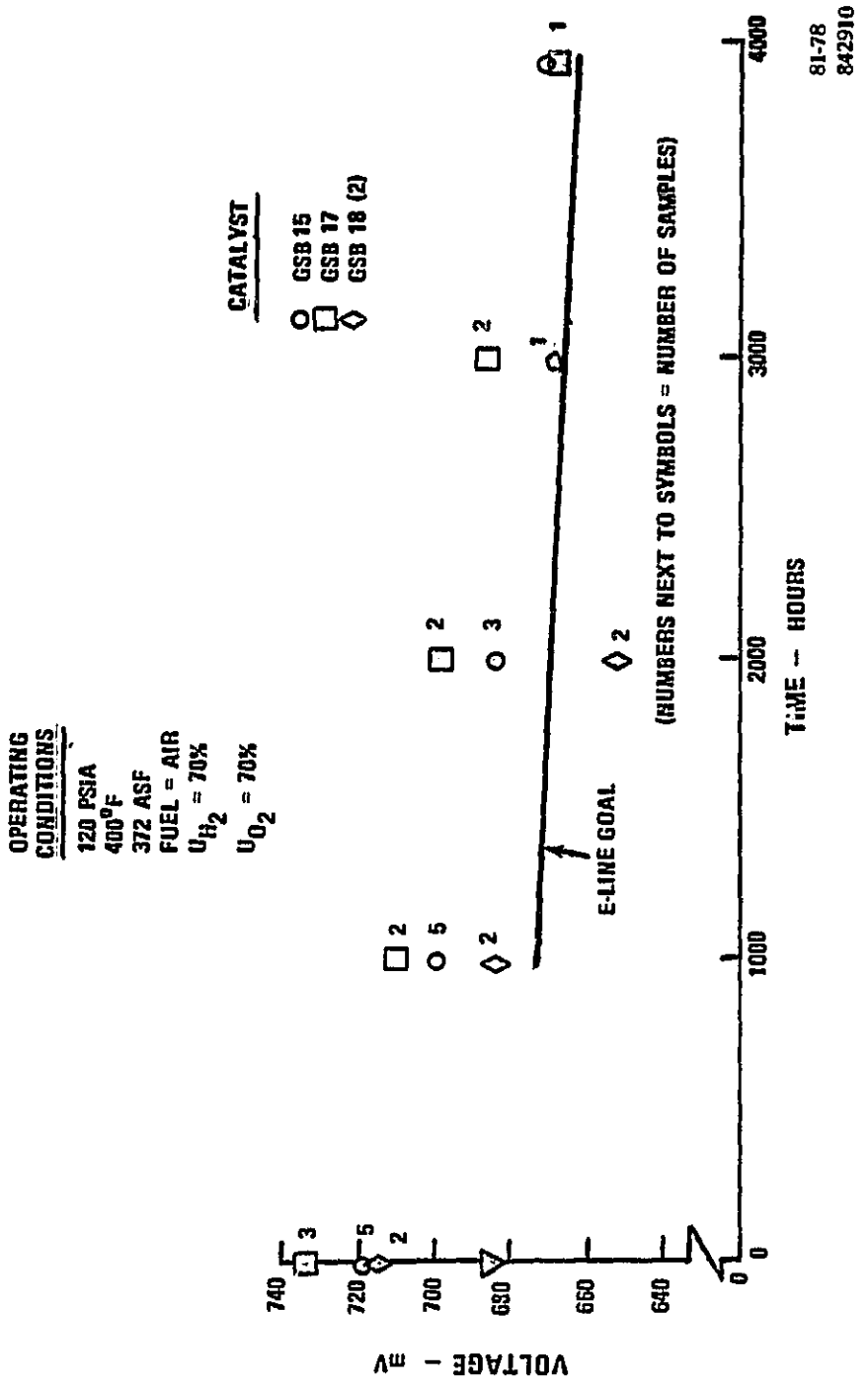

Figure 1-24. Cell Voltage vs. Time

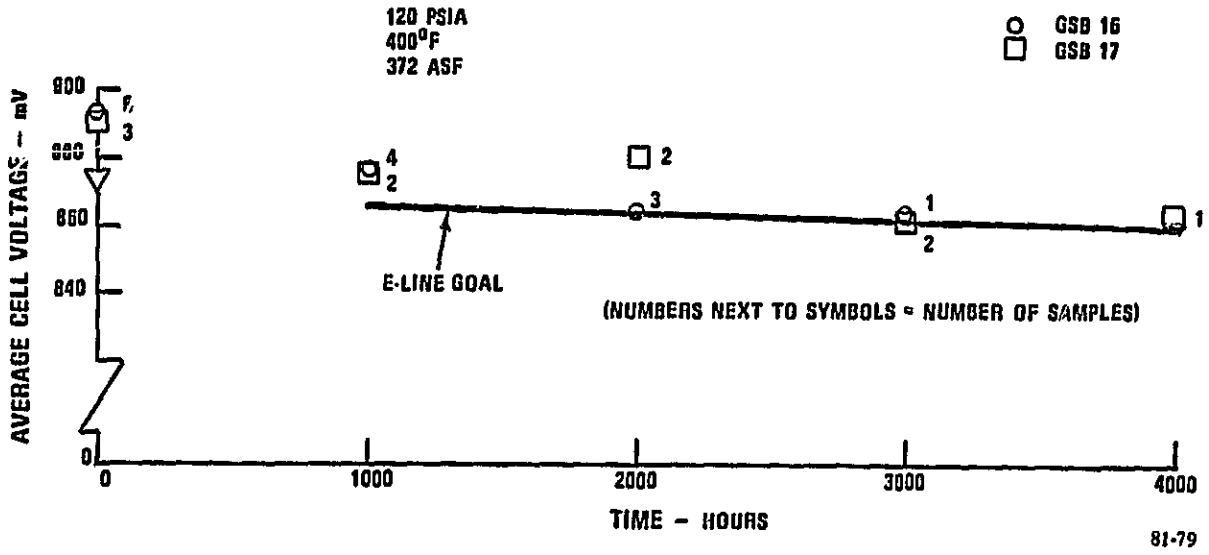

Figure 1-25. iR Free Performance of GSB-15 and GSB-17 Cathodes on Pure H_2 and O_2

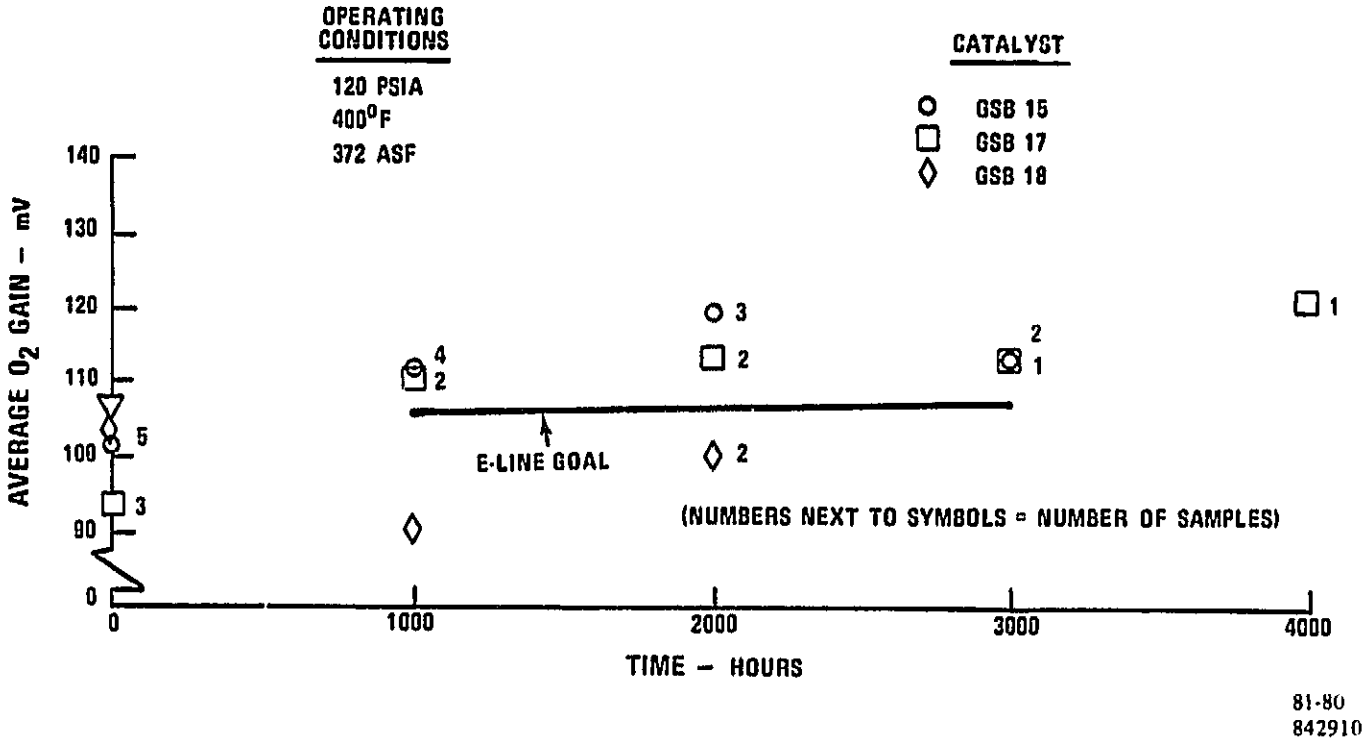

Figure 1-26. Diffusion Losses

SECTION 2
PROCESS DEVELOPMENT

Task 2 of Contract DEN3-191 continued the development of the ribbed substrate cell for higher temperature and pressure operation. The bulk of this effort was addressed to developing improved processing and fabrication techniques for the repeating and non-repeating elements of the cell structure. The approach was to continue work on improvements identified in previous DOE and EPRI programs. The objective was to produce significant improvements in the operational capabilities of the various cell components, then incorporate the improvements in the fabrication of cell elements. These were then evaluated on the basis of full-size stack endurance and performance tests discussed in Section 3.

This section reports on five separate areas of process development. The first part focuses on substrate processing with emphasis on the fabrication and preliminary technology development of a substrate forming machine; the second on lower cost electrode processing including matrix and wet seal improvement; the third on improving the cell separator plate processing; the fourth on intercell cooler optimization; and the fifth on improving the non-repeating stack parts. As the development of the various processing tasks progressed, the resulting improvements were incorporated into subscale cells and/or full-size stack tests for evaluation.

2.1 SUBSTRATE PROCESSING

Objective

The objective of this task was to develop the equipment and processing procedures to form large area (10-ft^2), electrode substrates, and to evaluate and select alternative substrate materials that reduce cost and meet functional, performance and endurance goals.

Summary

A pilot substrate forming machine capable of producing substrates up to 16 ft^2 was designed, fabricated and operated. The machine is shown in Figure 2-1. This design features the utilization of two continuous belts, one on top of the other, which form an endless continuously moving press. This integrates substrate formation and pressing into a single continuous operation. A total of 200 10-ft^2 substrates were continuously formed and pressed in one operation.

Several fiber precursors including an alternative pitch-based fiber were evaluated. The alternative pitch-based fiber was selected as the most promising and after some modifications the properties were improved to be comparable to those of the standard fiber. Subscale cells run to 1800 hours showed comparable performance.

Several substrate resins were evaluated and one was selected that resulted in significantly improved substrate properties as well as more stable handling characteristics. The selected resin was verified in a 3.7-ft^2, 20-cell stack test and used in substrates for all subsequent short stacks.

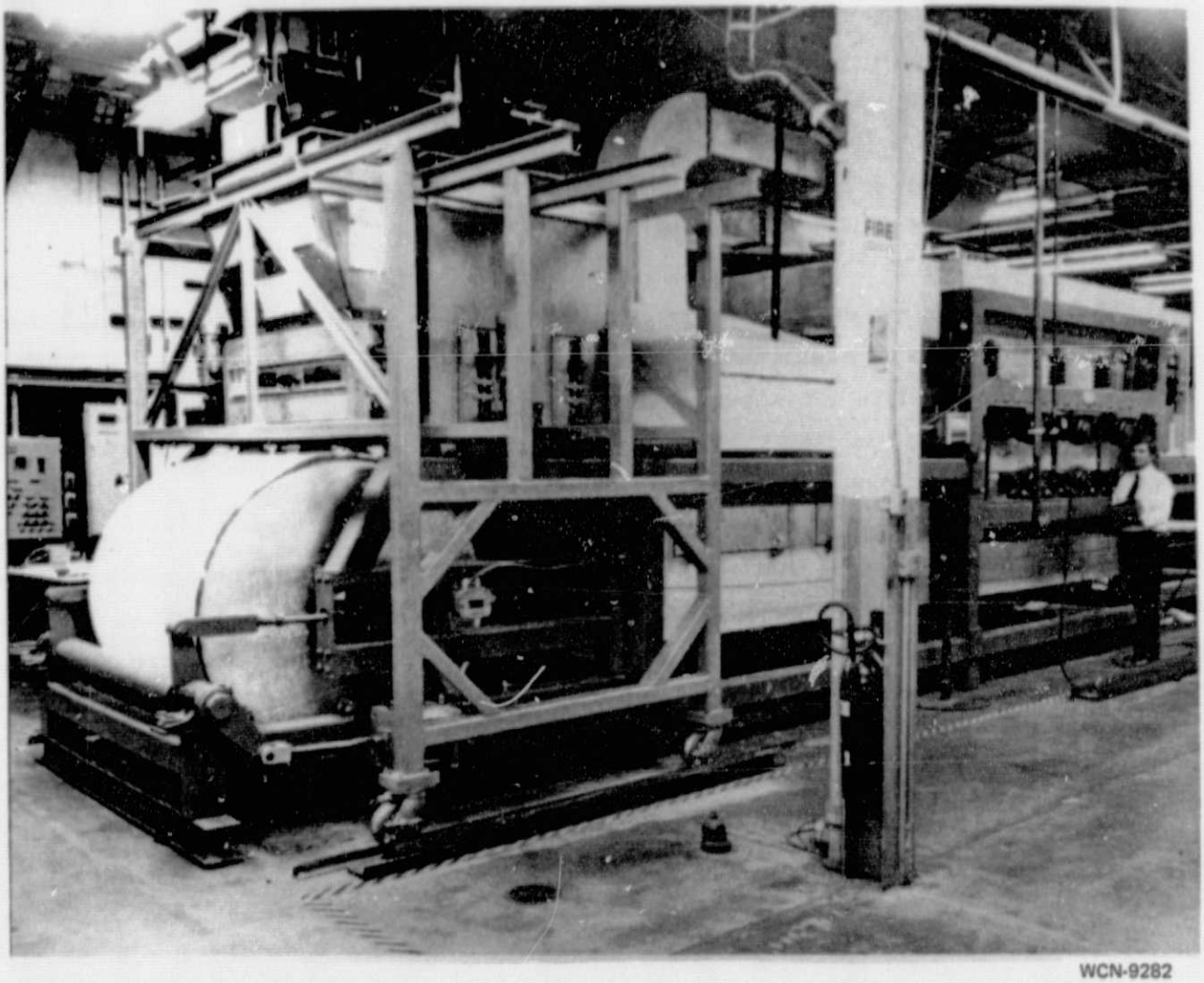

WCN-9282

Figure 2-1. Substrate Forming Machine

Discussion

Substrate Forming Machine - Prior to this program, electrode substrates, with active areas up to 3.7-ft^2, were made in three separate steps - substrate formation, densification, and microgrinding. To reduce costs, a new machine capable of forming and densifying to final thickness was conceived. This process would produce a superior substrate while eliminating two subsequent operations.

An additional objective of this effort was to investigate the technology of producing larger area substrates; however, existing machinery was unable to fabricate the larger area substrates. Consequently a new machine to form larger area substrates while incorporating the conceptual features discussed above was designed, fabricated and installed at UTC. The machine was designed to produce substrates up to 16-ft^2 of active area.

The substrate forming machine is a modified double belt press. The machine contains two continuous steel conveyor belts. Material is deposited onto the lower belt by a powder feeder. This material is then heated to melt the resin and then compacted and cured in the "belt press" zone to the desired thickness. The substrate blank is released and removed after exiting the press zone.

A separate UTC program had developed a new compound fiber/resin feeder system that was incorporated with the new larger area substrate forming machine. This feeder system was fabricated by UTC and used in conjunction with the substrate forming machine to conduct the fabrication trials.

Construction and functional demonstration of the double belt press section was completed at the vendor facility in August of 1981. The finished conveyor assembly, belts, and ovens were packaged separately, delivered to a prepared UTC site location, and installed. Major assemblies were checked out and trimmed individually and in combination in a series of dry runs to verify functional acceptability. The machine was ready for the first series of substrate processing trials by mid-April of 1982.

The feed system was checked out using a standard fiber/resin blend. Disturbances to the powder drop were caused by the exhaust ventilation and blowback from the gas-fired melt oven; this situation was corrected. A 50-piece, 10-ft^2 substrate trial run without edge seals was completed and parameters to produce parts of required thickness and density were determined. Localized thin zones occurring during the formation of the last few parts indicated that the powder drop uniformity was not being sustained. Powder drop trials conducted to isolate the problem identified that powder was bridging in the hoppers, impeding uniform powder flow to the feed brushes. Stirring devices were installed to prevent bridging, and the effectiveness of this modification was demonstrated by the successful formation of 10-ft^2 cooler holders for the first 10-ft^2 short stack. More than 600 lb of fiber/resin powder was fed to the system during processing, and powder drop uniformity was sustained throughout the run.

Substrate release difficulties encountered at the edge seal regions of the double belt press delayed the continuous formation of electrode substrates with integral edge seals. To provide substrates for 10-ft^2 electrode processing trials, 150 substrates without seals were formed on the steel conveyor with the belt press conveyor disengaged. Edge seal strips were then laminated, and the assembly pressed and cured using this conventional platen press approach.

Trials to improve substrate edge seal release were resumed. Processing conditions were adjusted to meet the density specification with active area fiber and satisfactory release was obtained. This completed definition of processing procedures required to initiate formation of substrates for the first 10-ft^2 short stack. Over 1000 trial substrates were processed to define these procedures. Figure 2-2 shows a substrate being removed from the machine.

A total of 200 10-ft^2 electrode substrates for the first 1[illegible] ft^2, 30-cell short stack were then continuously formed and pressed in one operation on the pilot substrate machine. Quality of the formed parts was excellent. Parts were heat treated and samples were submitted for full physical property characterization. All measured values compared favorably with those of conventionally formed substrates. In particular, the substrates were flat and strong, which aids in electrode processing and reduces handling scrap. Figure 2-3 compares a 10-ft^2 substrate with the smaller 2.2-ft^2 substrate.

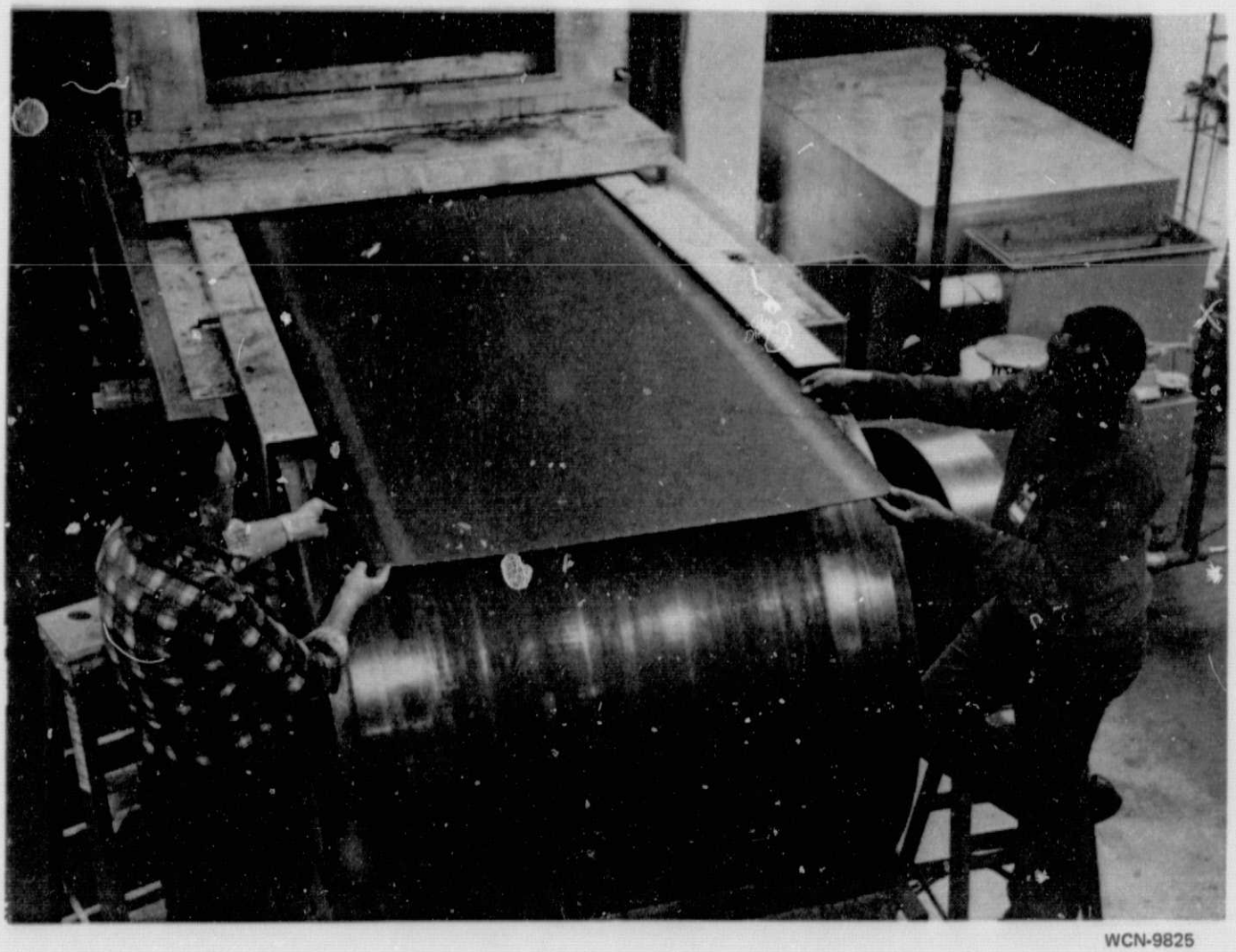

WCN-9825

Figure 2-2. 10-ft² Electrode Substrate Formed on Substrate Forming Machine

WCN-9827

Figure 2-3. Comparison of 10-ft^2, 11-MW Substrate and 2.2-ft^2, 40-kW Substrate

Work to improve the pilot forming machine was continued. A subscale powder metering device was designed, assembled, and temporarily installed within the powder transfer system to improve powder delivery rates to the powder feed hoppers. Functionality of the unit was verified. Full-scale implementation will provide automatic transport of powder to feed hoppers.

A continuous seal between the moving belts and the stationary oven frames was installed to prevent ambient air leakage into the press zone. This cooling air leakage had created a belt temperature maldistribution problem. The oven was instrumented to verify that the problem had been corrected. A spray system to automatically apply mold release to the upper press belt was installed and is now operational.

Faulty upper belt tracking and tensioning was corrected by recalibration and adjustment of the control mechanisms. A manually-activated override system was also incorporated. A more positive tracking/tensioning method was also determined and will be incorporated in the follow-on program. The feedback control system senses the position of the belt edge and steers the drive pulley accordingly.

A feedback device to automatically control powder feed rates was developed, installed, and tested on the smaller size substrate processing machine. A similar automatic powder feedback control was constructed and installed within the powder feed system of the pilot substrate forming facility. Plans are to utilize this control in the follow-on program to improve powder feed regulation, which will reduce material waste.

Carbon Fiber - An alternative carbon fiber was obtained and experimental lab-scale substrates were fabricated to the standard density. This resulted in a porosity of 64% for the alternative substrates as compared to 72% for the baseline substrates.

- The alternative-fiber substrates have a higher compressive yield and flexural strength than the baseline-fiber substrates. This is desirable from a handling point of view.
- Corrosion properties of the alternative-fiber substrate are comparable to the baseline-fiber substrate.

- Both the through-plane electrical conductivity and through-plane thermal conductivity are poorer for the alternative-fiber substrate than for the baseline-fiber substrate.
- The porosity of substrates made from the initial alternative fibers is too low to result in acceptable electrode performance.

The physical properties of the alternative fiber were acceptable, however, for a fibrous cooler holder. Cooler holders of 3.7-ft size were made from the alternative fiber on the substrate forming machine. There were no operational problems in substituting this fiber for the standard fiber. These cooler holders were hot pressed to the specification density, and then heat-treated at standard conditions. Two cooler holders were fabricated with the alternative fiber and evaluated in the first 20-cell stack, where the performance of the cooler was satisfactory.

Full-sized 3.7-ft^2 substrates were also formed from alternative carbon fiber and heat-treated to standard procedures. A 2-in. by 2-in. cell fabricated with components cut from full-size substrates was tested for 2000 hours. Performance was almost unchanged since the start of testing. The performance history at 200 ASF and ambient pressure was:

Time, hrs.	V, Cell, volts	H_2 Gain, mV	O_2 Gain, mV	iR, mV
Peak	0.600	24	85	28
2000 Hours	0.597	25	92	29

This substrate material has shown stable electrode performance but approximately 25-30 mV lower voltage than the standard fiber electrode.

The supplier then modified the fiber to reduce shrinkage during substrate heat treat processing. Excess shrinkage during heat-treating results in a substrate which is too dense; and performs poorly due to excessive diffusional losses. Lab substrates formed from this modified fiber had the increased porosity as desired, indicating that the through-plane shrinkage is relatively small. Other physical measurements indicated an improvement in thermal and electrical properties. Flexural strength decreased somewhat, but still exceeds the values obtained on substrates formed with standard fibers.

Two pairs of 2-in. by 2-in. electrodes were fabricated from the modified fiber for performance testing. The densities of these substrates were selected from the high end of allowable range, to confirm the relationship between pore structure, density, and performance. Performance of the higher density pair was at the low end of the acceptable band due to density-porosity induced diffusion penalties. The second pair of electrodes with lower density substrates started testing with initial performance at the high end of the acceptable band and completed over 1800 hours of operation on the endurance test bench. The performance of this cell was comparable to standard fiber substrates with the same catalyst lot.

The performance history at 200 ASF and ambient conditions was:

Time, hrs.	V, Cell, volts	H_2 Gain, mV	O_2 Gain, mV	iR, mV
Peak	0.616	26	82	23
1000	0.612	25	92	26
1800	0.606	24	89	27

Approximately 200 full-size electrode substrates were fabricated with the modified fiber, and substrate planform shrinkage was shown to be reduced from 7% to 2%. A 2-in. by 2-in. cell was assembled with a cathode made from the modified fiber and performance tested. The performance of this cell was comparable to standard fiber substrates with the same catalyst through 800 hours at 200 ASF and ambient conditions:

Time, hrs.	V, Cell, volts	H_2 Gain, mV	O_2 Gain, mV	iR, mV
Peak	0.646	20	76	29

Synthetic Fibers - Under the previous DOE contract, United evaluated a substrate produced from a low-cost rayon felt precursor. Under this program, commercially-available synthetic fibers were obtained, carbonized, and fabricated into substrates. This approach has several advantages over the approach evaluated in the earlier contract: (1) staple (long, chopped or discontinuous fibers) is the least expensive form of rayon fiber; (2) shrinkage of the rayon fibers will occur during carbonization of the unbonded fibers rather than during carbonization of a

formed part; (3) conventionally-densified substrate seals can be made from the carbonized rayon.

An approach to producing a carbon fiber from a rayon staple precursor was defined. Rayon staple from two suppliers was obtained and designated rayon "A" and rayon "B". Thermal gravimetric analysis (TGA) was performed after the impregnated rayon staple was heat-treated to 1000°C in a nitrogen atmosphere. The TGA results showed a carbon yield of 15 w/o for the untreated rayon, and 25 w/o to 35 w/o carbon yield for the treated samples. Treated rayon staple was carbonized, chopped, formed into a subscale substrate by the conventional process, carbonized, and graphitized to 2700°C. Results of physical properties characterization for this substrate are given in Table 2-1.

TABLE 2-1. RESULTS OF SUBSTRATE PROPERTY MEASUREMENTS

	Rayon "A" Fiber and Resin "C"	Rayon "B" Fiber and Resin "C"	Standard
Density, g/cm^3	0.42	0.47	0.57
Thru-Plane iR, mV/mil/100 ASF	0.045	0.080	0.031
Thru-Plane Thermal Conductivity, Btu/h-ft-°F	2.1	2.4	1.9
Compressive Yield Strength, psi	370	300	93
Corrosion Potential, mV	1155	1090	1180
Total Pore Spectra Porosity, %	71	66	71
Mean Pore Size, μ*	30	19	42

All samples graphitized @ 2700°C for 1 hour.

* New porosity measurements.

Electrodes were fabricated from substrates made with carbon fibers from rayon staples "A" and "B", and tested in 2-in. by 2-in. cells. Cell voltage was lower than cells containing standard substrates in all cases due to high diffusional losses attributed to the lower pore size and porosity.

The possibility of producing a low-cost carbon fiber from a phenolic fiber precursor was considered. Phenolic resins are easily carbonized, have a carbon yield of about 50%, and are commercially available.

Discussions were held with a producer of phenolic fibers who has experience with converting the phenolic fiber to a carbon fiber; the idea is technically feasible. Although the resin was cheap, the phenolic fiber was relatively expensive. This cost was equivalent to the current low-volume costs of pitch-based carbon fibers and does not include any heat-treatment processing costs. Therefore, we concluded that there was no merit at this time in pursuing carbon fibers derived from phenolic fibers.

It was concluded that the most promising candidate for near-term use would be the alternative pitch-based carbon fiber. The pitch fiber is compatible with the dry forming process and standard processing operations and is more easily adaptable when being tailored to substrate properties.

Alternative Resin - The evaluation of a modified phenolic resin system to improve shipping, storage, and in-process handling was conducted under this program. In particular, it was desired to increase the compressive yield strength of the substrates.

A family of resins with a range of melt flow properties was evaluated to determine if resin flow properties affect the physical properties of the substrates. Laboratory-size substrates made with the alternative resins were compared for selection of candidate systems for further evaluation. Full-size electrode substrates and cooler holders were formed from the selected alternative resin systems to evaluate processing characteristics and to fabricate substrates for test in demonstrator cell stacks.

Resins were obtained and lab-scale substrates were formed and heat-treated at 2700°C. The physical characteristics of these substrates were determined. Table 2-2 contains a summary of the properties of a substrate made from the four modified resins designated A, B, C, and D. It was shown that the substrates made from the modified resin had superior physical properties compared to substrates made from the standard resin. Resin "C" was selected for full-size 3.7-ft² trials.

TABLE 2-2. PHYSICAL PROPERTIES OF SUBSTRATES MADE WITH ALTERNATIVE RESINS

Physical Property	Resin "A"	Resin "B"	Resin "C"	Resin "D"	Standard
Through-Plane iR, mV/100 ASF/mil	0.018	0.016	0.017	0.017	0.031
Compressive Yield Strength, psi	125	134	157	153	93
Thermal Conductivity, Btu/h-ft-°F	3.0	3.2	4.8	3.9	1.9
Corrosion Potential, mV	1145	1195	1185	1170	1180

Approximately 200 substrates were made by the normal procedure, using the "C" resin, for evaluation in a 20-cell stack. No processing problems were identified with resin "C". In addition to these substrates, a number of experimental fibrous cooler holders were also made from resin "C". The electrode substrates and cooler holders were heat-treated to standard procedures. Six cathode substrates were used in the second of three 3.7-ft² 20-cell stack.

The resin supplier provided two additional modified resin systems, designed E and F, formulated to optimize substrate properties based on the results of this first series of tests. Lab-scale substrates were formed and the physical properties as shown in Table 2-3 were determined in comparison with resin "C" from the earlier series of modified resins. It was shown that substrates made from the modified

resin system "E" have higher corrosion resistance and significantly improved physical properties.

TABLE 2-3. PHYSICAL PROPERTIES OF SUBSTRATES MADE WITH ALTERNATIVE RESINS

Physical Property	Resin "C"	Resin "E"	Resin "F"
Through-Plane iR, mV/100 ASF/mil	0.017	0.023	0.023
Compressive Yield Strength, psi	157	145	158
Thermal Conductivity, Btu/h-ft-°F	4.8	4.6	4.7
Corrosion Potential, mV	1185	1210	1160

Using modified phenolic resin "E" approximately 400 3.7-ft^2 size electrode substrates and cooler holders were formed and heat-treated to the standard procedures. Physical property measurements taken on these full-size substrates confirm earlier subscale data which showed improved thermal conductivity, compressive yield, compressive modulus, and corrosion potential. These substrates were used in the third 3.7-ft^2 20-cell technology verification stack.

Cell stack test data has confirmed that electrode and cooler holder substrates formed with the modified resin system "E" and standard fibers exhibit improved properties. In addition, the "E" resin has advantages in raw material shipping, storage and in-processing handling. Consequently it was used in all subsequent electrode and holder substrates fabricated under this program.

2.2 ELECTRODE PROCESSING

Objective

The objective of this task was to continue the development of the ribbed substrate electrode for higher temperature and pressure operation, and to develop the process technology for fabrication of large area electrodes that reduce cost and meet functional, performance and endurance goals. The approach was to continue work on improvements in the cell matrix, wet seal and electrode processing technology initiated in earlier programs and to scale the fabrication process to 10 ft^2.

Summary

A cell matrix configuration that increases cross-pressure tolerance by a factor of 3 was successfully incorporated.

A lower cost "dry mix" catalyst formulation was incorporated that produced comparable performance to the standard "wet mix" formulations. Two advanced catalysts were scaled from laboratory processes and incorporated into the shop process to produce full-size electrodes. These advanced catalysts, the above "dry mix" catalysts and improved matrix were incorporated and tested in electrodes of the second and third 3.7-ft^2, 20-cell technology verification stacks.

Progress was made in the development of processing techniques for electrode fabrication. Procedures to develop a faster substrate wettability treatment, improved dry mix catalyzation, increased machining rate, and a stable matrix ink were completed in this program and verified in the four 3.7-ft^2 short stacks of 20 and 30 cells.

Scale-up of these techniques to a large area cell was accomplished by developing equipment to fabricate 10-ft^2 electrodes for verification in a 10-ft^2, 30-cell technology development stack.

Discussion

Improved Matrix - The objective of this task was to increase the capability of the matrix to resist higher gas breakthrough pressures. Matrices containing finer silicon carbide (SiC) were first evaluated in a program conducted under Electric Power Research Institute Agreement RP842-5, demonstrating a bubble pressure of 20 psi. This compares to a bubble pressure of 7 psi for the standard SiC. Effort under this program focused on improving the processing characteristics of the finer SiC and on producing a defect-free matrix.

Matrix curtain-coater inks were then formulated with the fine-particle SiC slurry and trials were conducted to evaluate the integrity of the matrix ink curtain. Problems were encountered in maintaining a stable matrix ink curtain. Gaps and tears would occur in the curtain after less than one hour of use. These problems were attributed to the formation of foam and fine bubbles in the matrix ink.

Curtain coater inks were then formulated with various surfactants and at different viscosities to prevent foam formation. Various trials were conducted, howev none produced a stable curtain or uniform matrix coverage.

An evaluation was then made of a matrix ink made from a mixture of two different particle sizes of SiC. A stable curtain and a uniform matrix coverage were obtained with this mixture of silicon carbide. Bubble pressure tests on samples containing 30% fine SiC show a 60% increase in breakthrough pressure over that of the standard matrix. Figure 2-4 shows the breakthrough pressure as a function of matrix composition.

The investigation of an alternative source of low cost silicon carbide was initiated to reduce material costs. Quantities of this material in different particle sizes were procured which meet purity and particle size distribution requirements. Matrix trials will be run on this material under the follow-on program.

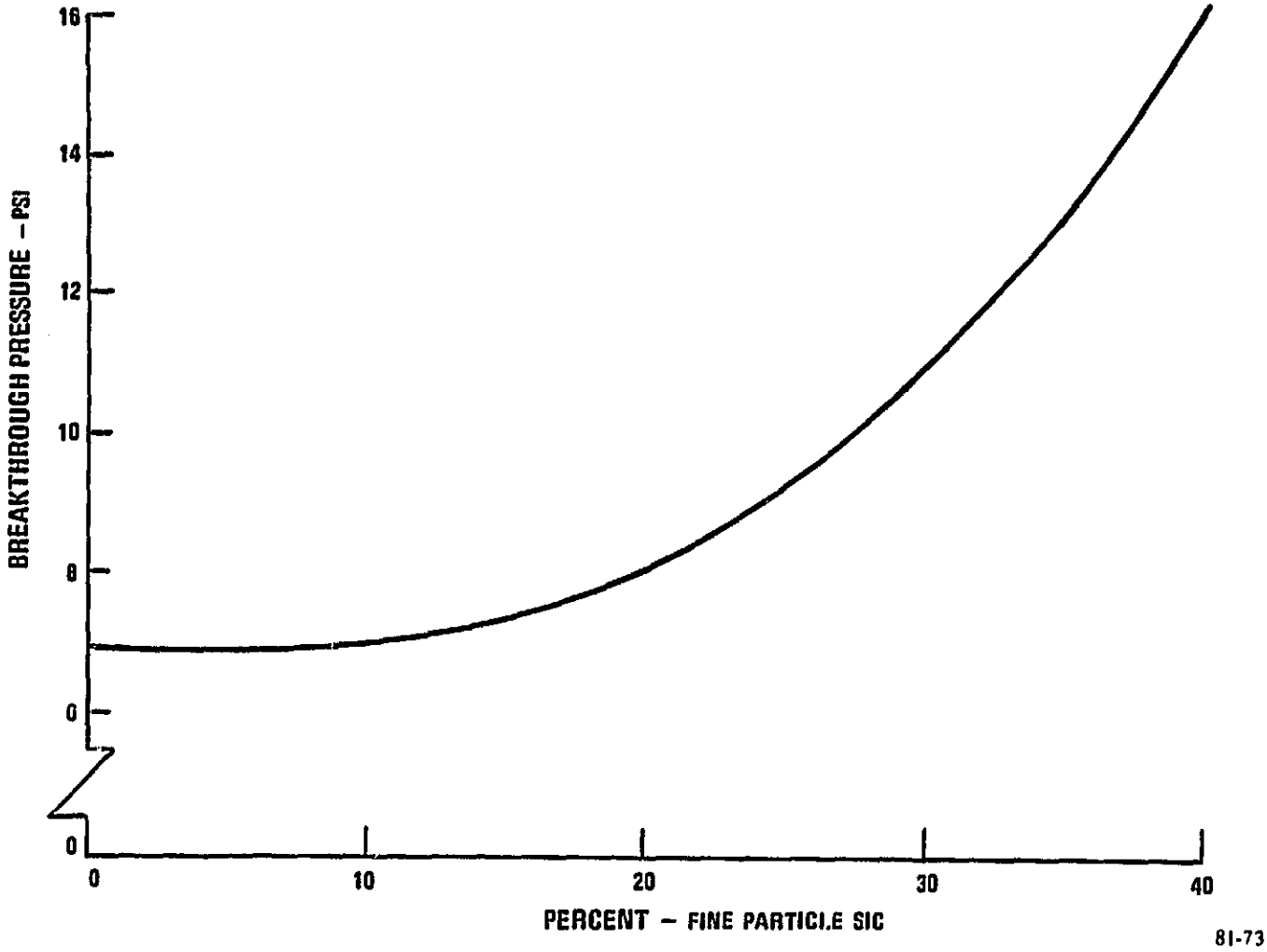

Figure 2-4. Matrix Cross-Pressure

Investigations conducted under this task have resulted in the identification and formulation of an increased breakthrough pressure matrix. This matrix has been incorporated into the fabrication of electrodes and evaluated in the thrid and fourth stacks.

Dry Mix Catalyst Processing - The purpose of this effort was to optimize a procedure for the fabrication of dry mix electrodes which will substantially lower processing and material costs. The baseline catalyst process uses a wet mix procedure which is time consuming and labor intensive. The dry mix process (U.S. Patent 4,17[illegible],159) produces a material suitable for use in a catalyst layer of a fuel cell electrode.

Both anodes and cathodes were fabricated by the dry mix process. Investigation of the catalyst layer indicated that particle size is in the proper range and well dispersed throughout the structure. Laboratory testing was carried out to optimize process conditions to achieve best electrode performance.

Subscale 2-in. x 2-in. electrodes were tested and evaluated against a standard catalyst structure. The dry mix anodes performed in a manner similar to the standard anodes, when tested at 375°F, 14.7 psia, 200 ASF, as shown in Table 2-4.

TABLE 2-4. ANODE PERFORMANCE COMPARISON

Electrode Type	H_2 Gain, mV
Dry Mix	20-29
Standard	23-29

Dry mix cathodes also were evaluated with two levels of Teflon and compared to standard electrodes prepared from the same catalyst batch also with two levels of Teflon. An ambient performance comparison at 200 ASF is shown in Table 2-5.

TABLE 2-5. CATHODE PERFORMANCE COMPARISON

Electrode Type	% Teflon	RL-1*/Air, volts	H_2/Air iR Free, volts	O_2 Gains, mV
Dry Mix	A	0.600	0.685	87
Standard	A	0.596	0.685	78
Dry Mix	B	0.558	0.644	94
Standard	B	0.575	0.660	90

*See Page 1-20

These data indicate that the dry mix electrode has initial performance comparable to a standard electrode at the A Teflon level. At the B Teflon level, the structure becomes too hydrophobic, as shown by the lower performance.

At this point work on dry mix catalyst processing was transferred to another contract, GRI 5080-344-0405. Development work done on this contract was used to process dry mix electrodes for the large area 10-ft^2 size electrodes. Several dry mix anodes and cathodes were processed for evaluation in the first 10-ft^2 30-cell short stack.

Electrode Processing for the Four 3.7-ft.^{2} Stacks - The objective of this effort was to scale advanced catalyst and catalyst layer application procedures from laboratory size to full size and test these on electrodes in short stack tests. Sufficient components for short stack testing at temperatures up to 405°F and pressures up to 120 psia were produced.

The first advanced catalyst to be transferred from laboratory scale to the shop fabrication process was designated C3B-17. This catalyst was chosen for its improved performance.

Electrodes for the first 3.7-ft^2 20-cell stack were processed with the major objective of evaluating the performance of scaled-up GSB-17 cathode catalyst. The anodes contained NOCAN™ catalyst. The anode substrates were all treated to improve wettability, U.S. patent 4,219,611, and contained a densified edge seal with backside interfacial seal. The cathodes had the same substrate and seal features, but different catalysts. Approximately one-third of the cathode substrates were catalyzed with the standard GSA-6 catalyst. These cells served as controls for comparative purposes. The remainder were catalyzed with the GSB-17 catalyst. One-half of these GSB-17 electrodes were made on cathode substrates treated to improve wettability. This treatment to improve wettability also facilitates acid filling at stack assembly.

Stack test results showed that some of the anodes which were tested opposite GSB-17 cathodes performed poorly. Analysis of these cells showed that the cause of the poor performance was that electrolyte had been preferentially transferred from the cathode substrate. A review of subscale (2-in. x 2-in.) endurance cell data also showed that a number of cells constructed with GSB-17 cathode catalyst exhibited the same anode sensitivity as seen in this stack.

Another experimental cathode catalyst, GSB-15, which had been tested on the endurance bench from laboratory prepared samples, did not exhibit this phenomenon. Consequently this catalyst was scaled-up to the shop process and full-size electrodes were fabricated. Subscale, 2-in. x 2-in., samples of these electrodes were tested to evaluate acid transfer from cathode to anode. The GSB-15 electrodes, with a 40% electrolyte fill of the substrate void volume, showed stable performance. At 120 psia test conditions, performance levels were 15 to 20 mV above the performance goal after 900 hours of testing.

Based on these results from the first short stack it was decided to test the GSB-15 cathode catalyst in the second 3.7-ft^2 20-cell short stack at an electrolyte fill of 30%. This avoids the electrolyte transfer from cathode substrates to anode substrates experienced in the first short stack. Projected stack life (acid availability) at future power plant conditions and with 30% electrolyte fill is greater than 40,000 hours.

This 20-cell short stack (# 2) contained five GSA-6 cathodes as controls. The cells with GSB-15 cathode catalyst used cathode substrates treated to improve wettability. Half of the experimental GSB-15 cells contained the improved SiC matrix formulation which has better processing stability and five cathode substrates were fabricated with the modified resin.

Initially this stack met the performance goal, but the decay in performance with time exceeded the goal allowance. Endurance testing of subscale samples of the same electrodes shows a similar performance decay with time as explained further in Section 3, Cell Stack Demonstration.

The third 3.7-ft^2 20-cell short stack was fabricated with GSB-15 cathode catalyst of increased Teflon content. The standard NOCAN™ catalyst was used on the anode. Both anode and cathode substrates were fabricated with the modified "E" resin, which provides increased substrate strength and better stability during substrate fabrication as discussed in Section 2.1. Both the anode and cathode substrates were treated to increase wettability and the matrix was composed of a mixture of fine-particle and standard-particle silicon carbide for increased breakthrough pressure resistance. A subscale (2-in. x 2-in.) verification cell cut from one full-size electrode gave the following performance at 120 psia and 372 ASF as a function of time.

Time	Cell Voltage, V	E-Line Goal, V	H_2-Air Performance, V
Initial	0.728	0.698	0.819
1000	0.712	0.670	0.811
2000	0.699	0.668	0.787

Substrates for the fourth 3.7-ft^2 30-cell short stack were fabricated with the modified "E" resin and all substrates were treated to increase wettability. To further increase electrode stability the Teflon level of the GSB-15 cathode catalyst was increased above that used in the third short stack. A more stable anode catalyst, HYCAN, was also used. The matrix contained a blend of fine and standard size silicon carbide for increased gas breakthrough pressure resistance.

Two subscale (2-in. x 2-in.) cells fabricated from the electrodes processed for this 30-cell stack were endurance tested. Performance at 200 ASF, 120 psia, 400°F, and 85/70 fuel/air utilization as a function of time was:

Build #	Hours	Cell Voltage, volts	E-Line, volts
6245	1508	0.772	0.762
	3700	0.746	0.756
	5529	0.743	0.754
	6128	0.741	0.753
	6983	0.732	0.752
6243	1665	0.750	0.761
	3840	0.720	0.756
	5686	0.716	0.754
	6214	0.724	0.753

10-ft² Electrode Processing - The purpose of this effort was to develop the process technology for fabrication of large area electrodes and construct electrodes for the first 30-cell short stack test. A new electrode processing facility capable of handling these larger electrodes was constructed.

A catalyst application machine capable of depositing catalyst on 10-ft² electrode substrates using the UTC dry application process was designed and fabricated. The finished machine is shown in Figure 2-5. The entire device is mounted on a movable carrier for ease of installation into an electrode processing line.

Catalyst deposition trials run on over 150 electrodes verified that a uniform deposit with good edge definition is obtained across the entire 10-ft² electrode substrate. This was confirmed by measurements taken of catalyst layer thickness and Pt loading at eight locations on the electrode. Catalyst waste was reduced from a value of 20% on an older machine to less than 2% on this device.

A UTC supplied oven was used to process the 10-ft² electrodes. Temperature uniformity within the oven is important to insure electrode catalyst uniformity. Temperature profiles were measured with an instrumented plate run through the oven. Side to side and front to back temperature variances were measured and found to vary no more than ±5°F which is acceptable.

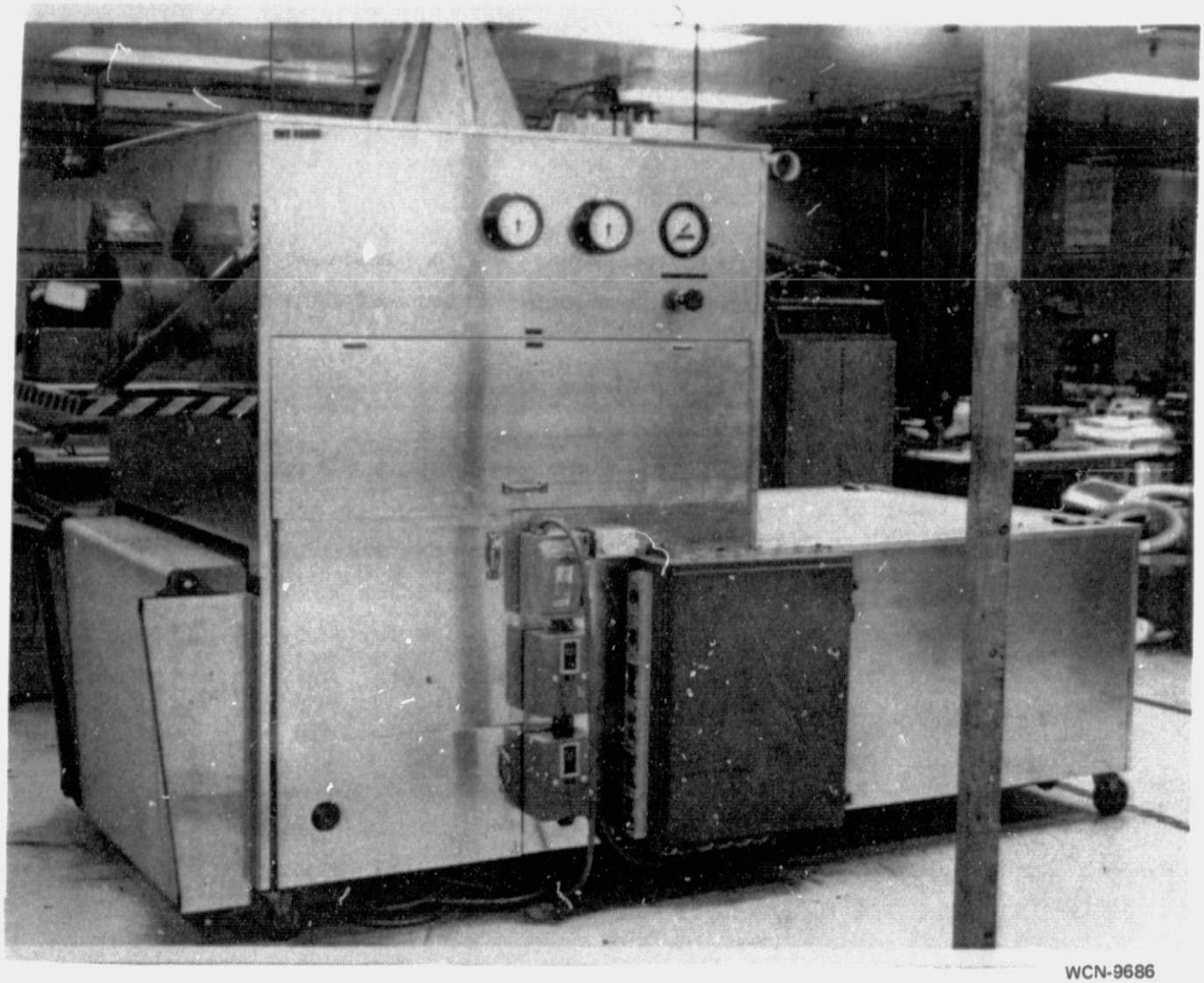

WCN-9686

Figure 2-5. Catalyzation Machine

The design and fabrication of an arbor and cutters to machine gas-flow fields into 10-ft^2 electrodes was completed along with a redesign of the milling machine to accommodate the 10-ft^2 electrode. Flow field machining of these electrodes was accomplished by machining each electrode in two passes. Trials were run on over 150 full-size parts, and thickness checks at 64 locations on an electrode indicate that both anode and cathode dimensions were within specification.

Vacuum pickup devices were fabricated and used in handling electrodes during the machining process step. This equipment was used in handling over 150 trial parts.

A semi-automatic device to apply interfacial backside seals and manifold flow divider seals was fabricated. The machine can apply both of these materials to the electrode simultaneously. It also has the capability to transport the coated part directly to the drying oven.

A UTC-supplied curtain coater was used for matrix application along with a UTC-supplied screen printer for fillerband application and a UTC-supplied dry line oven.

Electrode processing for this first 30-cell 10-ft^2 short stack occurred without any major difficulties in any of the processing steps. Electrode processing scrap was 16.7%, which was lower than expected due mainly to the high strength and flatness of the substrates. Substrates were fabricated with the modified "E" resin and all substrates were treated to increase wettability. The anode catalyst was the HYCAN formulation and the cathode catalyst was GSB-18. Both dry mix anodes and cathodes were processed along with the standard wet mix electrodes. The matrix was a blend of fine and standard particle size silicon carbide.

Two subscale (2-in. x 2-in.) cells fabricated from the electrodes processed for this 30-cell stack were tested on the endurance bench. One set was made by the standard wet mix method and the other by the dry mix catalyst process. Performance at 200 ASF, 120 psia, 400°F, and 85/70 fuel/air utilization was:

Build #	Type	Hours	Cell Voltage, volts	E-Line, volts
6266	Wet Mix	690	.763	.767
6267	Dry Mix	689	.758	.767

2.3 SEPARATOR PLATE DEVELOPMENT

Objective

The objective of this program was to improve separator plate technology and to scale this technology to larger plate areas to reduce cost and meet functional and performance goals. The approach was to investigate alternative material compounding, transfer compression molding, smaller particle size and higher purity graphite and shorter heat treating cycles in 3.7-ft^2 planforms. Successful results were incorporated in scaling the molding process to 10 ft^2.

Summary

An alternative material compounding method succeeded in improving the uniformity of the graphite-resin mixture that produced defect-free plates. Powder clean-up equipment and procedures were identified that also improved plate quality and yield. The molding process with these improvements was scaled to 10 ft^2 and produced plates for a 30-cell short stack test. A 20% shorter carbonizing cycle was tested and found acceptable for further development.

Discussion

Alternative Material Compounding and Transfer Compression Molding - Separator plates in the ribbed-substrate stack are flat plates formed from powder and resin by compression molding, and then heat-treated to produce the required physical properties. Initial activity addressed the problems of pits and holes developed in molded separator plates during the carbonization step. These defects were attributed to resin-rich areas in the graphite resin mixture prior to molding. An vendor proprietary alternative method of compounding the graphite/ resin mixture was selected for evaluation.

In addition, another activity addressed was an alternative molding process that showed potential for process cost reductions. This process, called transfer - compression molding or transfer molding, simplifies the process by utilizing only a single material preform but requires more complex equipment.

The initial material compounding trials were conducted using laboratory-scale equipment. Small quantities of molding compound were produced by this method. This material was of good quality and twenty-one 3.7-ft^2 plates were then molded by the transfer-compression molding process. The trial plates were microground to uniform thickness and then carbonized. Visual examination after carbonizing showed the plates to be almost totally free of defects which shows the alternative compounding technique to be effective in eliminating local resin-rich areas. A pattern of waviness was present that appeared related to flow of material during molding from the center of the plate radially outward to the edges. The amplitude of the waviness was not large (10 to 20 mils), and the plate flattened out completely during graphitizing. The physical properties of these plates were fully characterized. Selected property measurements are listed in Table 2-6 and compared to properties obtained for a typical compression-molded plate. The data show that plates molded by the transfer-compression method are equivalent to compression-molded plates.

TABLE 2-6. COMPARISON OF COMPRESSION AND TRANSFER-MOLDED SEPARATOR PLATE PROPERTIES

Property	Compression Molded	Transfer-Compression Molded
Flexural Strength, psi	6300	6400
Thermal Conductivity, Btu/h-ft-°F	53	57
Corrosion Potential, mV	1200	1235
Open Porosity, %	5.5	4.7
Density, g/cm^3	1.82	1.77

Visual inspection after graphitizing, however, showed these plates to contain a higher number of surface defects (small blisters and pits). The cause appears to be foreign material contamination which volatilized during graphitizing. Analyses showed traces of an iron-base material in the defects, and the most likely source of the contaminant is the graphite powder. This is discussed later in this section.

The objective of the alternative compounding method was to improve the uniformity of the graphite-resin mixture and thereby minimize resin-rich areas in the plates. Resin-rich areas can result in localized cracks when the resin shrinks during carbonizing. The fact that al plates molded in this program were free of defects after carbonizing demonstrates the effectiveness of the alternative method in producing uniform material. Based on these results, the alternative compounding method is considered a significant improvement over the standard method, and was incorporated into subsequent processing.

Smaller Particle-Size Graphite - Another approach evaluated to improve separator plate quality is the use of a smaller particle-size graphite powder. Preliminary work conducted prior to this program with 6-in. x 6-in. laboratory scale plates showed that finer powders improve strength and density. Molding compound was prepared from finer-particle graphite powder using the alternative compounding technique and two groups of fifty each, 3.7-ft^2 separator plates incorporating these features were molded. One group contained the smaller particle size graphite powder and the other group contained the standard graphite powder to serve as a control. Compression molding was chosen to minimize the number of variables being evaluated in the trial.

The two groups of plates were processed through carbonizing and graphitizing. After carbonizing, visual inspection showed that all plates were completely free of pinholes and other defects. Some waviness, confined to the plate edges, was present in both groups. The waviness that developed during carbonizing was eliminated during graphitizing, but edge cracks developed in about 30% of the plates with fine-particle graphite. The physical properties of the plates from

each group were fully characterized. These data are shown in Table 2-7. Properties of a standard plate that was processed at the same time are also shown for comparison. The data show that the properties of the experimental plates are slightly better than those of the standard plate. Plates from this trial were used for the second 20-cell short stack.

TABLE 2-7. COMPARISON OF ALTERNATIVE COMPOUNDING AND SMALL PARTICLE-SIZE GRAPHITE SEPARATOR PLATE PROPERTIES

	Standard Plate	Alternative Compounding	Alternative Compounding Small-Particle Size Graphite
Flexural Strength, psi	5900	6300	7500
In-Plane Electrical Resistivity, ohm-cm	0.002	0.002	0.002
Corrosion Potential, mV	1200	1200	1205
Open Porosity, %	5.5	5.0	5.9
Density, g/cm^3	1.82	1.82	1.83

Edge Waviness Trails - A series of five separator plate molding trials was conducted to determine whether variations in the molding process would reduce the tendency for plates to develop waviness during carbonization. The primary molding parameter investigated was the preform placement pattern in the mold since earlier work indicated this was a factor in plate flatness. Several preform patterns were utilized and approximately twenty plates were molded using each pattern. Most of these trials were conducted using molding compound prepared with the standard grade of graphite powder. One group of parts was also molded from fine-particle graphite powder using the preform pattern that appeared best from the trials with standard

material. Dimensional quality of the plates was documented after molding and microgrinding and revealed minimal effect on as-molded plate waviness.

Separator plates were provided for the third and fourth 20-cell short stack. These plates were made from molding compound which was processed by the alternative compounding method. High-purity graphite powder of the standard particle size was used and the plates were formed by compression molding. The separator plates were heat treated using standard procedures.

Graphite Powder Purity - It was concluded from previous activity in this program that the graphite powder was not consistently and sufficiently pure to ensure high plate yields. While lot sizes, processing equipment, and other parameters were examined, powder analysis indicated that the material could be cleaned of significant impurities with conventional processing equipment. The equipment and procedures to provide the required graphite powder cleaning were implemented and successfully demonstrated in concurrent programs. All work to develop the 10-ft^2 separator plate was conducted using the "clean" graphite powder as the standard material.

Lower Cost Carbonizing - The objective of this effort was to investigate shorter carbonizing cycles as a means of reducing separator plate cost. Trials were conducted to determine the feasibility of a shorter separator plate carbonizing cycle. A group of fifty 3.7-ft^2 plates was carbonized using a cycle 20% shorter than the standard cycle which is 172 hours long. These plates were then graphitized and characterized. The properties are shown in Table 2-8 and compared to those of standard plates. The data show the properties to be equivalent except that flexural strength is at the lower end of the range obtained on several lots of plates with standard processing. The difference in flexural strength is not considered significant and the shorter carbonizing cycle is a candidate for future consideration.

TABLE 2-8. COMPARISON OF STANDARD AND SHORTER SEPARATOR PLATE PROPERTIES

	Shorter Carbonizing Cycle	Standard Processing
Flexural Strength, psi	5900	6300 (5900 - 6600 range)
Flexural Modulus, psi x 10^6	1.1	1.1
In-Plane Electrical Resistivity, ohm-cm	0.002	0.002
Corrosion Potential, mV	1200	12( )
Density, g/cm^3	1.82	1.82

Development of Large-Area Separator Plates - The objective of this effort was to demonstrate the feasibility of forming and heat treating large area experimental separator plates, and to provide plates for the first 10-ft^2 short stack.

The initial approach was to form the large-area plates by pressing the graphite/resin molding compound between readily available flat plattens without edge constraint. Molding compound preform size, spacing, and other mold parameters were varied in the first mold trial and 50 separator plates were formed. The molding compound used was processed by the alternative method from standard resin and "cleaned" graphite powder to minimize the possibility of defects in the larger plate. Mold parameters were found to be consistent with those used to form smaller separators. A 10-ft^2 as-molded separator plate is compared to a 3.7-ft^2 separator plate in Figure 2-6.

Carbonization was conducted in two runs with half the molded parts in each run. The initial carbonizing run employed an oven cycle, approximately two times longer than the standard cycle. Plate density and flatness were satisfactory. The second run, conducted at the standard cycle developed for 3.7-ft^2 plates, also yielded satisfactory parts. The density and flatness of all plates were within criteria

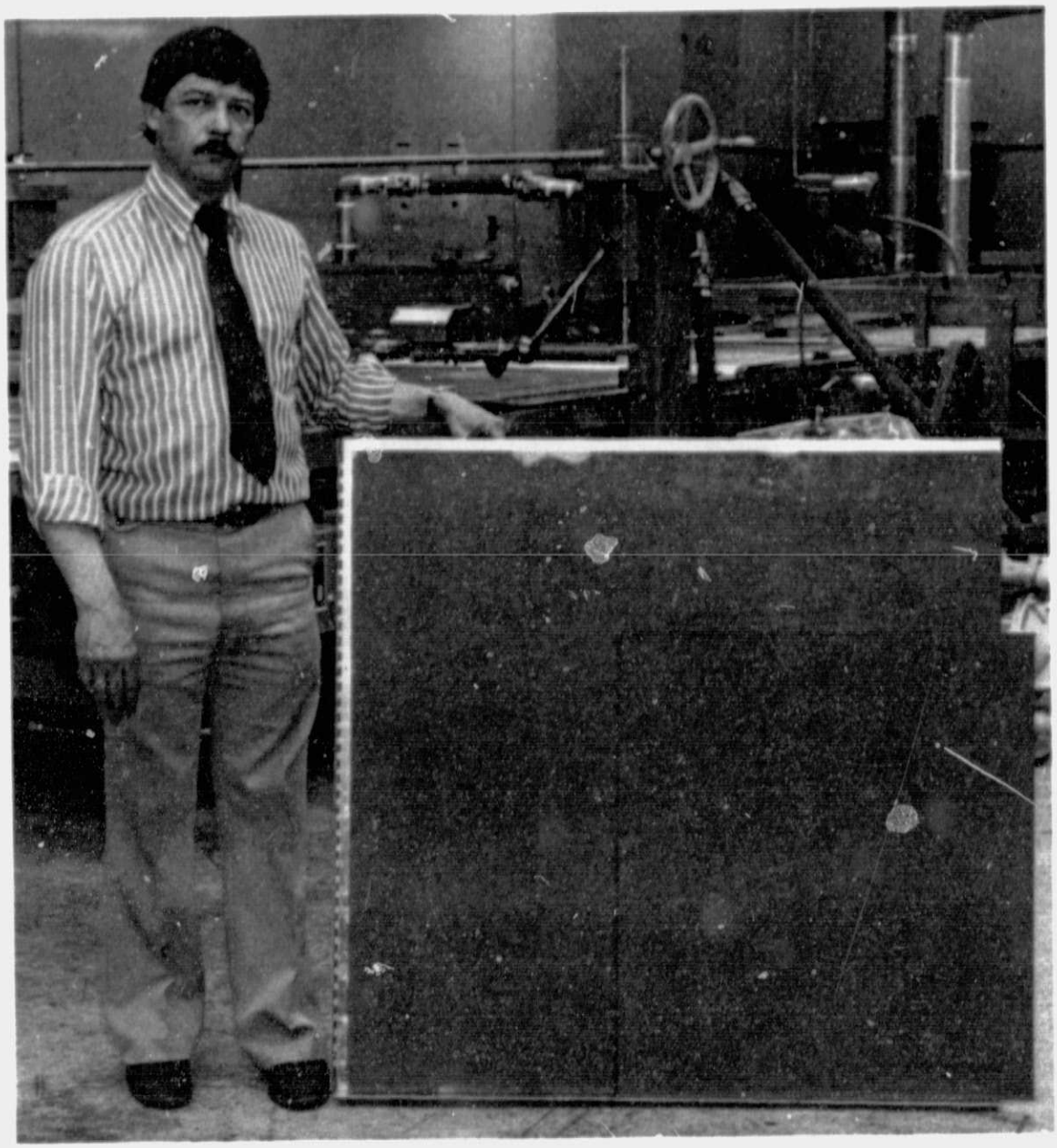

(WCN-10212)

Figure 2-6. Comparison of 10-ft^2, 11-MW Separator and 3.7-ft^2, 4.8-MW Separator

and 28 plates were selected for graphitization. Of the 28 graphitized plates 24 were cracked after graphitization. A majority of the plate cracks originated at an edge and propagated into the plate. Excluding these cracks, the plates were flat, with no blisters, pits, holes, or porous areas. Density, flexural strength, and flexural modulus met requirements, and dimensional shrinkage during heat-treat was as expected.

A second molding trial of 10-ft^2 separator plates was conducted to determine the cause of the excessive plate cracking experienced in the initial trial. One hundred plates were molded with the standard graphite and resin materials compounded by the alternative process on production-size equipment. Plate molding parameters were consistent with those of the first trial.

Samples from separator plates molded with flat plattens in the second 10-ft^2 plate trials were analyzed in detail for density, resin content, flexural strength, and flexural modulus to identify any irregularities in molding. The data have shown that average values of the plates measured are nominal, but with variations larger than desired. Modulus and resin content variations were significant, indicating that the resin and graphite had separated. Molding in this manner requires long material flow paths to make up for the material flowing outward to the unconfined edges, causing the resin and graphite to separate since they flow at different rates. It was then judged that the edge cracking was caused by the high internal stress generated by differential shrinkage rates existing within the plate.

Plates from this lot were then ground to thickness and carbonized without the edge cracking typical of plates from the first mold trial. Overall plate shrinkage was typical of the smaller 3.7-ft^2 plates, which generally excluded heat-treat temperature or cycle as a likely cause of the edge cracking.

Plates formed in the initial molding trial were also trimmed for heat-treat by scribing the plate along the trim line, and then snapping off the excess. To eliminate the possibility that this practice could also cause micro-cracks and

crack propagation under the thermal stress of subsequent heat-treat, plates from the second trial were trimmed by machine.

Following graphitization at standard conditions, eight of the ten plates processed to this stage had edge cracks. The approach for subsequent mold trials was to fabricate a new separator plate cavity-type mold to provide the necessary edge constraint and eliminate graphite and resin separation. A fabricator for the new 10-ft^2 separator plate mold was selected, the mold design was reviewed and approved, and fabrication and assembly of the mold was completed.

A trial was initiated to mold 200 separator plates of 3.7-ft^2 planform as part of the development program to evaluate the new 10-ft^2 mold design and also investigate ways to reduce separator material costs. These 3.7-ft^2 plates were formed in a scaled version of the 10-ft^2 mold design and established the initial forming parameters and flow characteristics for the subsequent 10-ft^2 plate forming. Additional activities included the evaluation of industrial graphite screening and impurity separation processes, material accountability step-by-step through plate molding, and the molding of thinner plates with the high purity material. These activities will be continued in a follow-on program.

From these trials, molding procedures were established and a first run of 150 plates of 10-ft^2 planform were molded. Samples were then obtained from a representative cavity molded plate for comparison with the plates formed earlier by simple pressing between flat plattens. As expected, the range of measured densities was much narrower for the cavity molded plates at 1.56 to 1.60 gm/cm^3 as compared to simple pressed plates which ranged from 1.42 to 1.60 gm/cm^3. These data indicate that the material flow towards edges has been properly controlled in the cavity mold.

Plates from this first 10-ft^2 plate forming trial with the cavity mold were ground to thickness and carbonized. Visual inspection of the plates after carbonizing revealed material "knit lines" evident as a change in surface coloration, which indicates incomplete meld of the preforms during molding. The plates were also

abnormally thick in the center; this confirmed that the condition is a result of excessive press deflection, which allows the material to begin curing before reaching the required molding pressures. A representative sampling of these plates was graphitized with a 70% yield. Physical property measurements were obtained for these plates with particular attention to flexural strength across the "knit lines". Selected property data, listed in Table 2-9, are compared to properties obtained for typical 3.7-ft^2 plates. The data indicate that flexural strength, modulus, thermal conductivity, electrical resistivity, and corrosion potential are acceptable and typical of smaller planform separator plates. The flexural strength and modulus measured across and along the "knit lines" do not vary significantly from average plate values.

TABLE 2-9. PROPERTIES OF 3.7-FT^2 AND 10-FT^2 SEPARATOR PLATES

	3.7-ft^2 Plate	10-ft^2 Plate
Flexural Strength, psi	5900	5934
Parallel to Knit-Line		6621
Perpendicular to Knit-Line		5513
Flexural Modulus, psi (x 10^6)	1.1	1.08
In-Plane Electrical Resistivity, ohm-cm	0.002	0.007
Corrosion Potential, mV	1200	1180
Typical Density	1.80	1.75

A second 10-ft^2 separator plate molding trial was completed using another press with inherently less deflection, and 300 plates were successfully molded. The deflection of this press under load was minimal, so the thick centers encountered during the initial mold trial were eliminated. No "knit lines" were detected under these molding conditions, indicating that the desired material flow and preform meld were achieved.

2.4 COOLER DEVELOPMENT

Objectives

The objectives of this task were to improve cooler thermal performance, reduce component and assembly costs, improve reliability, and to design and fabricate coolers for 3.7-ft^2 and 10-ft^2 stacks.

Summary

Thermal performance of the cooler assembly was improved by increasing the cooler tube diameter from 1/8 in. to 3/8 in., incorporating a clamshell cooler holder, and using cooler holders with a higher thermal conductivity. These changes allowed the number of cells served by one cooler to be increased from four to eight. Further improvement was accomplished by replacing the conventional cooler configuration requiring many tube connections with a serpentine cooler requiring significantly fewer tube connections.

Reliability of the cooler array was improved by increasing the thickness of the Teflon coating from 5 to 10 mils, incorporating chafe guards on the tube bends, developing a dry dielectric test for inspection of the final assembly, and minimizing the number of connections via use of the serpentine cooler. The ability of the cooler holder to prevent acid transfer to the cooler was improved by laminating a Teflon film between the cooler holder and the separator plate, using a cooler holder with a larger mean pore size than the electrode substrates, and using four-sided solid seals on the cooler assembly.

Cooler assemblies were fabricated for four 3.7-ft^2 stacks and the first 10-ft^2 stack. As they became available the above technology components were incorporated into the various stacks.

Discussion

Background - The cooler assembly consists of a metallic cooler array to contain the two-phase water coolant, a Teflon coating on the metal to prevent corrosion, and a cooler holder assembly which provides good thermal transport between the cells and cooler array as well as protection from acid. Development activity described in this section is presented in terms of these components. Cooler assemblies fabricated for each of the five stacks represented the state-of-the-art at the time they were made.

Cooler Array Configuration - At the start of this contract the cooler array for a 3.7-ft^2 cell consisted of 1/8-in. diameter copper tubes with extruded PFA (perfluoralkoxy-Tetrafluoroethylene) coating for corrosion protection, uncoated stainless steel headers, and mechanically-crimped connectors to join the tubes to the headers. The emphasis in this program was to improve the cooler array by simplifying the configuration and increasing the number of cells per cooler.

Heat transfer testing in a parallel GRI program showed that it was feasible to increase the number of cells per cooler by increasing the diameter of the cooler tube. An increase in diameter from 1/8 in. to 1/4 in. permits the number of cells per cooler to be doubled (from four to eight for a 3.7-ft^2 cell). The use of the larger diameter cooler tube made it feasible to replace the standard cooler configuration with a serpentine cooler configuration as shown in Figure 2-7. This cooler configuration contains no headers whereas the standard 3.7-ft^2 cooler contains two headers with 32 connections (see Figure 2-8). The combination of a simpler cooler array and more cells per cooler resulted in a simpler and cheaper configuration with improvement in reliability. The first, second and third 3.7-ft^2 stacks built under this program contained the conventional cooler configuration. The fourth 3.7-ft^2 stack was built with a 1/4 in. two-element serpentine cooler.

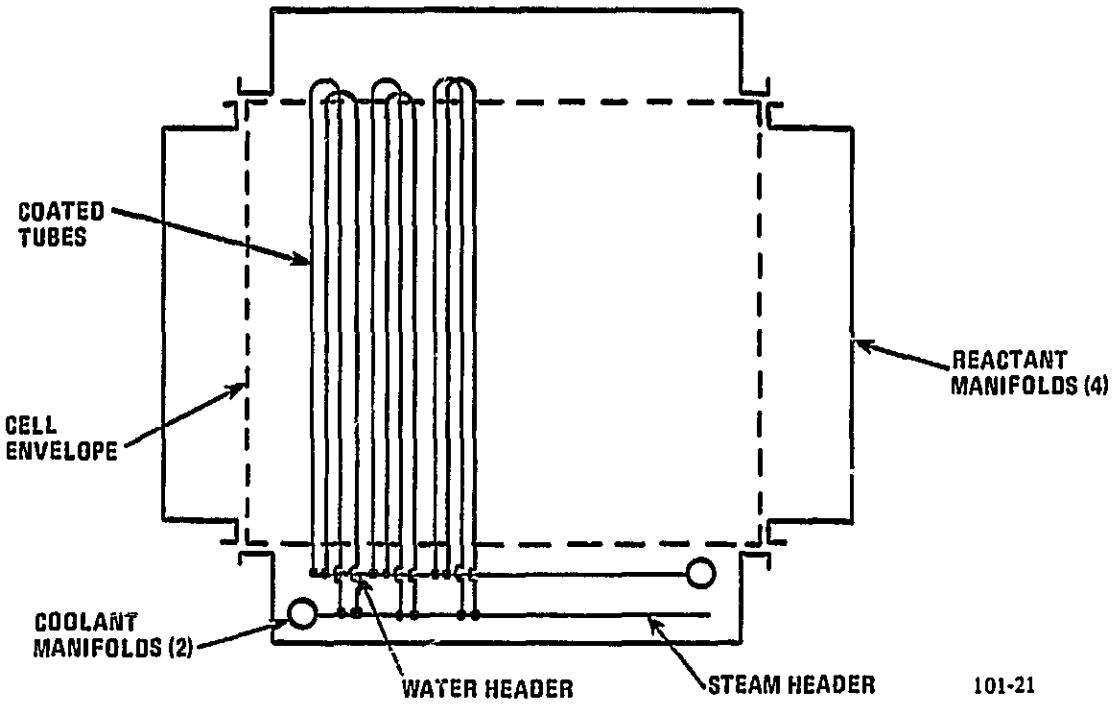

Figure 2-7. Schematic of Standard Cooler

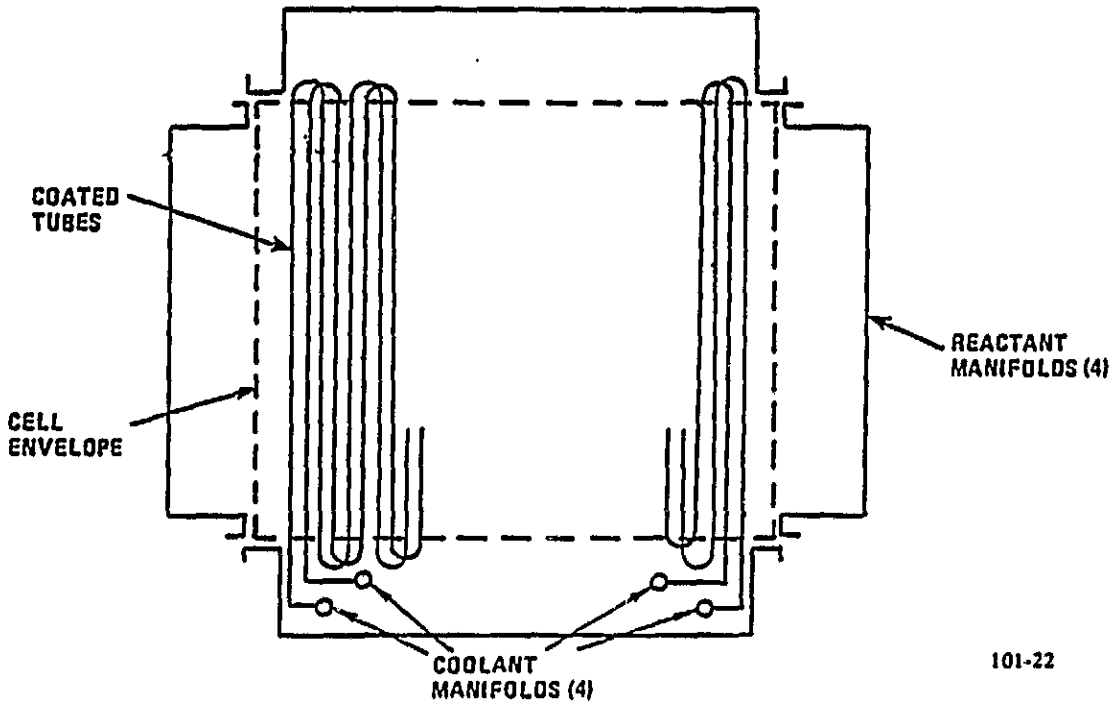

Figure 2-8. Schematic of Serpentine Cooler

A two-element serpentine cooler was designed for a 10-ft^2 stack. It was necessary to increase the tube diameter from 1/4 in. to 3/8 in. to obtain reasonable velocities and pressure drops. Each element contains 24 passes with a nominal pitch between tubes of 1.6 inches. The configuration and fabrication process were scaled successfully from the 3.7-ft^2 planform. The appropriate tooling and fixtures were fabricated and trials were conducted to prove out the fabrication process. Cooler assemblies for the first 10-ft^2 stack were fabricated.

Since the stainless steel cooler headers in 3.7-ft^2 stack tests show little corrosion, the feasibility of using a bare stainless steel cooler array with no dielectric coating was evaluated. Elimination of the dielectric coating would lower cost and improve heat transfer. A stainless steel cooler array fabricated to the standard configuration but with no dielectric coating was tested in the second 20-cell stack to determine the corrosion resistance of bare stainless steel under realistic cell stack conditions. The uncoated cooler failed after 700 hours of testing due to corrosion of an exposed tube. The failure occurred at the edge of the stack. The corrosion of the cooler was not extensive at locations other than the stack edge. The stainless steel manifolds had virtually no corrosion after the 700-hour test. It was concluded that an uncoated stainless steel cooler is not acceptable with the normal cooler configuration. However, a bare stainless steel cooler is viable with the totally encapsulated cooler concept under development in the On-Site Technology Program.

Cooler Array Coating - The conventional cooler arrays at the start of the program included copper tubes which contained an extruded nominal 5-mil PFA coating for corrosion protection. Thicker coatings of PFA and co-extrusions of PFA and Tefzel® (TFE-E copolymer) were evaluated under this program to improve durability. Tefzel® has a higher impact and abrasion resistance than PFA. Cooler tubing with the co-extruded coating and the standard PFA coating was subjected to thermal, electrical and mechanical testing. The results of thermal cycling from room temperature to 400°F, followed by dielectric testing in acid electrolyte up to 1000 volts, showed the co-extruded coating to be no better than equivalent to the standard PFA coating. Mechanical abrasion testing was conducted according to the

procedure of SAE test number ARP 1536. This test did not show any improvement for the co-extruded coating over the standard PFA, since both coatings withstood 3000 cycles to failure in the abrasion test. The conclusion is that each separate layer of the co-extruded coating is too thin to have properties that are representative of the bulk material; and that this co-extrusion is not an improvement.

Coolers with thicker PFA dielectric coating to improve reliability were evaluated. Cooler tubing with a nominal 10-mil coating, which is twice the standard thickness, was subjected to the same mechanical abrasion test described above. The thicker coated tube withstood 16,000 cycles to failure compared to 3,000 cycles for the standard coating. The increase in abrasion resistance is attributed to a higher quality extruded coating in addition to the increased thickness. These 10-mil PFA coatings were successfully extruded on 1/8-in., 1/4-in., and 3/8-in. copper tubing. The thicker coating resulted in an immediate improvement in manufacturing yield by eliminating defects which resulted in failures during dielectric testing. Coolers for the first and second 3.7-ft^2 stacks were fabricated with 5-mil coatings. Coolers for the third and fourth 3.7-ft^2 stack and the first 10-ft^2 stack were fabricated with 10-mil coatings. Testing showed that the thicker coating increased the thermal resistance of the standard cooler assembly by about 35%. This increase was offset by incorporation of the two-piece clamshell cooler holder, described later, which reduced thermal resistance by 30%.

A program was started to investigate the addition of carbon fillers to the standard extrusion coating for cooler tubing with the objective of doubling the thermal conductivity. Two candidate compositions to increase the thermal conductivity of the coating were selected for further evaluation. Both compositions project to a two-fold increase in thermal conductivity with melt flow properties compatible with extrusion coating. This effort will continue under the follow-on program.

A 4000-volt dry dielectric test was developed to identify pinhole defects in the PFA cooler tube coating. This test was used on cooler assemblies made for the third and fourth 3.7-ft^2 stack and the first 10-ft^2 stack. It is effective in preventing defective coolers from being used in stacks.

The cooler tube bends which extend beyond the planform of the cooler holder are subject to possible damage during fabrication and stack assembly. A piece of shrink tubing was placed on these exposed bends to act as a chafe guard to minimize the possibility for accidental damage to the PFA coating.

Cooler Holder Assembly - The conventional cooler holder consists of a one-piece fibrous substrate made from the same material as the electrode substrates, but with a higher density for improved thermal conductivity. The concept of a two piece clamshell holder for improved heat transfer was evaluated. Methods to prevent acid transfer to the cooler assembly were developed. Improved cooler holder materials were defined.

In the conventional design used at the start of this program, only 50% of the tube surface was in direct contact with the cooler holder. An alternative configuration with a two-piece holder that completely surrounds the cooler tube was evaluated to decrease the thermal resistance between these components. Thermal performance testing was conducted on a two-piece clamshell cooler configuration in a heat transfer rig. Data from the thermal test rig showed that this two-piece assembly has a thermal resistance about 30% lower than that of the standard one-piece configuration. This result was subsequently confirmed by stack testing. Thermal testing was conducted at 30-psi and 12-psi axial loads to simulated stack conditions before and after initial axial load loss. Thermal performance was the same at both loads. A resistance test showed no significant penalty across the two-piece assembly at loads down to 12 psi. The two-piece configuration was used in the cooler assemblies fabricated for the third and fourth 3.7-ft^2 stacks and the first 10-ft^2 stack.

Construction of the cooler holder assembly was modified also to minimize the potential for contact between the cooler array and the acid in the cells. A method of laminating the cooler holder to the separator plate with an FEP film was developed under the parallel NASA/DOE On-Site Technology Development Program and was applied in this program.

This approach will improve reliability by preventing acid transfer caused by wicking through the separator plate and/or evaporation - condensation between the surface of the separator plate and the cooler tube. The pore size of the cooler holder was increased to make it larger than that of the electrode substrate, which is the reverse of the conventional configuration. This will lead to a further improvement in reliability by eliminating a driving force for acid transfer by wicking from adjacent cells. The cooler assembly edge seal was changed from a two-sided solid seal configuration to a four-sided solid seal configuration using commercial grade graphite strips. This reduces the cross-sectional area at the edge of the cooler holder available for acid transport by wicking and by flow of acid-saturated fuel through the cooler holder. Cooler assemblies for the fourth 3.7-ft^2 stack and the first 10-ft^2 stack were fabricated with these features.

Several variations in the fibrous cooler holder were evaluated. The thermal conductivity of the fibrous cooler holder was doubled by a change to a modified phenolic resin as explained more fully under Section 2.1 Substrate-Processing.

The technology improvements and cooler features evaluated in short stack tests are shown in Table 2-10.

TABLE 2-10. COOLER FEATURES EVALUATED IN SHORT STACK TESTS

Feature	Stack				
	3.7-ft² #1	3.7-ft² #2	3.7-ft² #3	3.7-ft² #4	10-ft² #1
Tube OD, in.	0.125	0.125	0.125	0.250	0.375
Coating Thickness, in.	0.005	0.005	0.010	0.010	0.010
Configurations Header Type (H) or Serpentine (S)	H	H	H	S	S
Tube Pitch, in.	0.590-1.298 avg 0.757	0.590-1.298 avg 0.757	0.590-1.298 avg 0.757	0.656/0.680	0.800
Cells/Cooler	5	5	4	8	8
Nom. Design ΔT, °F	75	75	50	50	50
Stack Operating Pressure, psia	50 and 120	120	120	120	120
Cooler Holder Config. One Piece (1) or Clamshell (CS)	1	1	CS	CS	CS
Bumpers	No	No	Yes	Yes	Yes
Cooler Holder Pore Size Rel. to Cell Pore Size	Smaller	Smaller	Smaller	Larger	Larger
Interfacial FEP Film	No	No	No	Yes (0.005 in)	Yes (0.005 in)
Resin in Cooler Holders (1) Standard (2) Modified	1	1	2	2	2

2.5 NON-REPEATING PARTS DEVELOPMENT

Objective

The objective of this task was to identify lower cost approaches for fabricating selected non-repeat cell stack hardware. Specific components and processes addressed were the reactant manifold seals and stud-welding of coolant manifold feeder tubes.

Summary

Improvements were demonstrated in material preparation and assembly of reactant manifold seal frames through simplified design and simpler tooling with no penalty to component quality and performance. Additional improvement was judged achievable through the use of stud welding as a manufacturing process for joining coolant manifold feeder tubes to the manifold. Tests of configurations fabricated by this method demonstrated the integrity of the bond.

Discussion

Simplified Reactant-Manifold Seal. The objective of this task was to reduce the time required to fabricate the reactant manifold seal frame. The approach taken was to simplify the seal frame design to reduce labor through simpler detail fabrication, and to simplify tooling to reduce setup time. Trials to fabricate the seal frame assembly successfully demonstrated reductions in all aspects of material preparation and seal frame assembly. It was concluded that the improved design was acceptable for power section use.

The seal frame configuration was redesigned under this program to simplify the corner joint, and to simplify the tooling and setups required to fabricate the assembly. The simplified seal frame configuration is shown in Figure 2-9 in comparison with the first generation design. Both designs employ Teflon materials for dielectric separation between the cell stack and the reactant manifolds, and

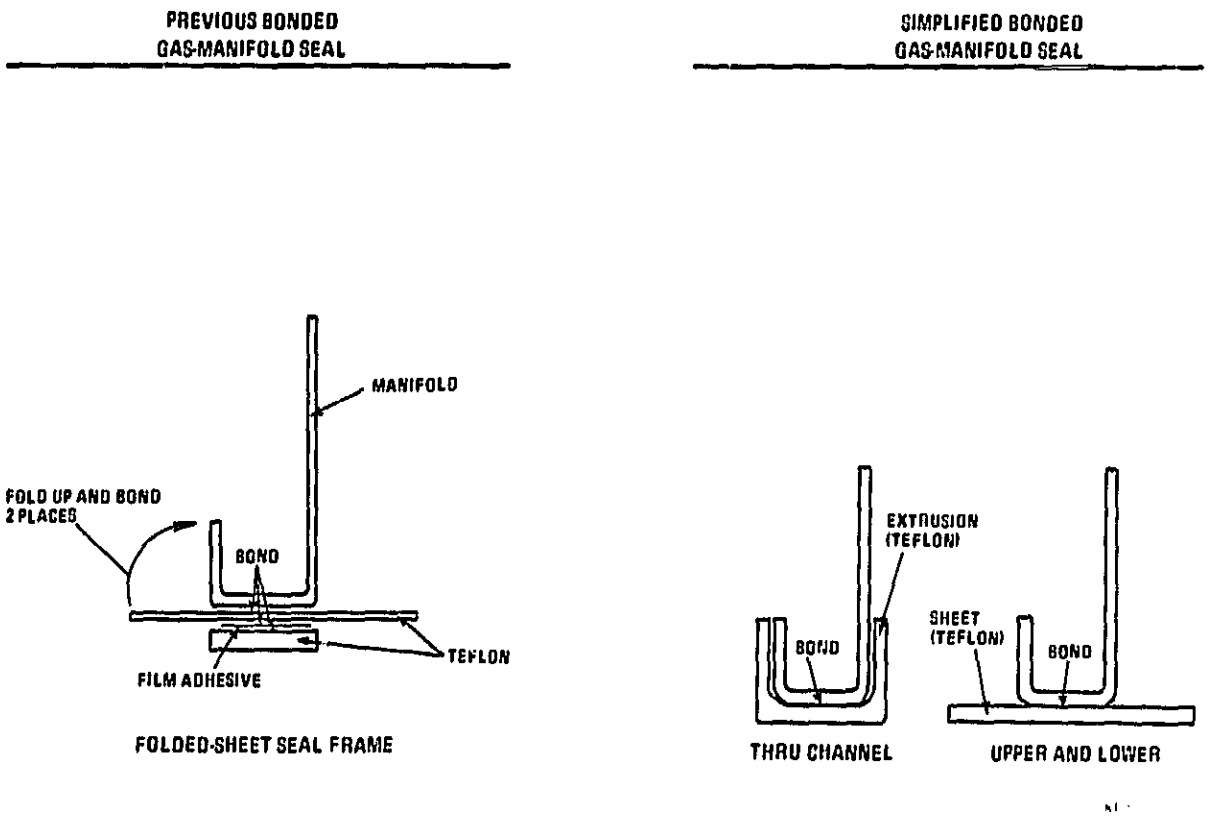

Figure 2-9. Seal Configuration Cross-Section

consist of a foot and sidewalls. The foot is used in combination with a conformable gasket to bear against the cell stack and distribute the seal loads. The sidewalls provide the required dielectric length between the cell stack and the metal manifold. The major feature of the simplified design is the substitution of an extruded "U"-channel shape with preformed sidewalls, which eliminates the tooling required to form and bond sheet material into sidewalls. The extrusion also combines the two pieces of sheet material required to form the sidewalls and foot into a single finished shape, and eliminates the extra bonding operation required to join the two sheets. The complexity of folding and overlapping materials in the corners was eliminated by substituting a simple butt joint at those locations.

Technically, the tasks of joining Teflon seal details to each other and to the metal ducting were successfully demonstrated in earlier programs, and the procedure has been employed in both full-size and short-cell stacks. These seal-frames were tested at power plant operating conditions and fulfilled all technical requirements. There was no separation or loosening of the joints noted through 8200 hours of this testing, and no change in leakage was attributable to the bond. In addition, the bonded frame successfully passed dielectric breakdown tests in a full-size power section when tested to Underwriter Laboratories Specification UL-795. Activity under this program was directed at maintaining the integrity of this design, while simplifying the configuration.

The initial effort was directed toward the fabrication of a seal frame that is integral with the reactant manifold. The conceptual advantages of the integral, or bonded seal, frame are:

- Elimination of the costly gas seal material required between frame and manifold in "loose" frame assemblies.

- Verification of frame dielectric and leakage integrity prior to assembly on the cell stack.

- o Simplification of installation of the seal-frame on the cell stack.
- o Bond of Teflon seal details strengthened by locking all details in place and minimizing thermal expansion to the levels of the steel manifold.
- o Provision of handling protection for the manifold corrosion coating.

Tooling to fabricate an integral seal frame was designed and fabricated to provide a simple setup and loading surface, where pre-cut seal frame details and a reactant manifold would be positioned and clamped together for oven bonding, as shown in Figure 2-10. The loading system, which is not shown, provided the required bonding pressure. Full-length manifolds were selected for these trials to eliminate scaling effects.

The initial oven-bonding trial of a simplified seal design was completed, and results support the technical feasibility of this approach. Heating of the clamped assembly successfully bonded all Teflon details to each other, and to the manifold. The Teflon-to-Teflon bonds were excellent. However, the Teflon-to-metal bond had only moderate to poor adhesion due to an oxide buildup on the bare metal manifold used in this trial. Standard PFA-coated manifolds were used in subsequent trials to eliminate this problem. Clamping loads during bonding were sufficient to maintain the required bonding pressure throughout the oven cycle, but some Teflon extrusion was noted. The carbon steel plate against which the seal frame bears during bonding was stiffened to improve the load distribution in later trials.

Fixes implemented to improve adhesion and eliminate extrusion were successfully demonstrated during the second oven-bonding trial or the simplified seal design. The major remaining deficiency was tearing in the sheet stock material due to material dimensional instability. As shown in Figure 2-11, the tearing observed in the first two trials initiated at the outside edge of the sheet material and ran inboard along the inner edge of the butt joint. Concurrent materials testing had shown that the sheet stock grew when heated, which suggested that the tear was a result of excessively high loads on the butt joint during oven-bonding. Tearing

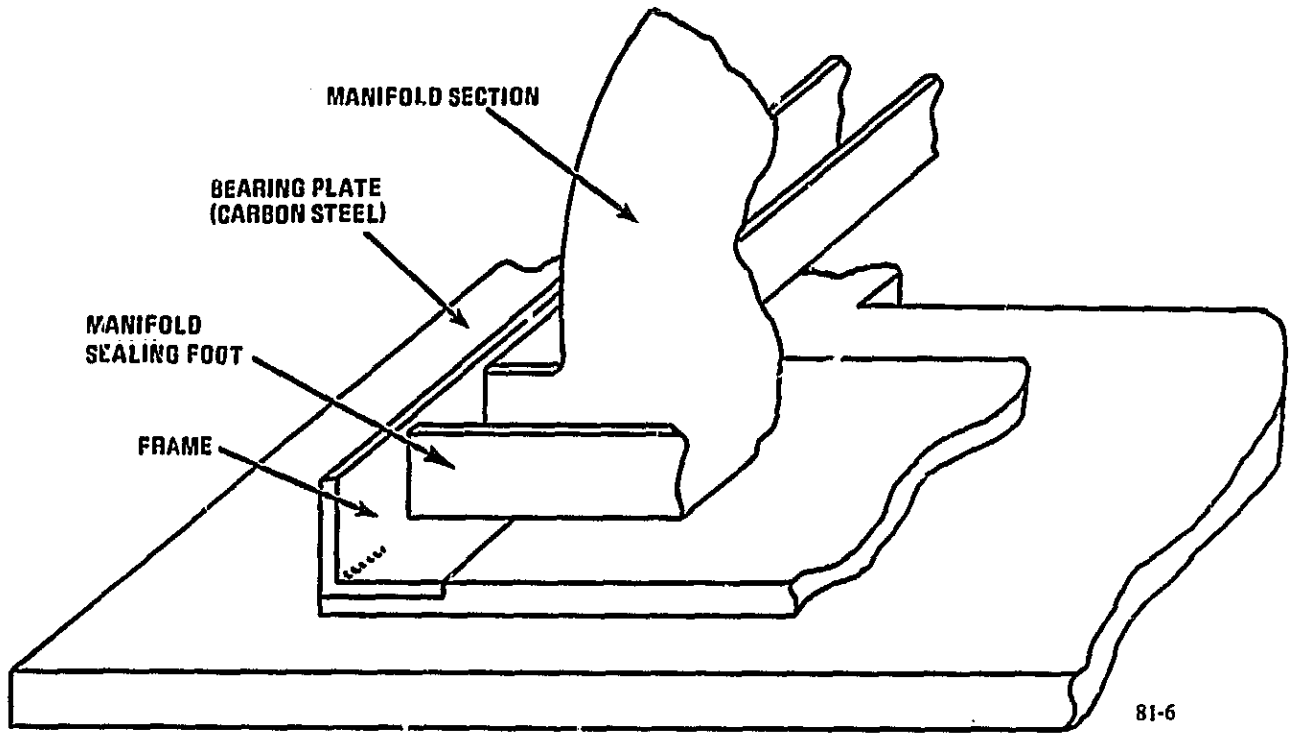

Figure 2-10. Seal Frame Configuration 1

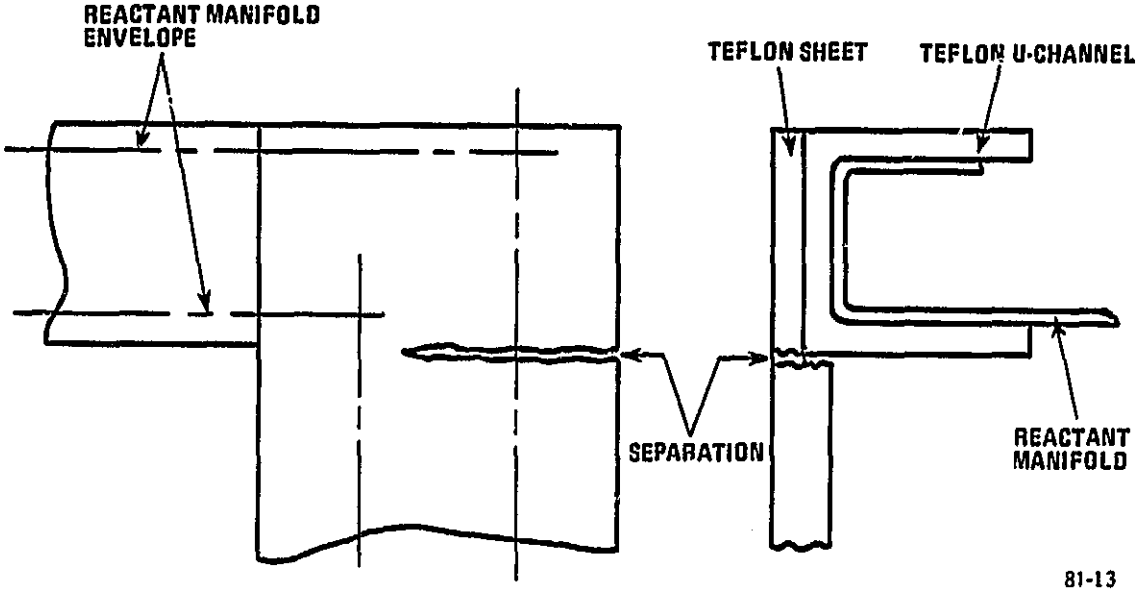

Figure 2-11. Seal-Frame Separation

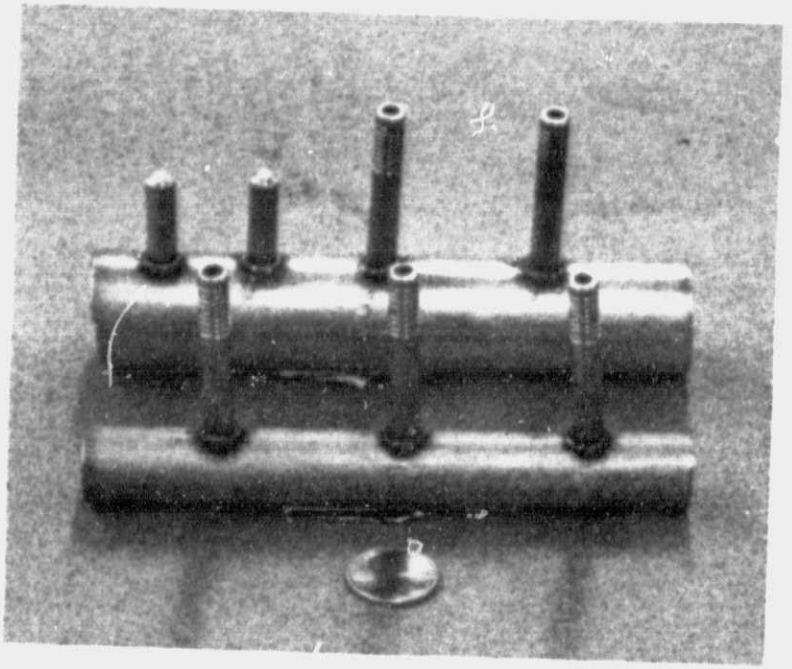

(WCN-8536)

Figure 2-12. Manifold Samples

was most likely to have occurred during cooldown, when the unrestrained outer edge of the sheet material cooled and began to shrink.

A series of tests was then conducted to identify a commercially available Teflon sheet material with better dimensional stability. Materials with controlled dimensional properties were obtained and tested to the ANSI/ASTM D3292-78 procedure at the oven-bonding temperature for comparison with the material specification against the original material. Two candidate materials were selected for additional oven-bonding trials based on test performance and cost. The change in length of both materials exceeded the purchase specification, but the change was only half that of the original materials. In addition, pre-test heat-treatment was shown to be effective in reducing the measured change in half again.

An oven-bonding trial employing one full-size sheet of each of the two candidate materials was completed, at conditions reproducing those of the earlier trials. The oven-bonding of these materials was completed without tearing or indication of duress in the critical area. Oven-bonding of a final full-size trial assembly using dimensionally stable material was also completed without tearing.

Oven-bonding of the final full-size trial assembly concluded the activity to develop a lower cost reactant manifold seal. In the course of this activity, fabrication parameters were defined for surface preparation, material pretreatment, and bonding requirements. The latter item included the determination of seal frame cold loading, load follow-up material encapsulation for dimensional control during thermal cycling, and oven requirements. It was concluded that the simplified seal frame meets all technical requirements.

Stud-Welding of Coolant Manifold Tubes. Stud-welding was investigated as a lower cost manufacturing process for joining coolant manifold feeder tubes to the manifold. Stud weld rods were joined to short sections of coolant manifolds to define fabrication and inspection procedures (see Figure 2-12). A full-length manifold was then fabricated to demonstrate the feasibility of this approach. All operations were satisfactorily developed to fabricate leak tight, structurally sound coolant manifolds that provide the required flow distribution. It can be

concluded that the stud- welded manifold is satisfactory for operational verification in a full-size cell stack assembly.

Stud weld rod was joined to short sections of a coolant manifold in the initial development phase to determine the basic fabrication and inspection procedures. Welding equipment and weld parameters were defined from these samples, which were then machined to form the coolant flow-control opening. Preliminary tooling requirements were also defined for the operations which include fixturing for alignment, feeder tube indexing, welding, hole machining and deburring.

The samples were leak tight in hydrostatic testing at three times the maximum system pressure. Microscopic examination of the feed tube and manifold cross-section revealed satisfactory weld penetration and no weld porosity that might reduce the structural strength of the assembly, or provide a leakage path. A micrograph of a typical cross-section detailing a tube-to-manifold weldment is shown in Figure 2-12. Cross-sectioning also indicated that the flow-control opening was within dimensional requirements and that burrs were satisfactorily removed.

Tooling to fabricate a full-length manifold was designed and constructed to simulate production processes. Longer sample sections were fabricated on this set-up to verify procedures determined from the initial trials and to confirm that the tooling achieved the required feeder tube spacing and alignment with the manifold. Pressure test, microscopic examination of weld cross-sections, and dimensional inspections were all satisfactory and final procedures were established.

Full-length stud-welded coolant inlet and exit manifolds were fabricated using the procedures and tooling determined from the trials in scale. Both manifolds were free of bowing or other distortion due to weldment; this is attributable to the short heat cycle inherent with this weld system. Hydrostatic pressure test of the completed assemblies indicated that one feeder tube with incomplete weldment and repair was made by conventional welding, without distortion to the feeder tube or

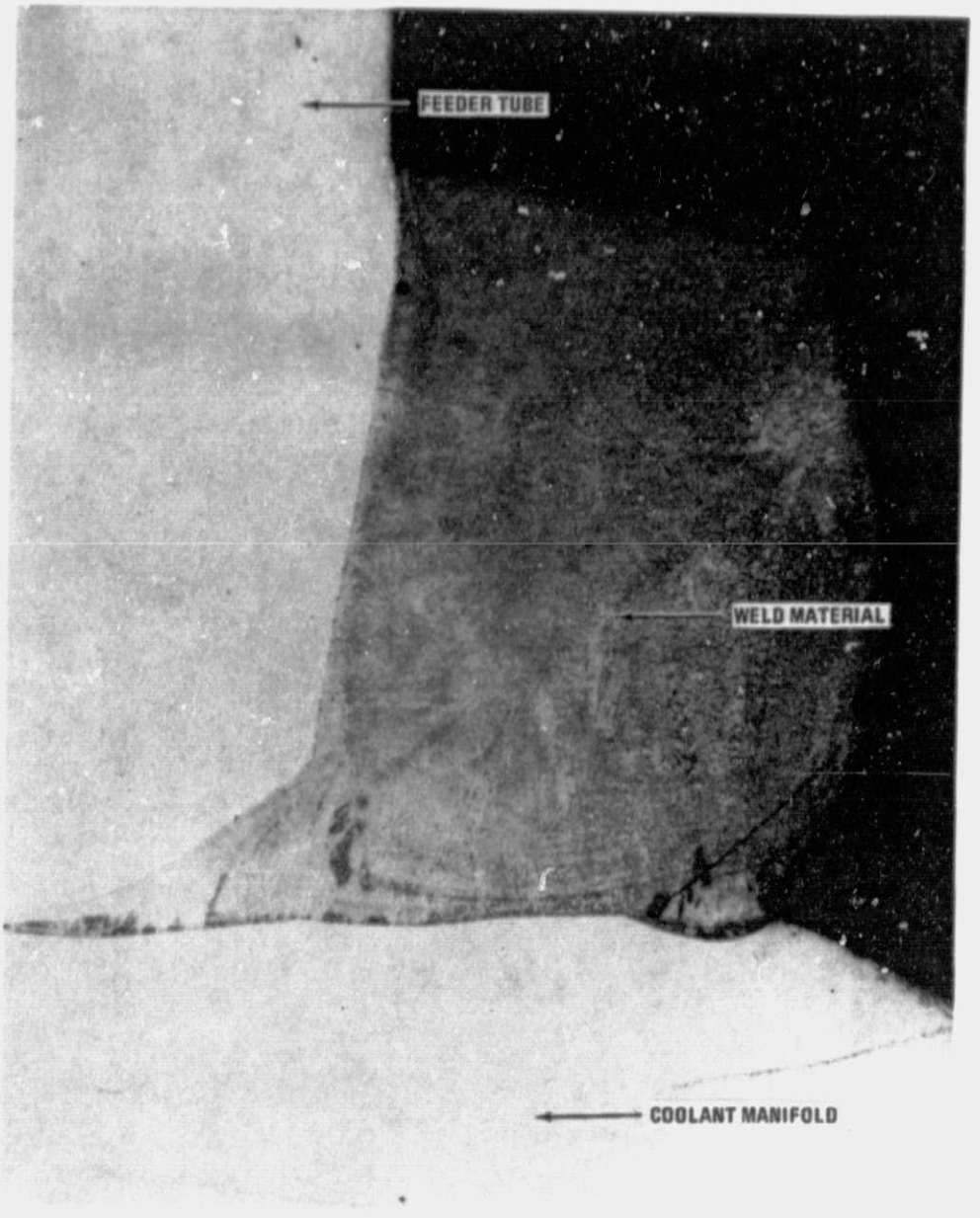

Figure 2-13. Cross-Section of Stud-Welded Feeder Tube

manifold. Flow tests of the assemblies at simulated power plant conditions indicated that the flow rates from tube to tube were uniform and within specification, which concluded this activity.

SECTION 3

CELL STACK DEMONSTRATION

Task 3 of Contract DEN3-191 was directed at demonstrating, in short stacks of full planar area cells, the technology improvements from the Task 2 development efforts in full-size short stacks. Catalysts tested and recommended in Task 1 were used for the cathodes. The approach for the initial effort was to build and test 3.7-ft^2 active area short stacks of 20 and 30 cells. The last stack built was the first with a 10-ft^2 active area using 10-ft^2 components scaled and fabricated in Task 2. Cell stacks were tested at the 120 psia, 405°F conditions contemplated for future fuel cell power plants. This section discusses the four short stacks built and tested under this contract.

Objective

The objective of this task was to demonstrate in short stack tests the functional and performance capability and the endurance characteristics of cell stack components developed in previous tasks. The short stack of full-size cells contains sufficient repeating components to provide a proper simulation of the operating parameters of a full-height cell stack.

Summary

In this contract four short stacks with a 3.7-ft^2 ribbed substrate cell configuration and one short stack with a 10-ft^2 ribbed substrate cell configuration were assembled and tested. The combined total test time accumulated on these stacks was 11,775 hours.

Four short stacks containing cells of the 3.7-ft^2 ribbed substrate configuration were assembled and tested. The first two short stacks were assembled, tested for 350 hours and 1525 hours, respectively, and then disassembled for a post-test analysis of the stack components. The third and fourth stacks were assembled and

endurance tested, for 5400 hours and 4500 hours, respectively. These last two stack tests will be continued in a follow-on program. The first 10-ft^2 short stack was assembled and testing initiated; this testing will be completed in a follow-on program.

These stack tests have demonstrated the functionality of the ribbed substrate cell and materials configuration at 120 psia/405°F conditions in 3.7-ft^2 and 10-ft^2 planform. Initial catalyst performance attained the E-line goal in full-size stack hardware. Durability was demonstrated to 4500 and 5400 hours respectively in two 3.7-ft^2 stacks.

These stacks were operated at 120 psia reactant gas pressures and 405°F average cell temperatures. The cell operating conditions were at current densities, reactant utilizations and load profiles that correspond to future power plant operating conditions. An endurance goal of at least 1500 hours was established for each stack. Other test objectives include the definition of the following cell and stack operating parameters.

- Performance over a range of power levels.
- Cell and stack performance stability.
- Reactant gas utilization effect on performance.
- Reactant gas cross-pressure tolerance.
- Reactant gas leakage rates.
- Stack internal resistance.
- Stack compressive axial load.
- Cell electrolyte inventory.

Discussion

First 3.7-ft^2 Short Stack (20-Cell) - The special features contained in this stack included the following:

- Fifteen cells with GSB-17 cathode catalyst and five cells with the baseline GSA-6 cathode catalyst.
- Electrode substrates with integral edge seals.
- Separator plates fabricated by transfer-compression molding.
- Cooler assemblies with cooler holders fabricated from alternative carbon fibers (two coolers), extruded protective coating on the tube array and graphite cover plate for improved electrolyte management.
- Five cells per cooler, four coolers per stack.
- Two-pass reactant gas flow paths.
- Cell electrolyte volume nominally 40% full at the beginning of life.
- Initial stack compressive axial load of 30 psi.

The objectives that were accomplished with this stack can be summarized as follows:

- Operation at 50 and 120 psia reactant pressures.
- Operation at 405°F average cell temperature.
- Performance evaluation of GSB-17 cathode catalyst.
- Acceptable reactant gas leakage rates.
- Acceptable stack internal resistance.
- Stack compressive axial load reduction was documented.

This stack was operated at both 50 psia and 120 psia reactant gas pressures. It was the first stack to be operated at 120 psia reactant gas pressures and 405°F average cell temperature. The performance comparison of the GSB-17 cathode catalyst cells to the GSA-6 cathode catalyst cells is shown in Figure 3-1. This figure also compares the performance difference between operation at 50 psia and 375°F and at 120 psia and 405°F, and shows the superior performance achieved with the GSB-17 cathode catalyst cells. However, the cell performance stability of the GSB-17 cathode catalyst cells was not typical of the baseline cells with GSB-6 cathode catalyst. Figure 3-2 presents the cell performance history of this stack. Diagnos-

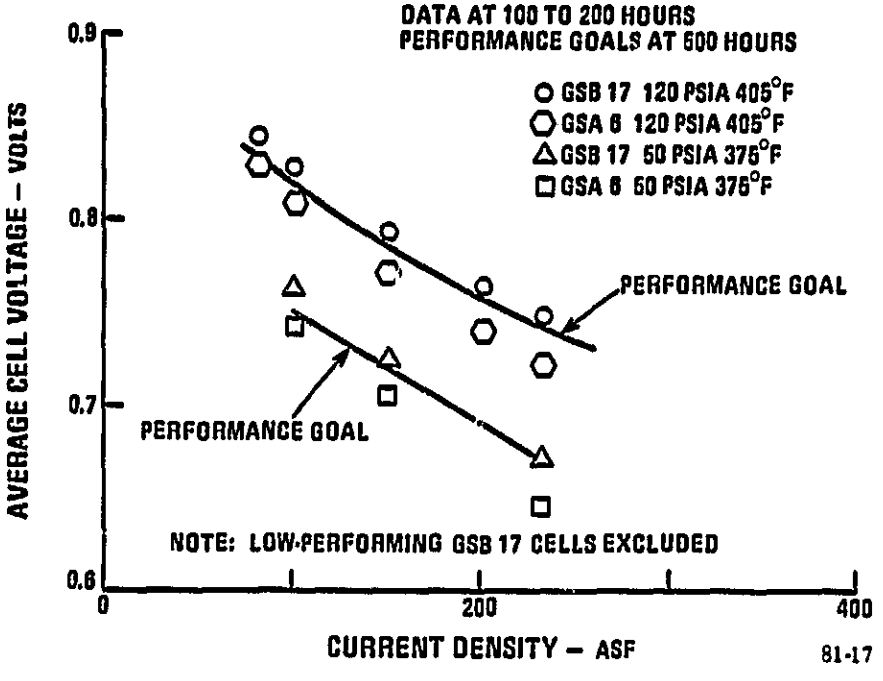

Figure 3-1. Average Cell Voltage vs. Current Density

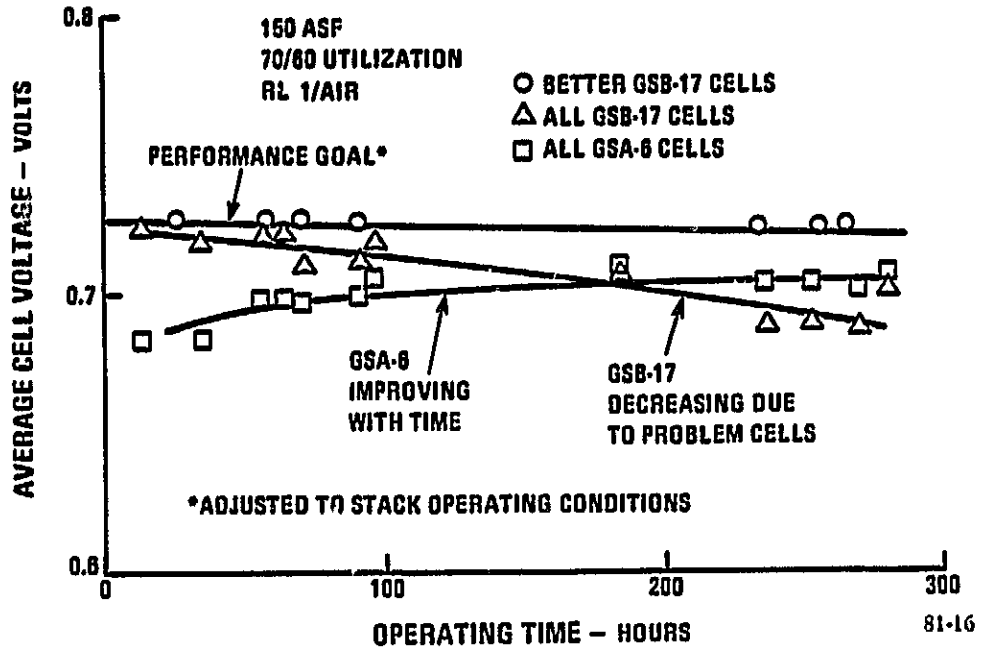

Figure 3-2. Performance History

tic tests indicated that the performance instability of certain GSB-17 cathode catalyst cells was caused by low anode performance. The test was terminated to investigate the instability of the GSB-17 catalyst. It was determined during the post-test analysis that this poor anode performance was caused by excess electrolyte in the anodes. This data is shown in Figure 3-3, which is a plot of electrolyte volume in the anode versus the anode hydrogen gain.

To further investigate the anode performance problem, ten cells from this stack were reassembled and tested for a brief (60-hour) test period. The objective of this test was to determine the controlling factors which affect electrolyte redistribution within the cell package and within the cell stack. It was concluded that the electrolyte redistribution is related to the electrode properties. The cell package electrolyte inventory data also indicated that the properties of the GSB-17 cathode catalyst cells were significantly different from the baseline GSA-6 cathode catalyst cells in that there was a larger variation in the electrolyte volume in the former.

The reactant gas leakage rates in this stack were low and acceptable. The reactant gas cross-leakage rate at 1.0 in. H_2O pressure differential increased during this stack test from 0.2% to 0.8% of the rated power fuel flow. This increase in leakage, although not exceeding the goal of 1% of rated power fuel flow, is attributed to the excessive electrolyte redistribution in the cell packages.

The average cell internal electrical resistance was low and acceptable at 13.3 mV per 100 ASF for cells adjacent to separator plates. The internal resistance of the standard cooler assemblies and for the cooler assemblies with alternative carbon-fiber holders were 6 and 9 mV per 100 ASF higher, respectively.

The compressive axial load on the stack was initially set at 30 psi and at the end of the test this axial load was reduced by 61%.

The test time for this stack was brief, since the test was terminated to evaluate the cause of the electrolyte redistribution into the anodes of the GSB-17 cathode

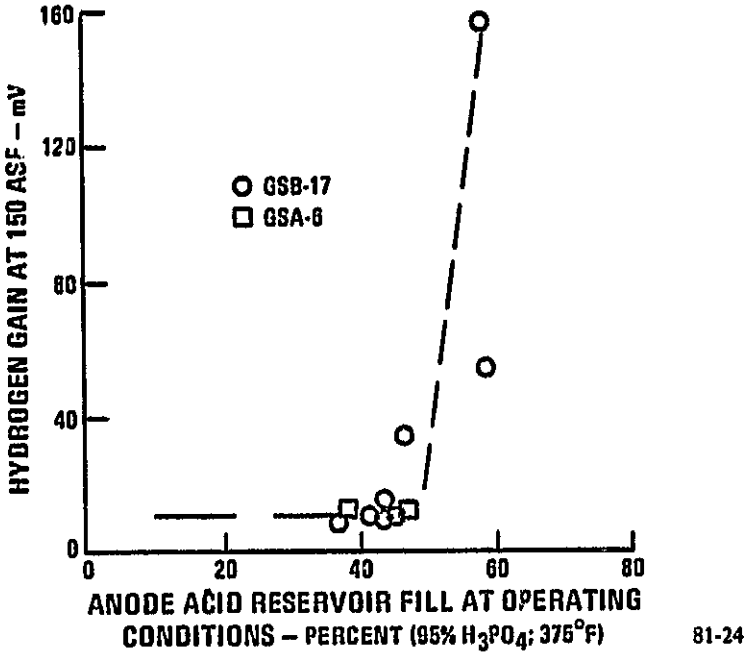

Figure 3-3. Acid Reservoir Fill vs. Hydrogen Gain

catalyst cells. The total test time was 349 hours with four thermal cycles. Of this test time 65 hours were at 120 psia and 405°F.

Second 3.7-ft^2 Short Stack (20-Cell) - The special features contained in this stack include the following:

- Fifteen cells with GSB-15 cathode catalyst and five cells with the baseline GSA-6 cathode catalyst cells.
- Modified resin in the electrode substrate of five cells.
- Commercial-grade graphite strips in the cooler assembly seal edge.
- Uncoated stainless steel cooler array in one cooler assembly.
- Five cells per cooler, four coolers per stack.
- Two-pass reactant gas flow paths.
- Cell electrolyte volume nominally 30% full at the beginning of life.
- Initial stack compressive axial load of 30 psi.

The objectives accomplished with this stack can be summarized as follows:

- Operation at 120 psia reactant gas pressures and 405°F average cell temperature for over 1500 hours.
- Performance evaluation of GSB-15 cathode catalyst cells.
- Confirmation of predicted reactant gas utilization effects on performance.
- Determination of reactant gas leakage rates, and identification of the causes of leakage rate variations.
- Verification of acceptable stack thermal and electrical internal resistance.
- Stack compressive axial load reduction.
- Cell electrolyte inventory.

The average cell performance for the cells with GSB-15 cathode catalyst is presented in Figure 3-4. The cell performance history for these cells is presented in Figure 3-5. These cells achieved the performance goal at early life, 375 hours, but the performance decay rate was higher than projected. The consequences of an air manifold seal failure and the failure of the uncoated stainless steel cooler array are explained further below.

The cell performance of the five baseline cells with GSA-6 cathode catalyst was 50 to 60 mV below that of the GSB-15 cells.

The anode and cathode diffusion losses are shown in Figure 3-6. The hydrogen performance gain of 10 mV at 200 ASF is the expected value, and the cell-to-cell uniformity indicates that the electrolyte distribution between anode and cathode is not adversely affecting cell performance as it did in the first stack tested under this task. The oxygen gain of 77 mV at 200 ASF is also at the expected level. During this diagnostic test the air manifold seal failed. A subsequent laboratory investigation showed that the cause was oxidation of a seal-positioning adhesive in the 120 psia oxygen environment.

The cell performance sensitivity to reactant gas utilization is shown in Figure 3-7. The voltage response to both the air and fuel flow are at the expected level. The expected cell voltage response has been predetermined analytically and emphirically. The important characteristic of utilizations response is the slope of the response as opposed to the absolute voltage level.

The reactant gas leakage rate was greater than expected and diagnostic tests indicated that this cross-leakage was localized in four cells. This local cross-leakage was caused when the air manifold seal failed and the reactant gas cross-pressures fluctuated ± 3 psig. The cross-leakage increased again when the uncoated stainless steel coolers failed. The leakage rate when the stack was first assembled was 0.3% of rated power fuel flow at 1 in. H_2O cross-pressure. This increased to 0.7% after the manifold seal failed and was 4.4% at the end of the stack test. The reactant gas cross-leakage goal is less than 1% of the rated power fuel flow rate.

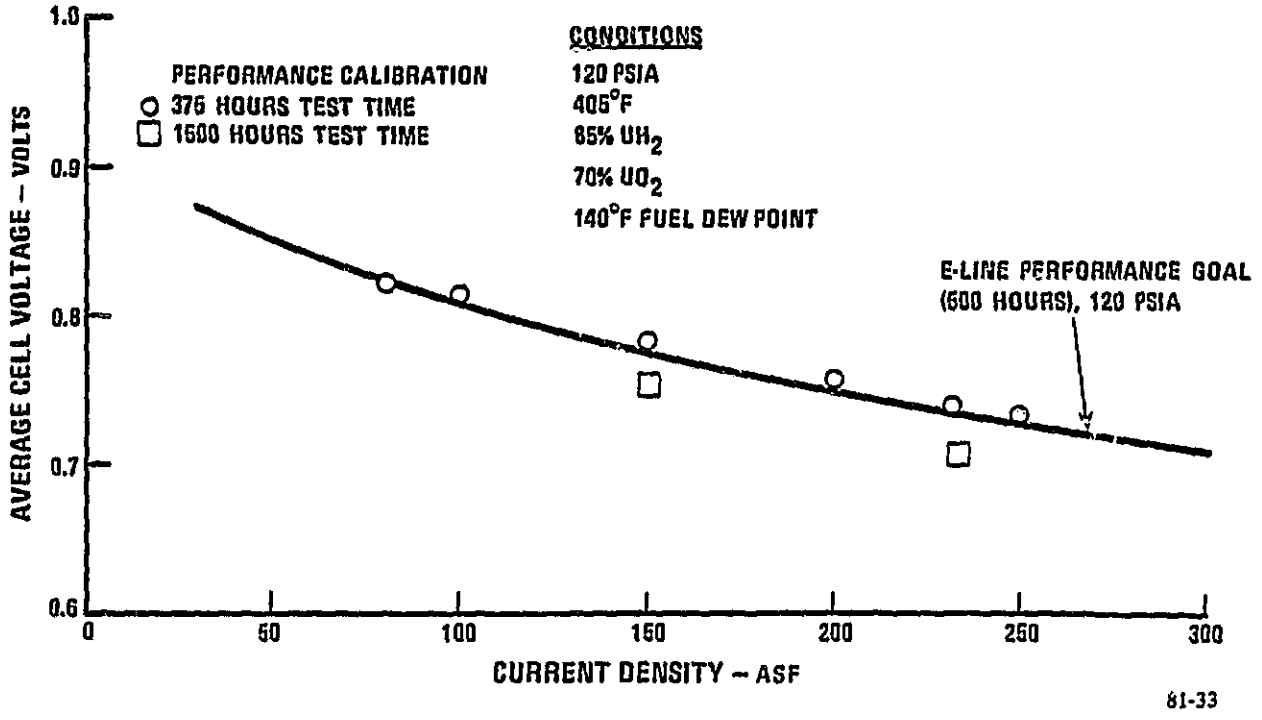

Figure 3-4. Average Cell Voltage vs. Current Density

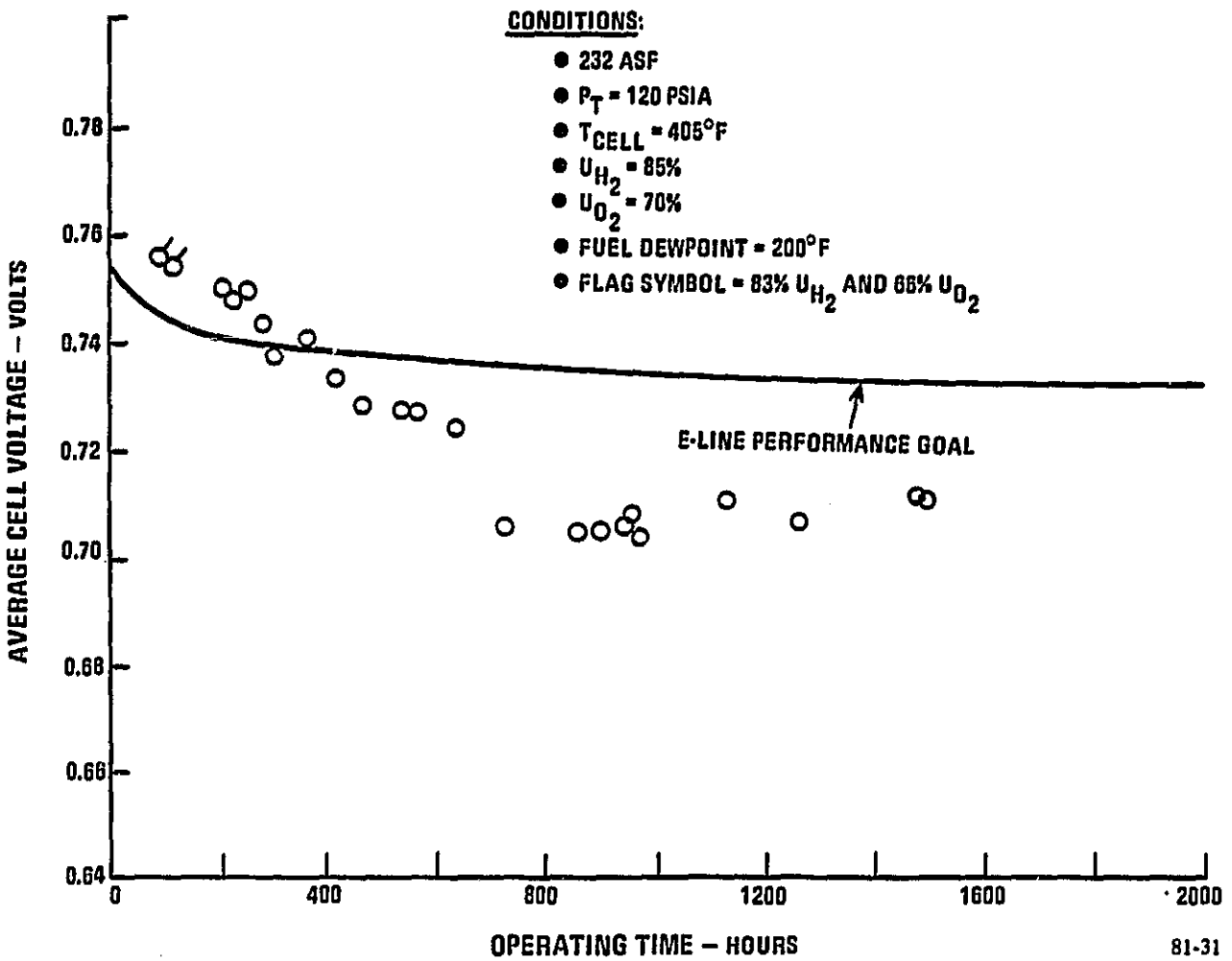

Figure 3-5. Performance History of GSB-15 Cells

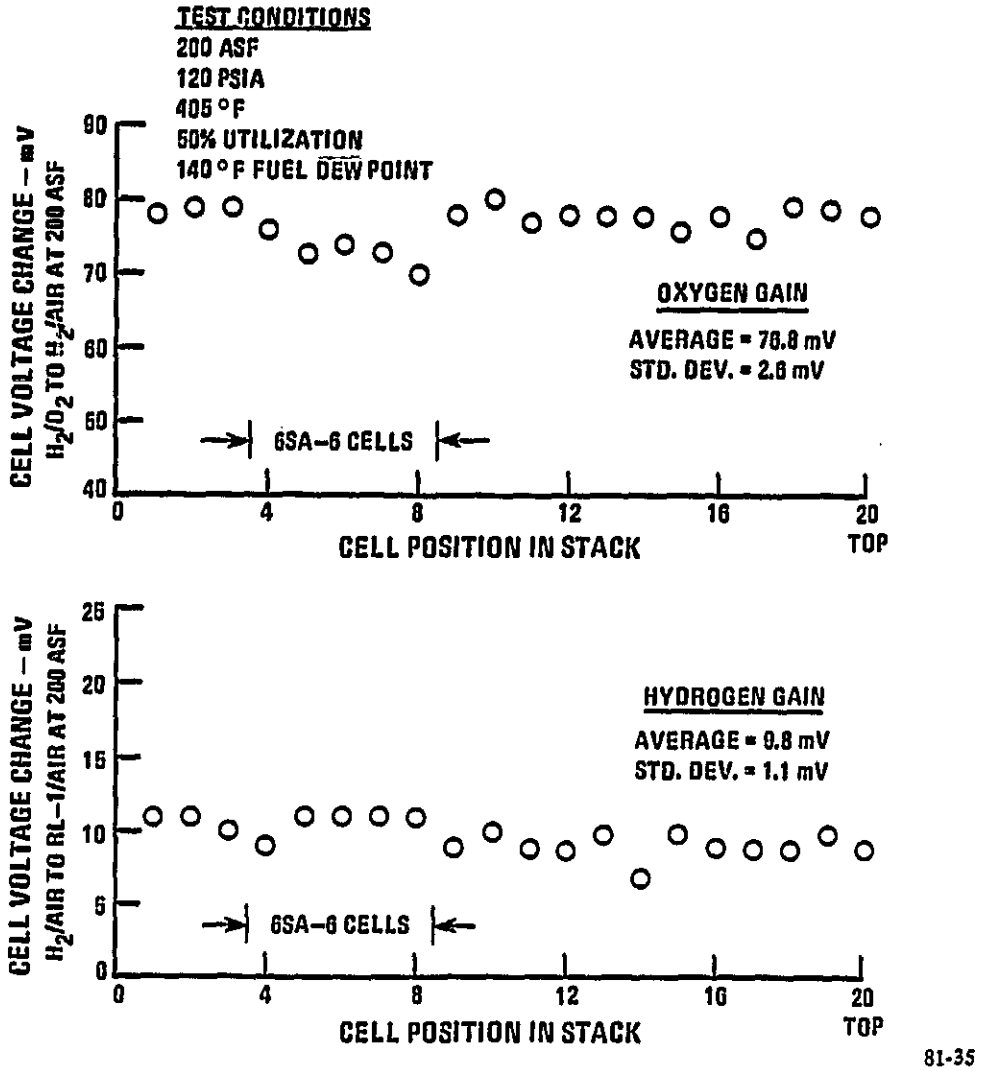

Figure 3-6. Hydrogen and Oxygen Gain Data Summary for 20-Cell Stack

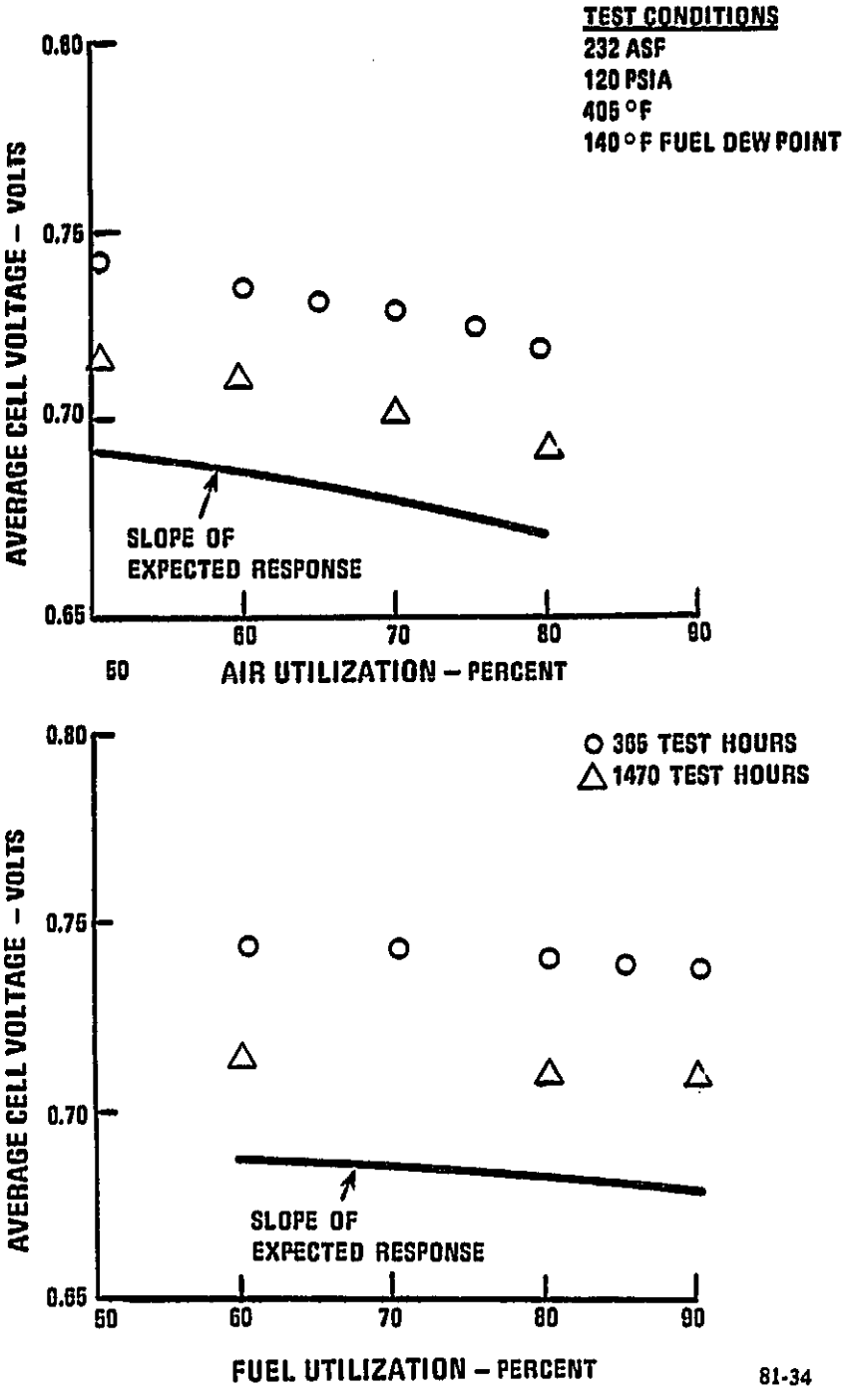

Figure 3-7. Reactant Utilization vs. Average Cell Voltage

The stack thermal properties were at the expected value. The effective thermal resistance of the stack was 0.020 hr-ft^2-°F/Btu. The effective thermal resistance for the uncoated stainless steel cooler assembly and the standard cooler assembly were 0.009 and 0.018 hr-ft^2-°F/Btu, respectively. Figure 3-8 presents this data. The uncoated stainless steel cooler array developed leaks due to corrosion and was replaced after 760 hours of stack operation. This cooler array was included in the stack assembly as a corrosion evaluation of stainless steel at actual acid cell conditions. The failure of this cooler array caused fuel starvation to the stack and a step loss in cell performance resulted, see Figure 3-5.

The cell package internal electrical resistance remained unchanged and was at a low and expected level. The internal resistance of the cell packages adjacent to separator plates averaged 11.1 mV per 100 ASF. The cell packages adjacent to the cooler assemblies averaged only 3.3 mV per 100 ASF greater than separator plate cells. The internal electrical resistance data are presented in Figure 3-9.

The stack compressive axial load was initially set at 30 psi. At the end of the test the axial load was reduced by 75%. Figure 3-10 presents these data and compares the reduction in axial load with that of the third and fourth stacks.

The post-test visual inspection of the repeat components in this stack showed them to be unchanged.

The post-test inspection also determined the electrolyte inventory. These data indicated a normal distribution of electrolyte within the cell packages and within the stack.

The test program for this stack was terminated after achieving the goal of 1500 hours. The total test time was 1526 hours which included 14 thermal cycles. All of this test time was at 120 psia reactant gas pressures and at 405°F average cell temperature.

Third 3.7-ft^2 Short Stack (20-Cell) - The special features contained in this stack include the following:

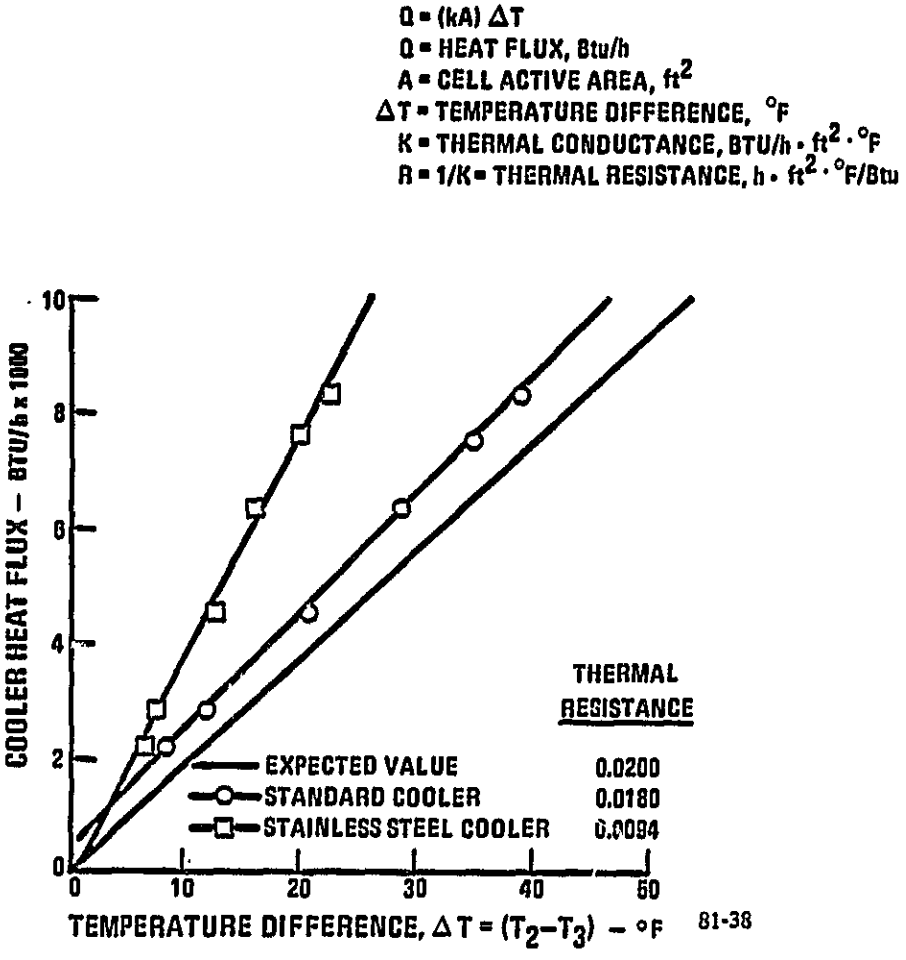

Figure 3-8. Cooler Assembly Thermal Analysis for 20-Cell, 3.7-ft² Stack

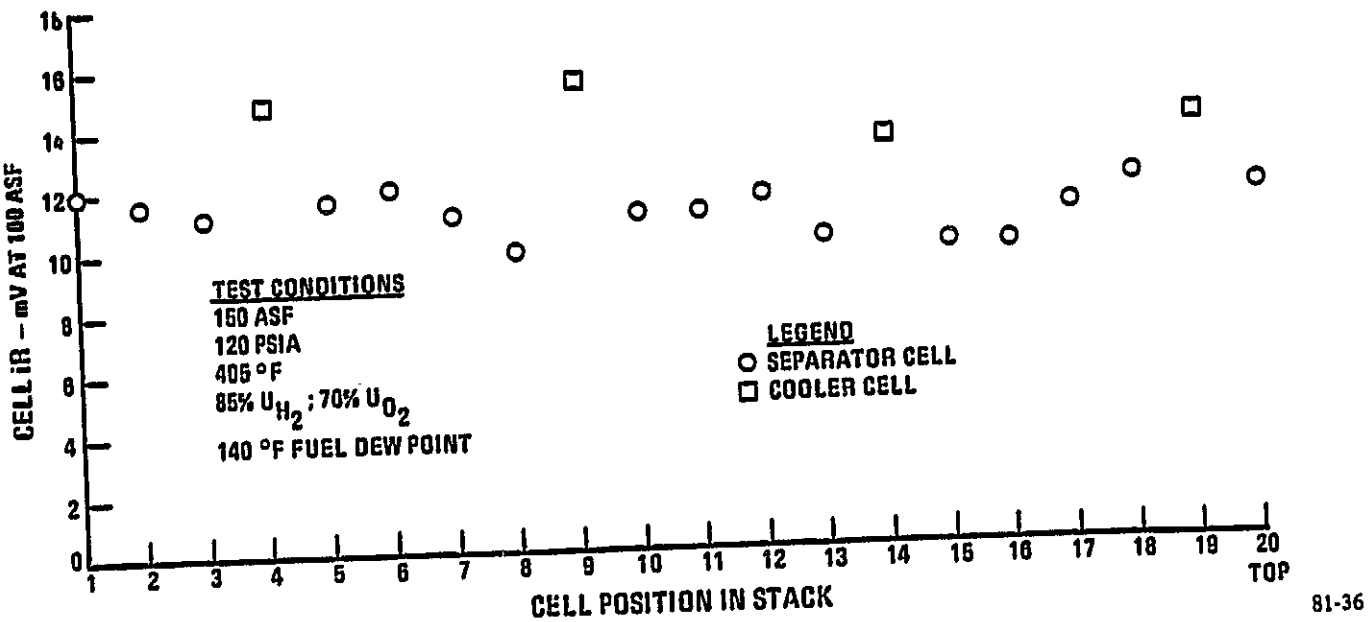

Figure 3-9. Cell iR in 20-Cell Stack

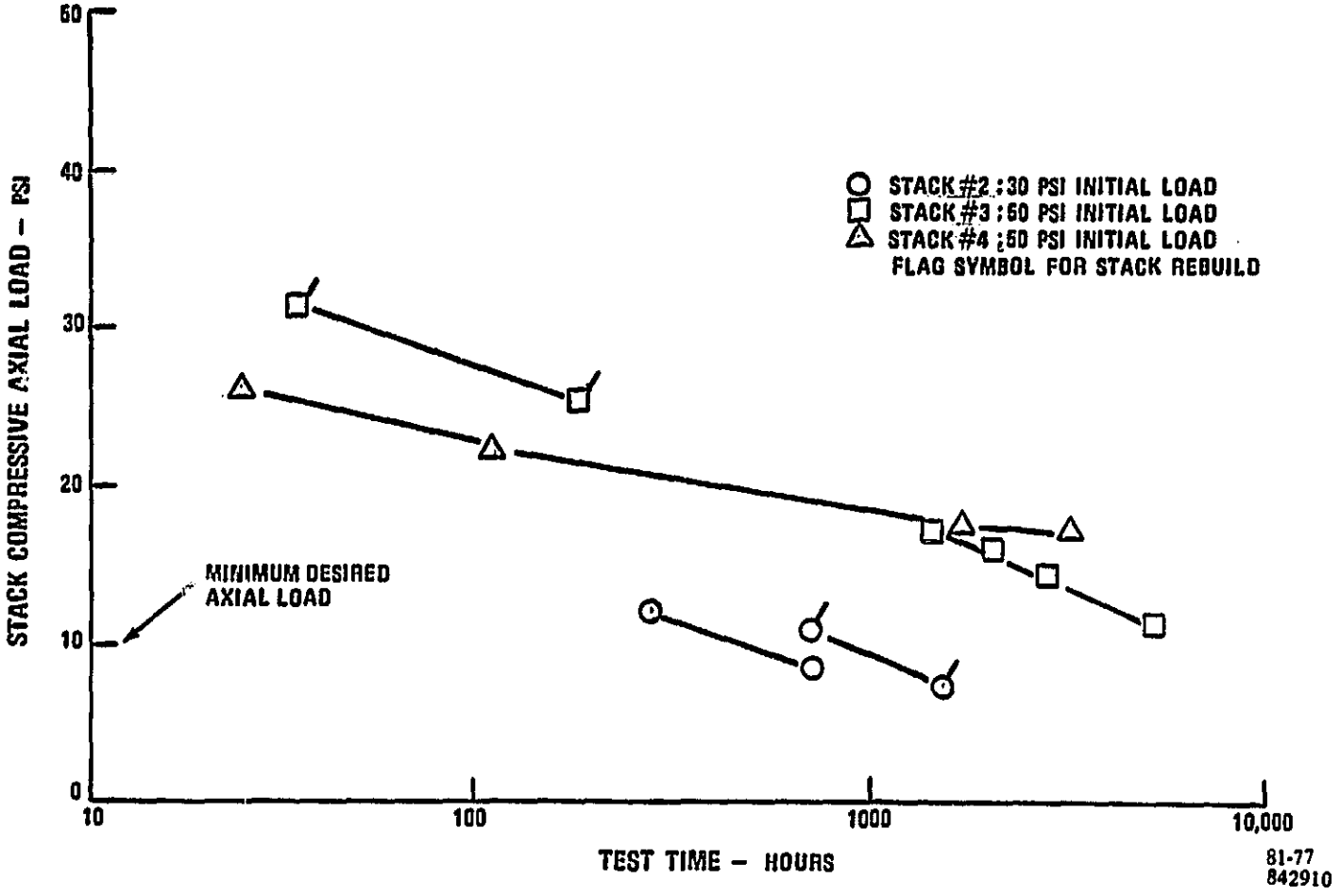

Figure 3-10. Axial Load vs. Time

- Twenty cells with GSD-15 cathode catalyst.
- Modified resin in the electrode substrates and in the cooler holders.
- Improved cross-pressure tolerant matrix.
- Separator plates fabricated with molding compound processed by the alternative method.
- Cooler tube arrays with 10-mil coatings with bumpers.
- Two-piece cooler holders with sealed edges.
- Four cells per cooler assembly, five coolers per stack.
- Two-pass reactant gas flow paths.
- Cell package electrolyte reservoir nominally 30% full at the beginning of life.
- Initial stack compressive axial load of 50 psi.

The endurance test program for this stack accumulated 5400 hours under this contract and will continue, with a goal of accumulating 8000 hours of operation under the follow-on program. This endurance test was conducted at 120 psia reactant gas pressures and at 405°F average cell temperature. The cell operating conditions were 232 ASF, 85% fuel utilization, 70% air utilization and 140°F fuel dewpoint.

The cell performance for this stack is presented in Figures 3-11 and 3-12. Figure 3-11 presents the performance calibration data. These data are compared to the E-line and to the 4.8-MW power plant performance goal adjusted to 5000 hours. Figure 3-12 presents the cell performance history. These data indicate that the performance is approximately 35 mV below the time-adjusted E-line performance goal after 5400 hours of operation due to catalyst degradation.

Diagnostic tests have been conducted periodically throughout this endurance test program. These tests have documented the following:

- Reactant gas utilization effect on performance.
- Stack electrical and thermal characteristics.

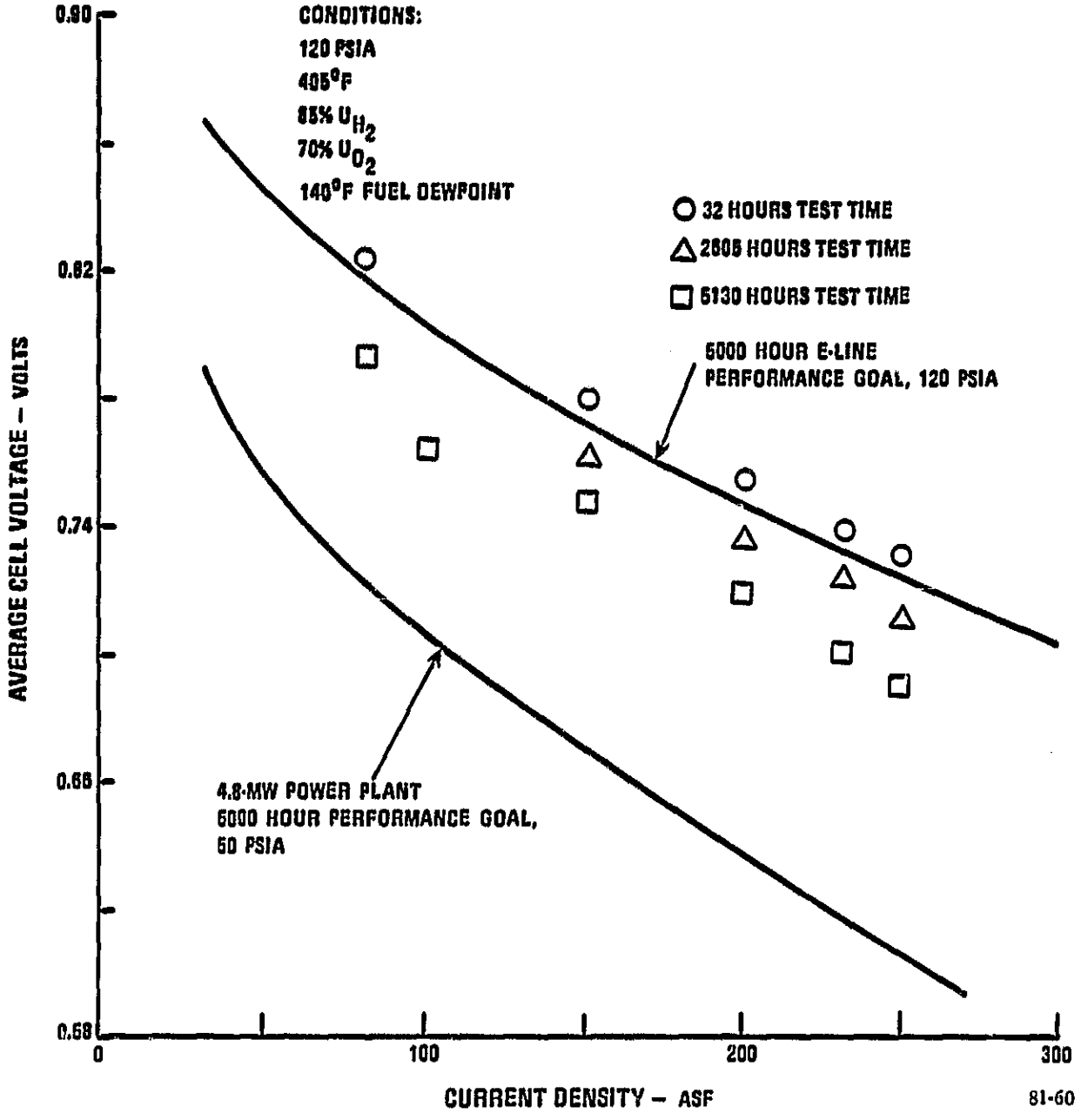

Figure 3-11. Average Cell Voltage vs. Current Density

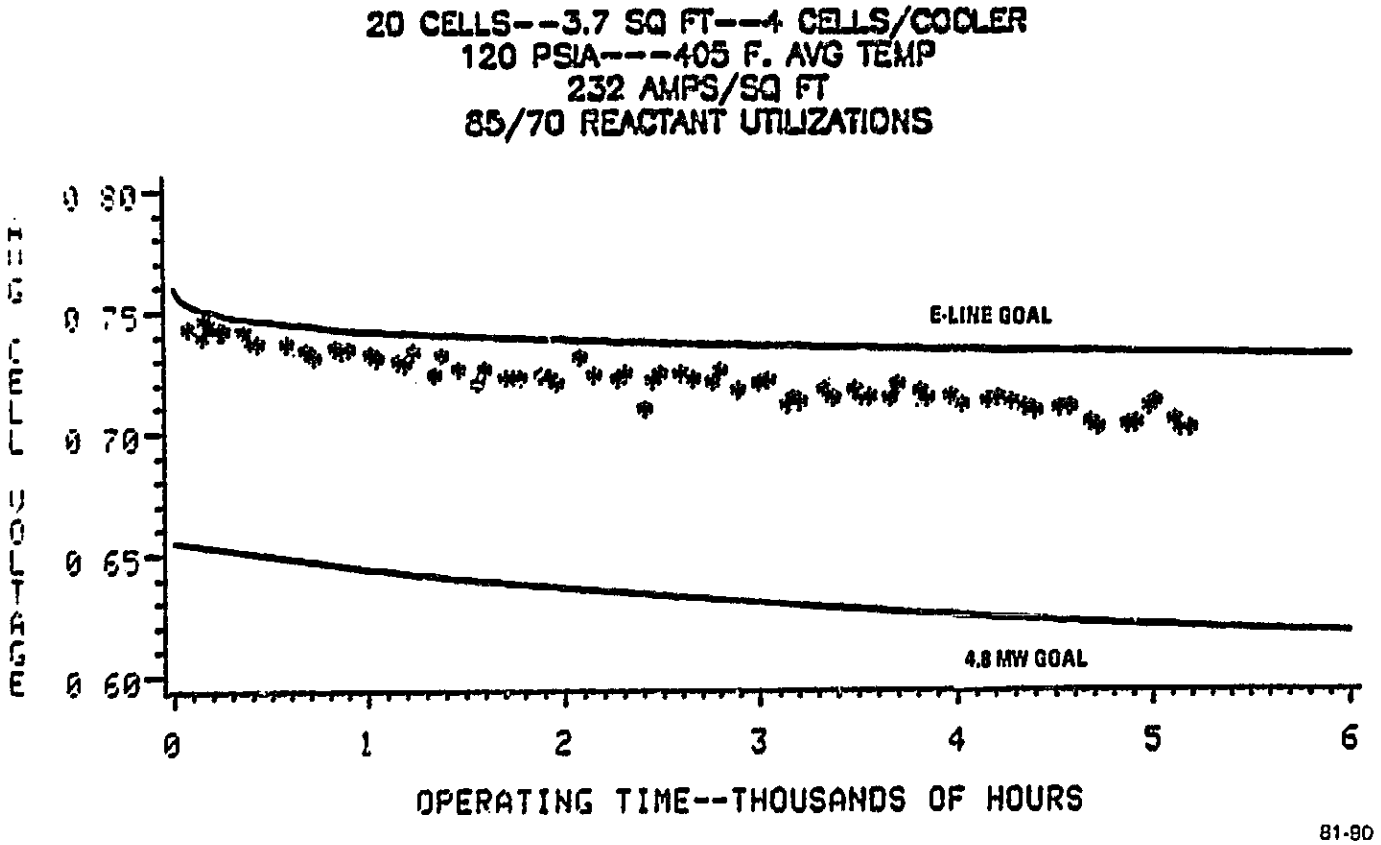

Figure 3-12. Performance History

- Stack compressive axial load reduction with test time.
- Reactant gas cross-pressure tolerance and leakage rates.

The cell performance sensitivity to reactant gas utilization is shown in Figure 3-13. The voltage response to both the air and the fuel flow is at the expected level.

The stack thermal properties are presented in Figure 3-14. The effective thermal resistance of the stack remains unchanged throughout the duration of this endurance test. The resistance is also at the expected level for these components and for this stack configuration of four cells per cooler.

The cell package internal electrical resistance has also remained unchanged and is at a low and expected level. The internal resistance of the cell packages adjacent to separator plates averaged 11.1 mV per 100 ASF after 5200 hours of stack operation. The cell packages adjacent to the cooler assemblies averaged only 3.8 mV per 100 ASF greater than separator plate cells. The internal electrical resistance data are presented in Figure 3-15.

The stack compressive axial load was initially set at 50 psi. The reduction in axial load with test time is presented in Figure 3-10.

The cell package reactant gas cross-pressure tolerance data are presented in Figure 3-16. They show the effect of gas cross-pressure on open circuit voltage for each cell in the stack. The data indicate that cell #18 developed excessive cross-leakage. This leakage was caused by a test facility gas cross-pressure excursion during stack operation. This excursion, at approximately 3000 hours of operation, was at 6 psi for an excessive time duration of 6 minutes.

The endurance test was interrupted after completing 5400 hours of operation because of the high reactant gas leakage. The stack was returned to assembly for inspection of the repeat components and to obtain physical property data on cell packages, separator plates and on one cooler assembly. Other than the localized damage to the cathodes of a few cells, the repeat components were in good condition. The visual

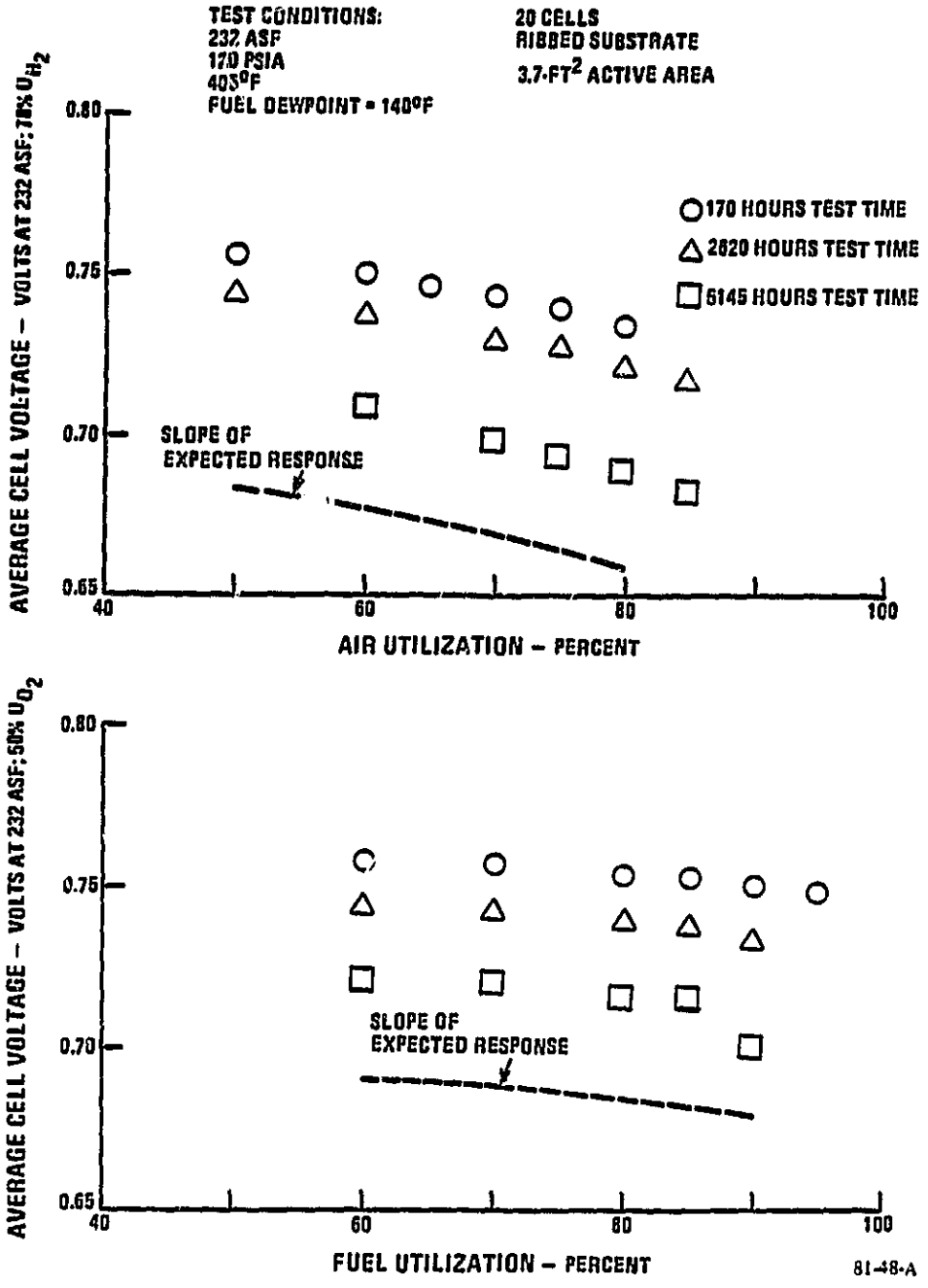

Figure 3-13. Reactant Utilization vs. Average Cell Voltage

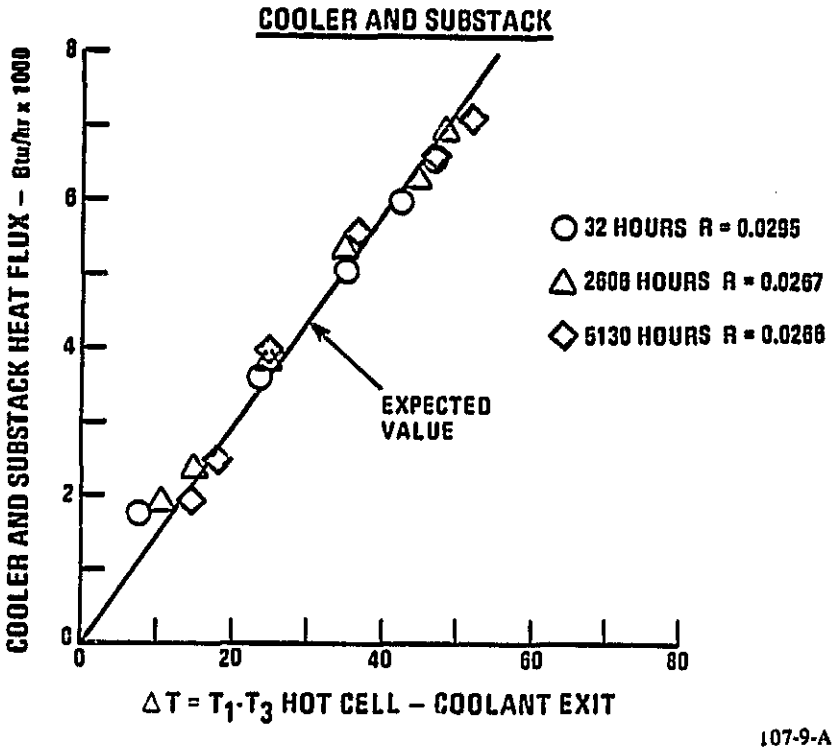

Figure 3-14. Thermal Properties

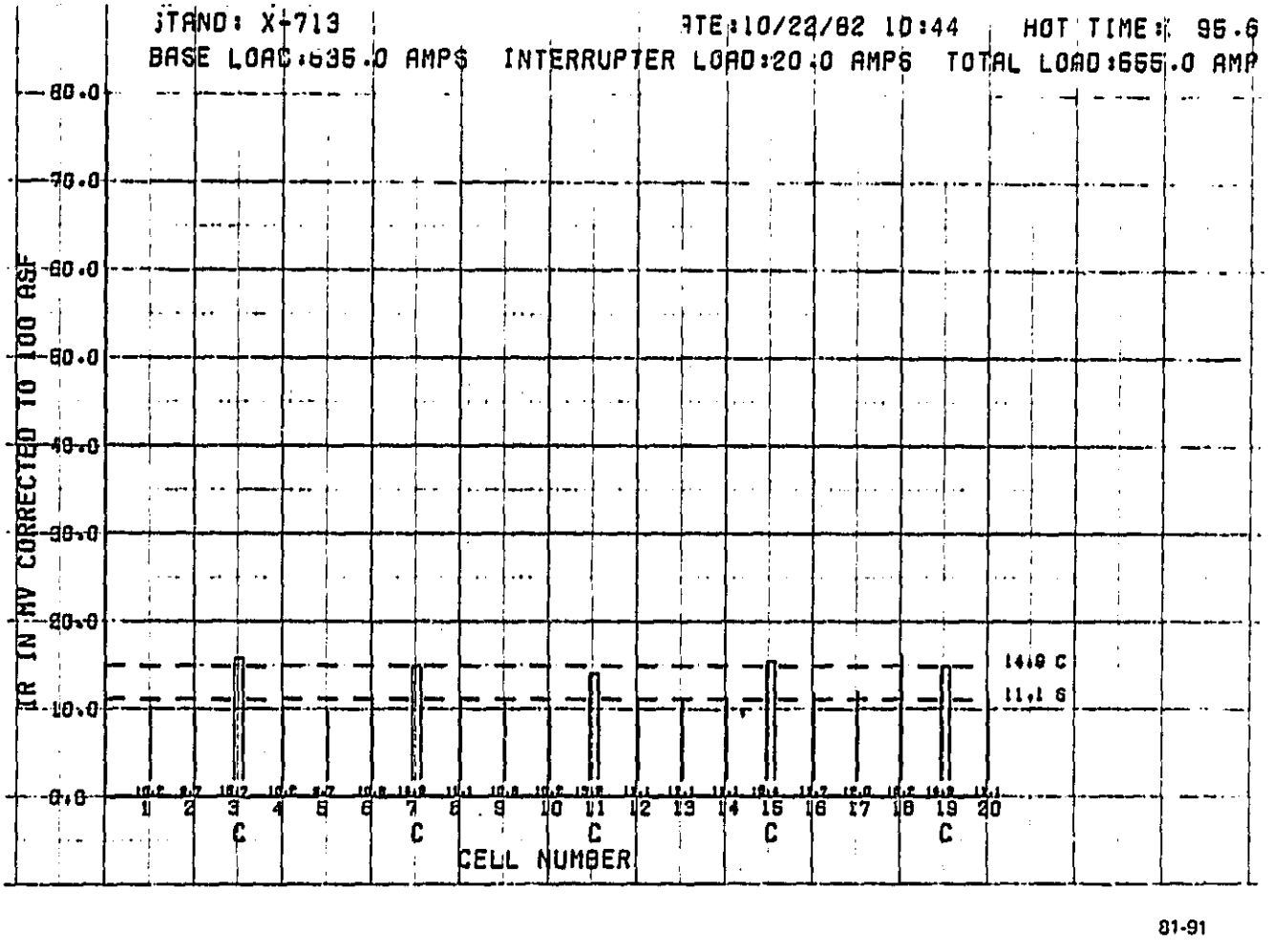

Figure 3-15. Cell iR in 20-Cell Stack

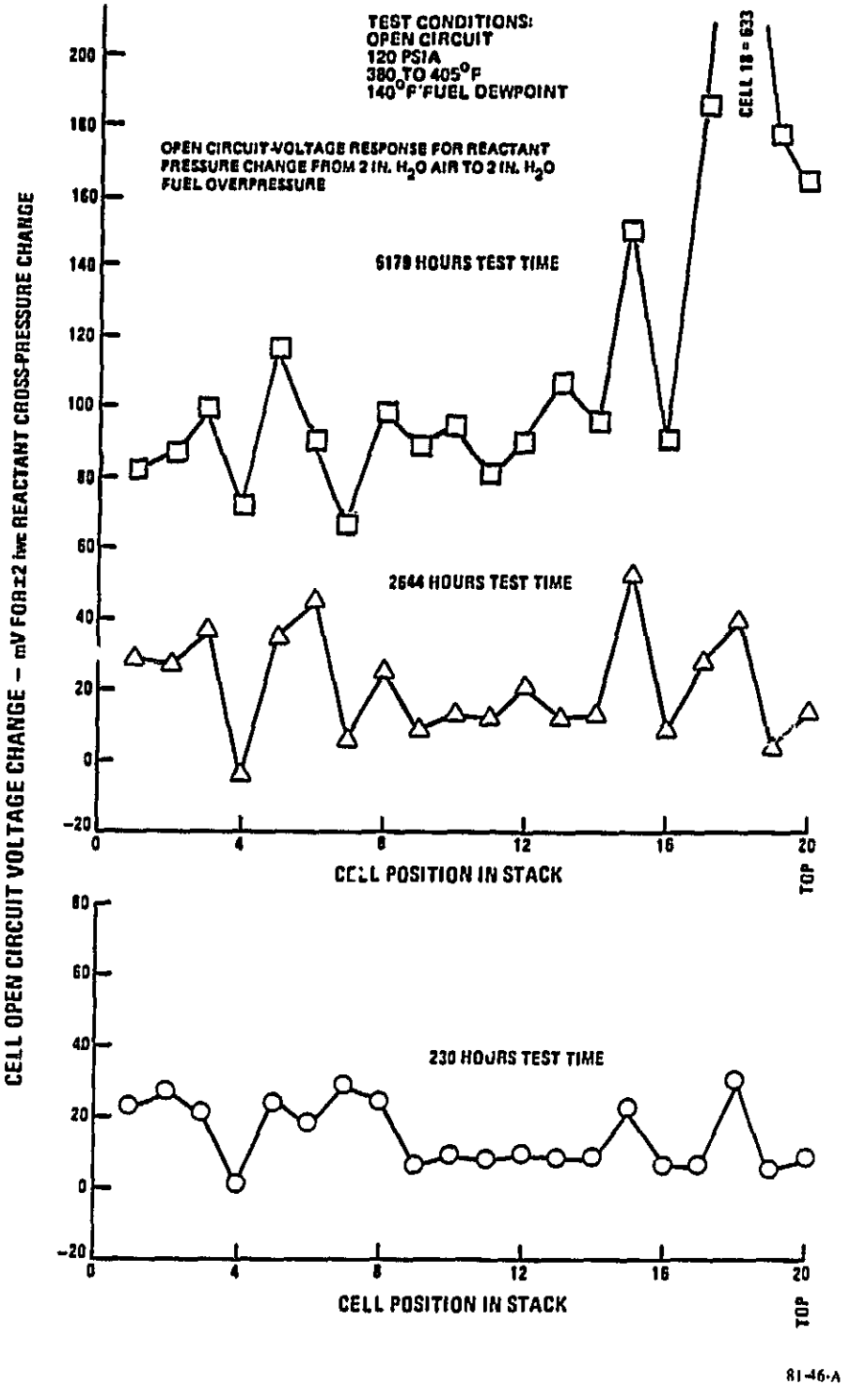

Figure 3-16. Reactant Cross-Leakage Diagnostic Test Data

inspection indicated that the damage caused by the cross- pressure excursions was local to the edge seals, the back side seals and the filler band-catalyst layer interface.

Property data are summarized in Table 3-1. The column labeled "Sample Value Before Test" refers to property data obtained from samples of untested parts. Scatter in data is the explanation for some specific properties showing an apparent improvement in 5400 hours of operation. The conclusion from this data is that no property shows significant downward change after 5400 hours of stack testing. More test data is obviously required to establish trends.

Electrolyte inventory data was obtained on a limited number of cells from this stack. These data indicated that the electrolyte loss rate was in reasonable agreement with the theoretical model prediction.

The stack was reassembled. The cells and separator plates used for physical property data analysis were replaced with used cells from the second stack tested in this program task. The stack returned to test and additional endurance is planned to obtain additional property data on repeat components. The total test time on this contract was 5400 hours, which includes 26 thermal cycles.

Fourth 3.7-ft^2 Short Stack (30-Cell) - The special features contained in this stack include the following:

- Thirty cells with GSB-15 cathode catalyst and HYCAN anode catalyst.
- Modified resin in the electrode substrates and in the cooler holders.
- Two-element serpentine coolers with 10-mil coatings with bumpers.
- Two-piece cooler holders, four-sided seal and a pore structure larger than the electrode substrate.
- Eight cells per cooler, four coolers per stack.

TABLE 3-1. 3.7-FT^2, 20-CELL STACK, PROPERTY DATA SUMMARY

Component	Sample Value Before Test	5400 Hour Sample	5400 Hour Data
ELECTRODE			
Compressive Strength	147 psi	Cell 15 Anode	157 psi
		Cell 15 Cathode	209 psi
Compressive Modulus	1897 psi	Cell 15 Anode	1370 psi
		Cell 15 Cathode	2341 psi
Edge Seal Density	1.1-1.2 Grams/cc for 0.75 inches from outboard edge	Cell 5 Anode	1.2 for 0.75 in.
		Cell 5 Cathode	1.1 for 0.75 in.
		Cell 6 Anode	1.1 for 0.75 in.
		Cell 6 Cathode	1.2 for 0.75 in
Load Deflection	8.3 Mils/50 psi	Cell 15	6.4 Mils/50 psi
Load Relaxation	12.5 psi/150 hrs.	Cell 15	13 psi/160 hrs.
SEPARATOR PLATE			
Flex Strength	5810 psi	Plate 7/8	6960 psi
		Plate 8/9	6620 psi
		Plate 17/18	6357 psi
Flex Modulus	1.06 x 10^6 psi	Plate 7/8	1.24 x 10^6
		Plate 8/9	1.21 x 10^6
		Plate 17/18	1.14 x 10^6
COOLER ASSEMBLY			
Electrical Resistance - Cooler to Holder	Infinity	Cooler 18/19	9000 Ohms
Snivvy Deposits	None	Cooler 18/19	None
Cooler Tube Erosion	None	Cooler 18/19	None

- Two-pass reactant gas flow paths.
- Cell electrolyte volume nominally 30% full at the beginning of life.
- Initial stack compressive axial load of 50 psi.

Figure 3-17 is a photograph of this 30-cell stack assembled into the containment vessel and with the containment vessel cover removed.

The endurance test program for this stack has accumulated 4500 hours under this program and will continue, with a goal of accumulating over 20,000 hours of operation under the follow-on program. This endurance test is being conducted at 120 psia reactant gas pressures and at 405°F average cell temperature. The cell operating conditions are 200 ASF, 83% fuel utilization, 70% air utilization and 140°F fuel dewpoint. Operation at 200 ASF corresponds to future power plant full power operating conditions.

The cell performance for this stack is presented in Figures 3-18 and 3-19. Figure 3-18 presents the performance calibration data through 3215 hours of operation. These data are compared to the E-line performance goal and to the 4.8-MW power plant performance goal adjusted to 2000 hours. Figure 3-19 presents the cell performance history. These data indicate that the performance is 44 mV below the time-adjusted E-line performance goal after 4500 hours of operation.
Diagnostic tests have been conducted periodically throughout this endurance test program. These tests have documented the following:

- Reactant gas utilization effect on performance.
- Reactant gas cross-pressure tolerance and leakage rates.
- Stack electrical and thermal characteristics.
- Stack compressive axial load reduction with test time.

The cell performance sensitivity to reactant gas utilization is shown in Figure 3-20. The voltage response to both the air and the fuel flow is at the expected level.

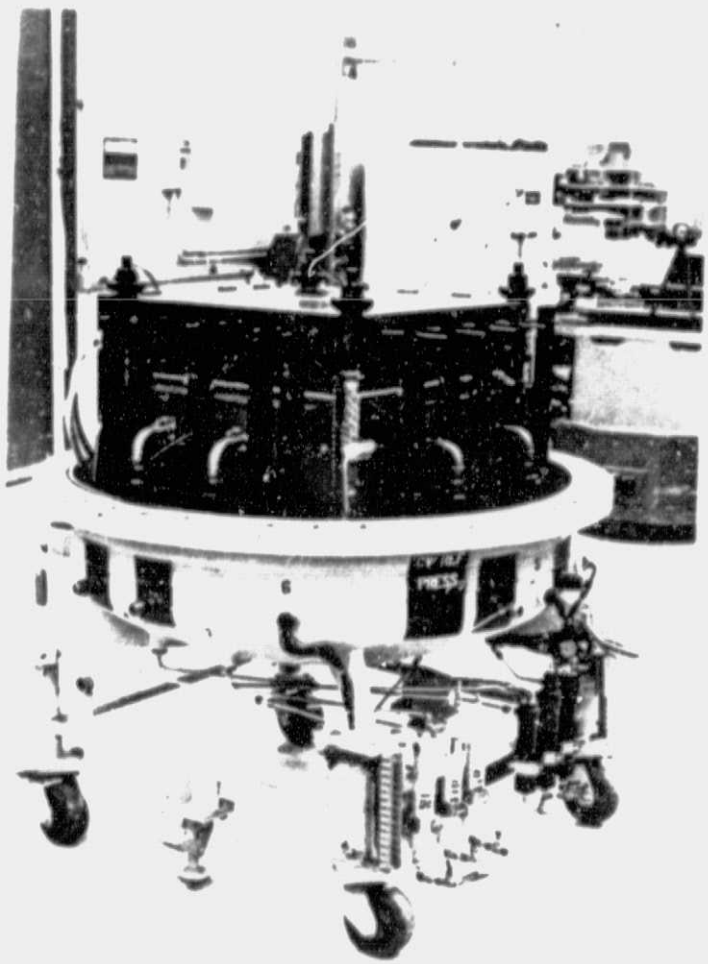

FC19286

Figure 3-17. Rig Assembled in Containment Vessel

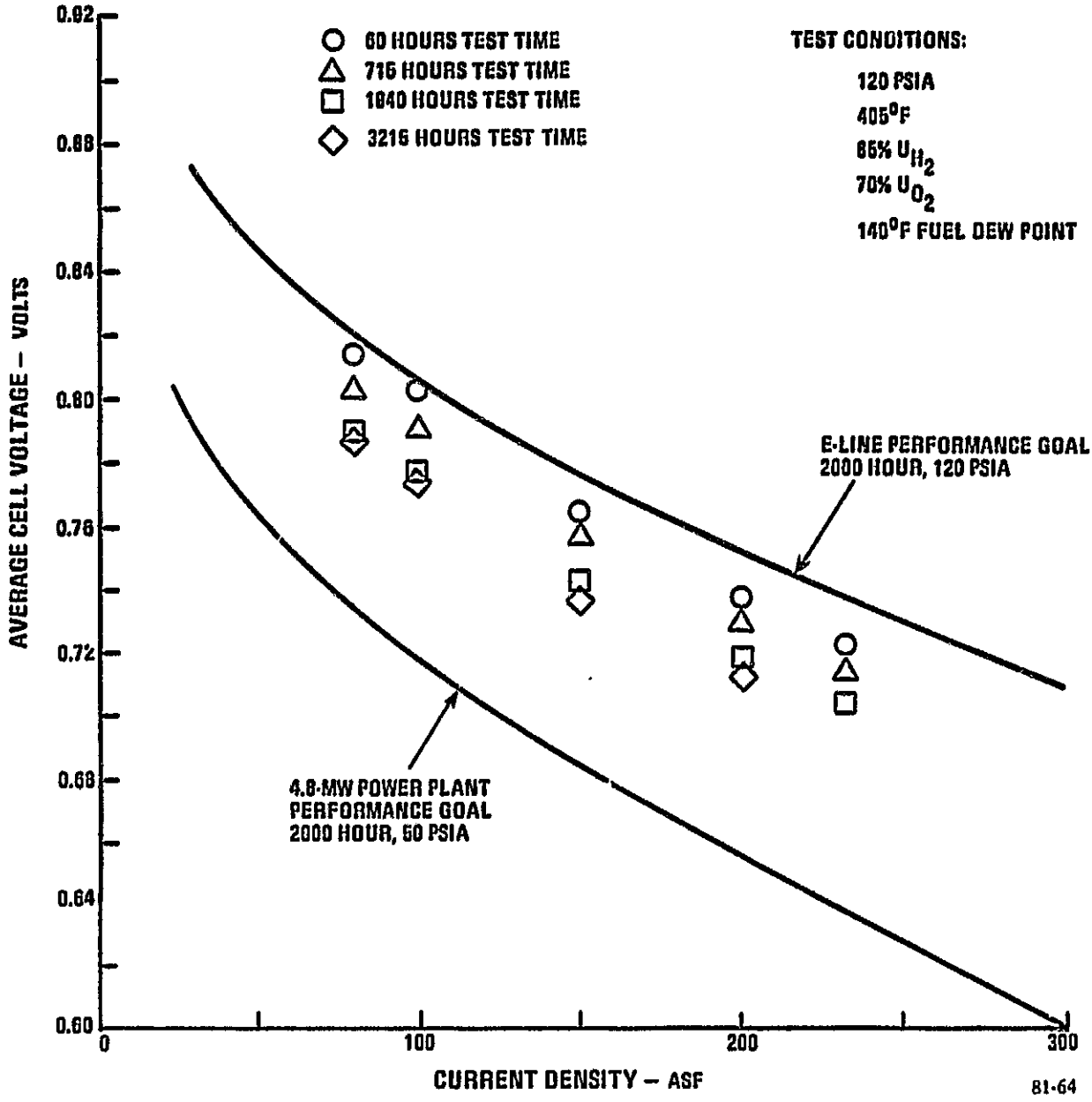

Figure 3-18. Average Cell Voltage vs. Current Density

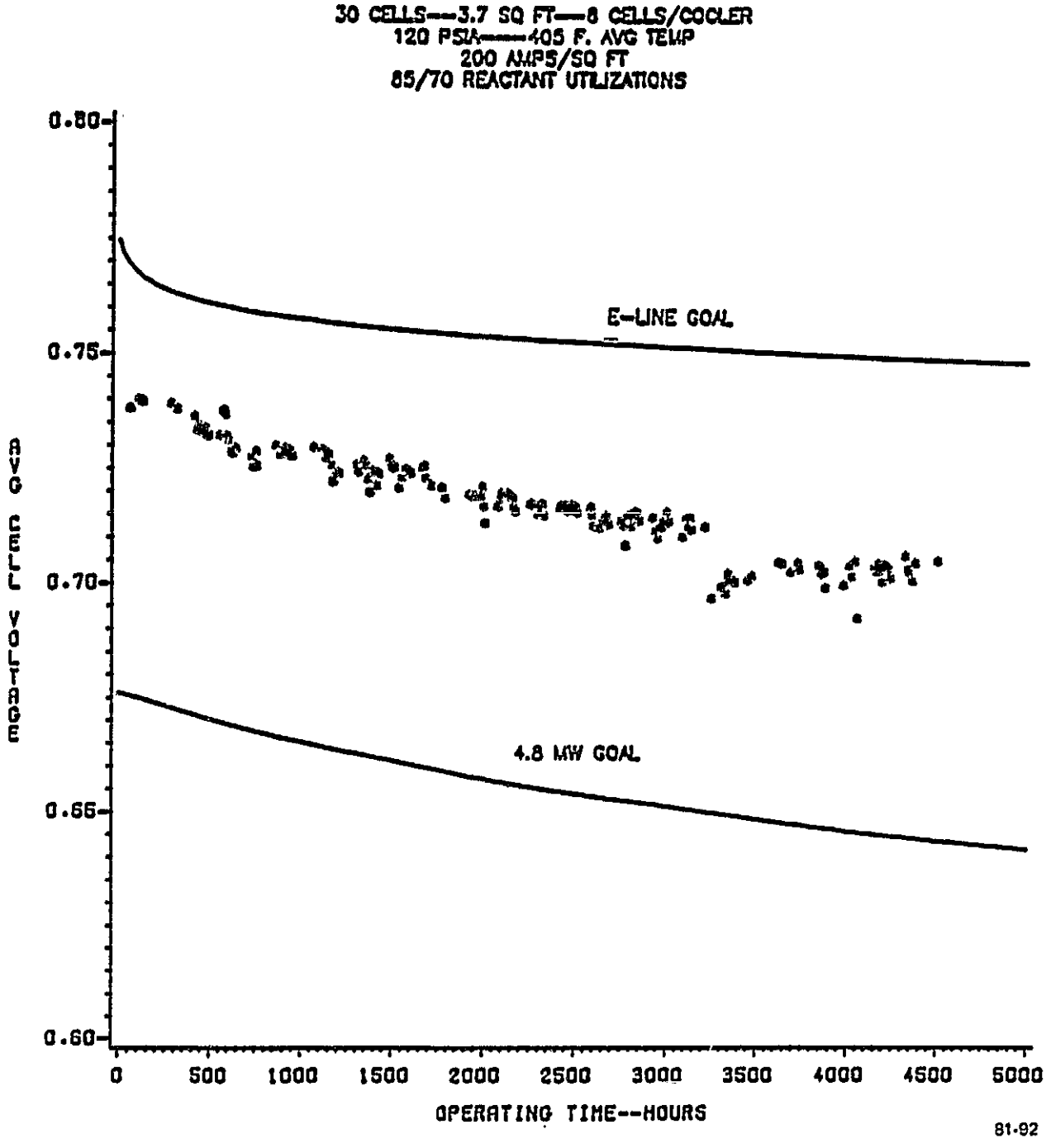

Figure 3-19. Performance History

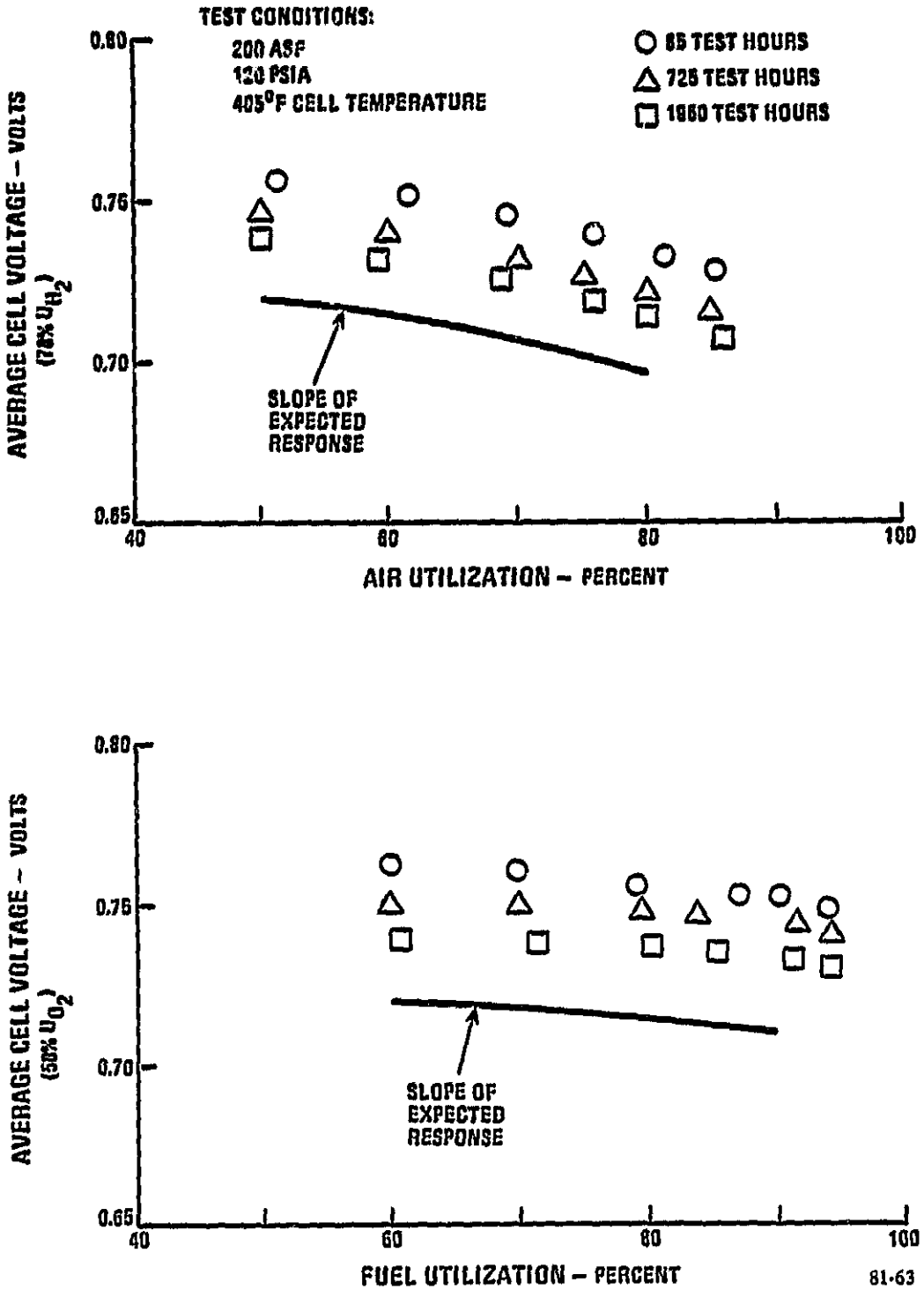

Figure 3-20. Reactant Utilization vs. Average Cell Voltage

The reactant gas cross-pressure tolerance data are presented in Figure 3-21. These data show the effect of cross-pressure on open circuit voltage for each cell in the stack. It can be seen from these data that the stack cross-pressure tolerance remains low and acceptable (below 20 mV change in voltage). The reactant gas cross-leakage rates have also remained low and acceptable. There has been a very slight change in leakage throughout the duration of the test, increasing from 0.06% of rated power fuel flow at 1 in. H_2O cross-pressure after 100 hours of operation to only 0.29% after 4500 hours of operation. Leakage below 1.0% of rated power fuel flow is acceptable.

The stack thermal properties are presented in Figure 3-22. The effective thermal resistance of the stack remains unchanged throughout the duration of this endurance test. The resistance is also at the expected level for these components and for this stack configuration of eight cells per cooler.

The cell package internal electrical resistance has also remained unchanged and is at a low and expected level. The internal resistance of a cell package adjacent to separator plates averaged 12.4 mV per 100 ASF after 1936 hours of operation. The cell packages adjacent to the cooler assemblies averaged 21.6 mV per 100 ASF greater than separator plate cells. The internal electrical resistance data are presented in Figure 3-23.

The stack compressive axial load was initially set at 50 psi. The reduction in axial load with test time is presented in Figure 3-10. These data indicate that the axial load rate of reduction is at the expected value.

The endurance test program for this stack will continue under the follow-on program. The objective is to evaluate cell performance characteristics as well as to determine changes in the physical properties of the repeat components over this length of operating time. A total of 4500 hours of operation with 15 thermal cycles have been accumulated under this program.

First 10-ft^2 Short Stack - The first stack containing cells of the 10-ft^2 ribbed substrate configuration was assembled and testing initiated under this contract.

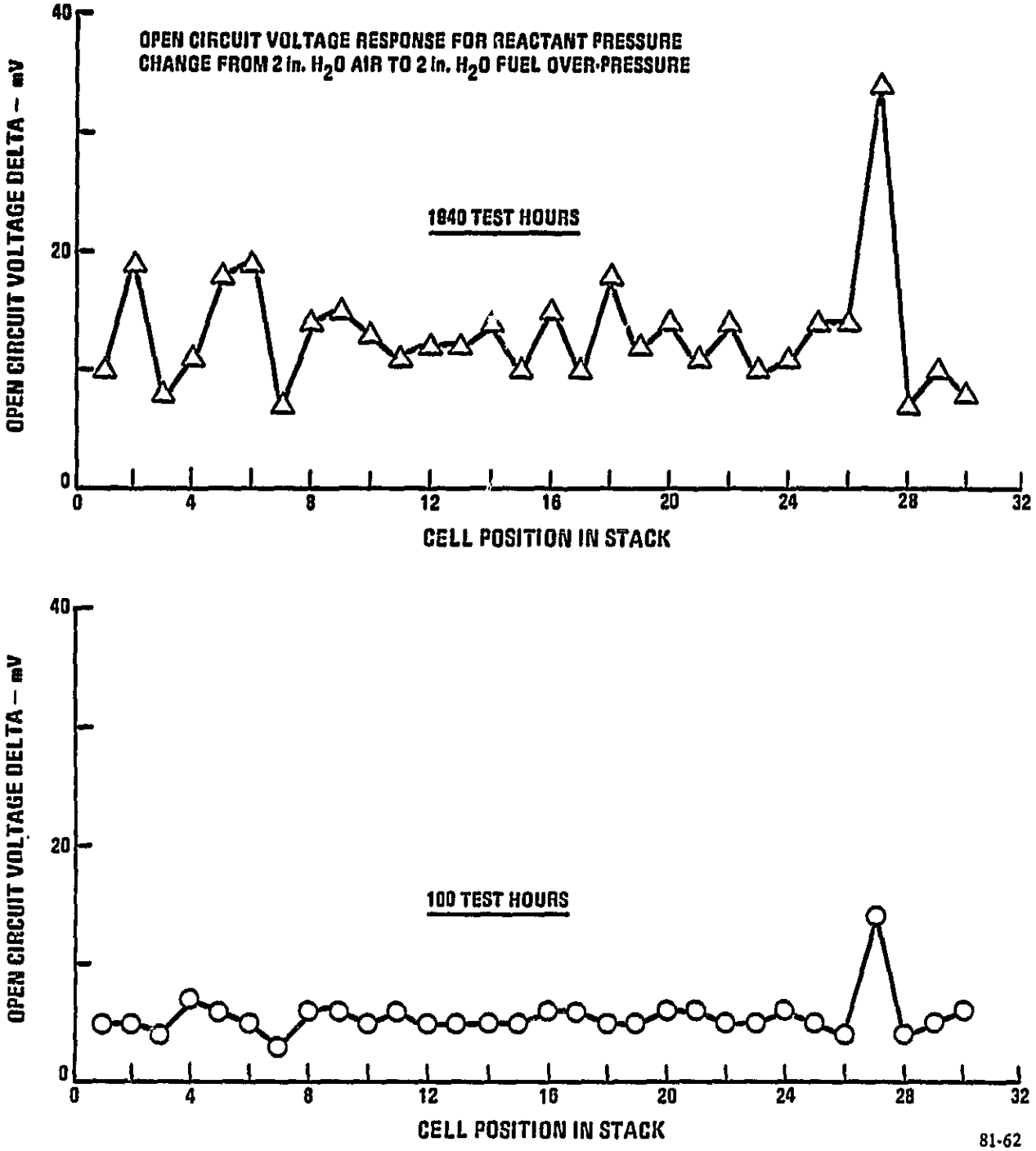

Figure 3-21. Reactant Gas Cross-Leakage Diagnostic Test Data

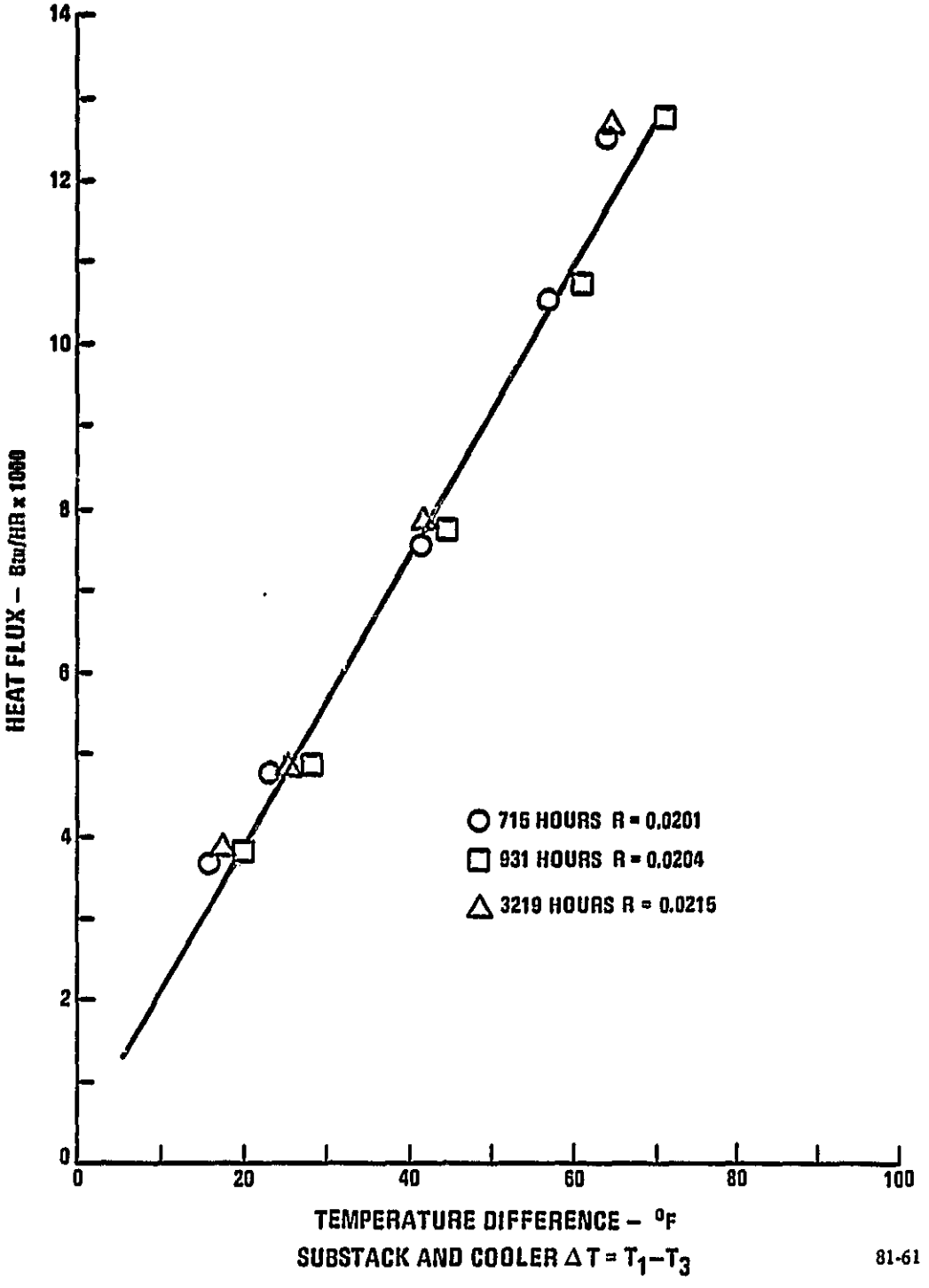

Figure 3-22. Thermal Properties

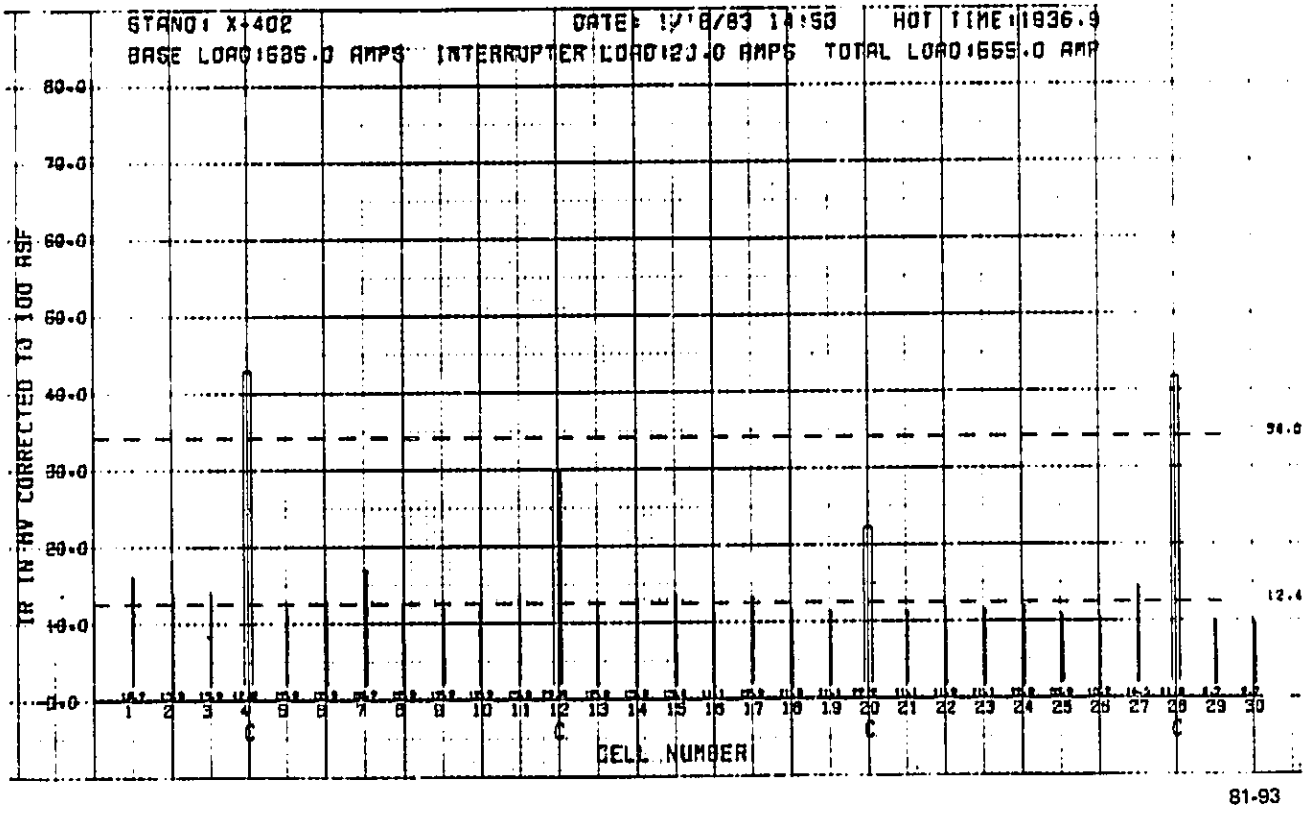

Figure 3-23. Electrical Properties

Testing will continue under the follow-on program. The objective of this stack test is to evaluate functional capability of the first 10-ft^2 stack repeat and some non-repeat components in a 1500-hour test operating at 120 psia reactant gas pressures and at 405°F average cell temperature. The cell operating conditions are 200 ASF, 85% fuel utilization, 70% air utilization and 140°F fuel dewpoint.

The special features contained in this stack include the following:

- Thirty cells with GSB-18 cathode catalyst and HYCAN anode catalyst.
- Modified resin in the electrode substrates and the cooler holders.
- Two-element serpentine cooler, 3/8 in. copper tube with 10-mil coating with bumpers.
- Two-piece cooler holder, four-sided seal and a pore structure larger than the electrode substrate.
- Eight cells per cooler, four coolers per stack.
- Two-pass reactant gas flow paths.
- Cell electrolyte volume nominally 30% full at the beginning of life.
- Initial stack axial compressive load of 50 psi.

The stack was assembled using 10-ft^2 components fabricated under the component technology development tasks. Figure 3-24 is a photograph of this 30-cell stack assembled into the containment vessel and with the containment vessel cover removed.

The stack was operated for 113 hours over a range of conditions. An initial performance curve, for the non-cooler cells, is given in Figure 3-25. The cooler cells have abnormally high electrical resistance and are deleted from Figure 3-25 to give a more realistic picture of cell performance. These data are the initial performance calibration data and are compared to the E-line and to the 4.8-MW power plant performance goal adjusted to 500 hours.

The test program on this stack has completed 113 hours of operation including 3 thermal cycles. The test will continue under the follow-on program.

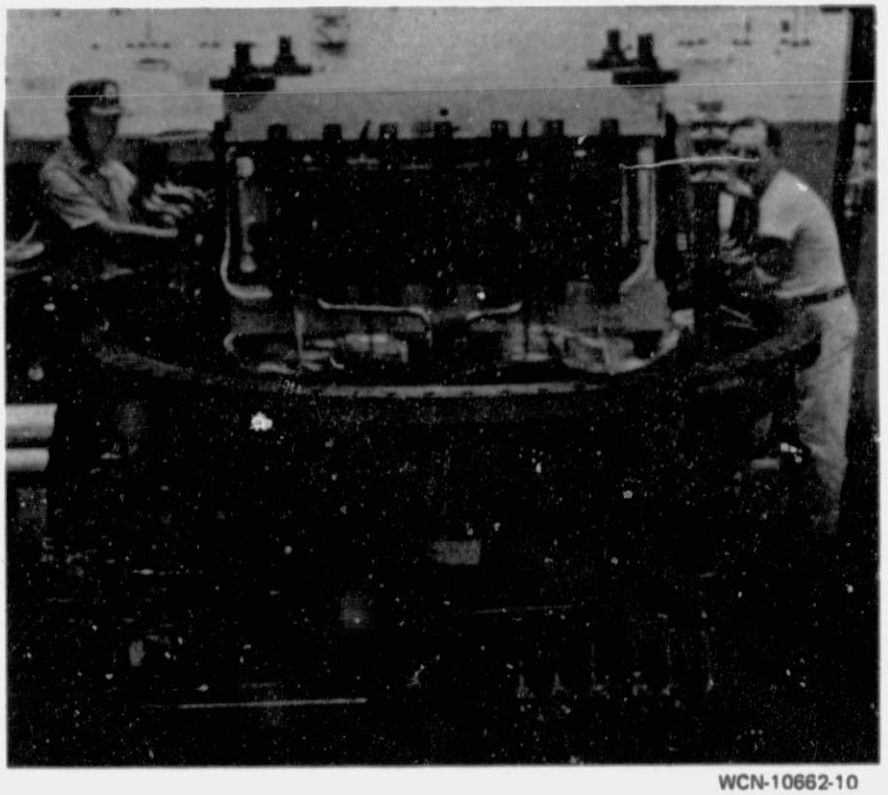

WCN-10662-10

Figure 3-24. 10-ft^2, 30-Cell Short Stack Mounted in Containment Vessel Base

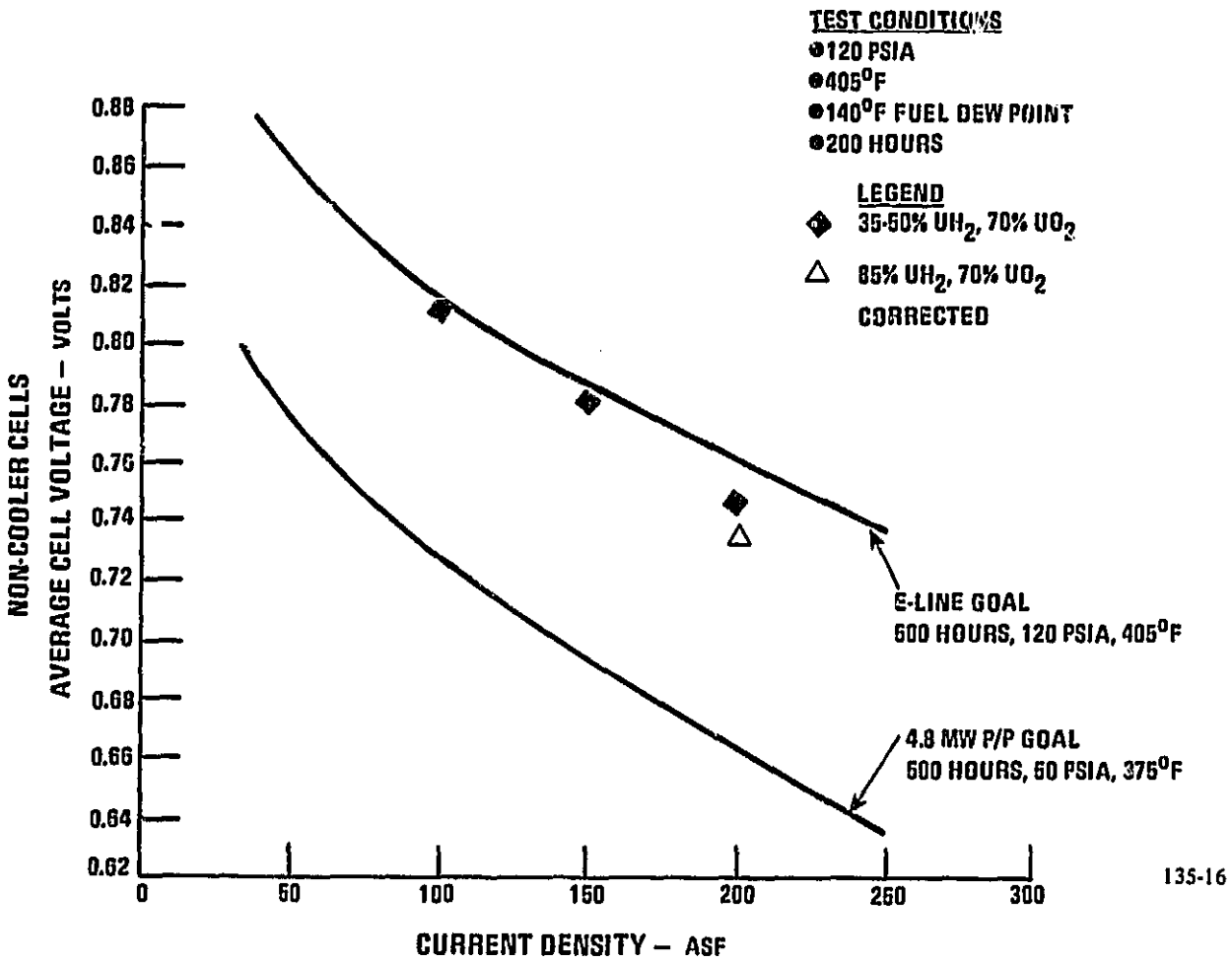

Figure 3-25. Performance Calibration, 10-ft², 30-Cell Stack

SECTION 4

CELL STACK CONCEPTUAL DESIGN

Task 4 of Contract DEN3-191 was directed at evolving a conceptual design of a larger area cell stack contemplated for future power plants. The design activity considered advanced technology and lower cost materials described in Section 2 and also advanced system concepts such as a two-gas power section. The constraints of a truck transportable, lower heat rate, highly integrated, lower cost power plant were applied. The major areas studied are discussed below.

The last short stack discussed in Section 3 was constructed from this conceptual design configuration.

Objective

The objective of this task was to continue a conceptual design activity initiated in the previous DOE Contract DE-AC-03-76 ET 11301, of a ribbed substrate cell stack with a larger (nominally 10-ft^2) area capable of operating at the higher pressures and temperatures contemplated for future power plants and to guide component development activities.

Summary

A conceptual design of a future stack designed to operate at 120 psia was completed. The stack consists of 460 cells with a nominal active area of 10½-ft^2 and a nominal planform of 42 in. x 42 in. Cooler pitch is five cells/cooler. (Since this work was done early in this program technology has progressed to allow up to eight cells per cooler.) Two-pass flow is used for both reactants to minimize flow channel tolerance requirements and the potential for flow maldistribution. A flow orientation of air-in at the fuel exhaust was selected because it has no impact on performance and allows an anode exhaust condenser to be eliminated from the future power plant.

Interstate truck transportation constraints were reviewed. A power section pallet with an overall height of 11 ft. 6 in. and a weight of 70,000 lb can be shipped on a conventional flat bed trailer. A pallet with an overall height of 12 ft. 8 in. and a weight of 80,000 lb can be shipped on a low-boy trailer. The selected 460-cell Cell Stack Assembly (CSA) is shippable as a separate vessel or as a pallet.

Discussion

Cell Configuration - The cell configuration consisting of planform dimensions, flow channel dimensions, and reactant flow orientations was conceived. Limits were established based on manufacturing constraints, flow uniformity requirements, and water recovery considerations for a nominal 200 ASF design point.

Two-pass fuel flow and air flow were selected to minimize both the potential for reactant maldistribution and the tolerance requirements on flow channel dimensions. The anode configuration consists of a channel depth of 35 mils and width of 46 mils with a rib coverage of 54%. The tolerance requirement for the channel configuration is 3 mils on the depth and 2 mils on the width. This configuration requires a 200-cfm anode recycle to meet distribution requirements at low power. The cathode channel is 45 mils deep by 55 mils wide with a rib coverage of 52%. Tolerance requirements for the cathode are the same as for the anode.

System studies had shown that it might be feasible to eliminate the power plant anode exhaust condenser. The net water transport from the oxidant stream to the fuel stream was estimated for various fuel and air manifolding arrangements. Four candidate configurations were studied. The results, shown in Figure 4-1, show that Configuration D meets the requirements for water recovery with no anode exhaust condenser at rated power. The potential for fuel starvation at various power conditions was evaluated and margins found acceptable. The calculations showed that even though the local cathode potential at the air-in/fuel-out corner is considerably higher than average, it is not significantly dependent on fuel flow distribution.

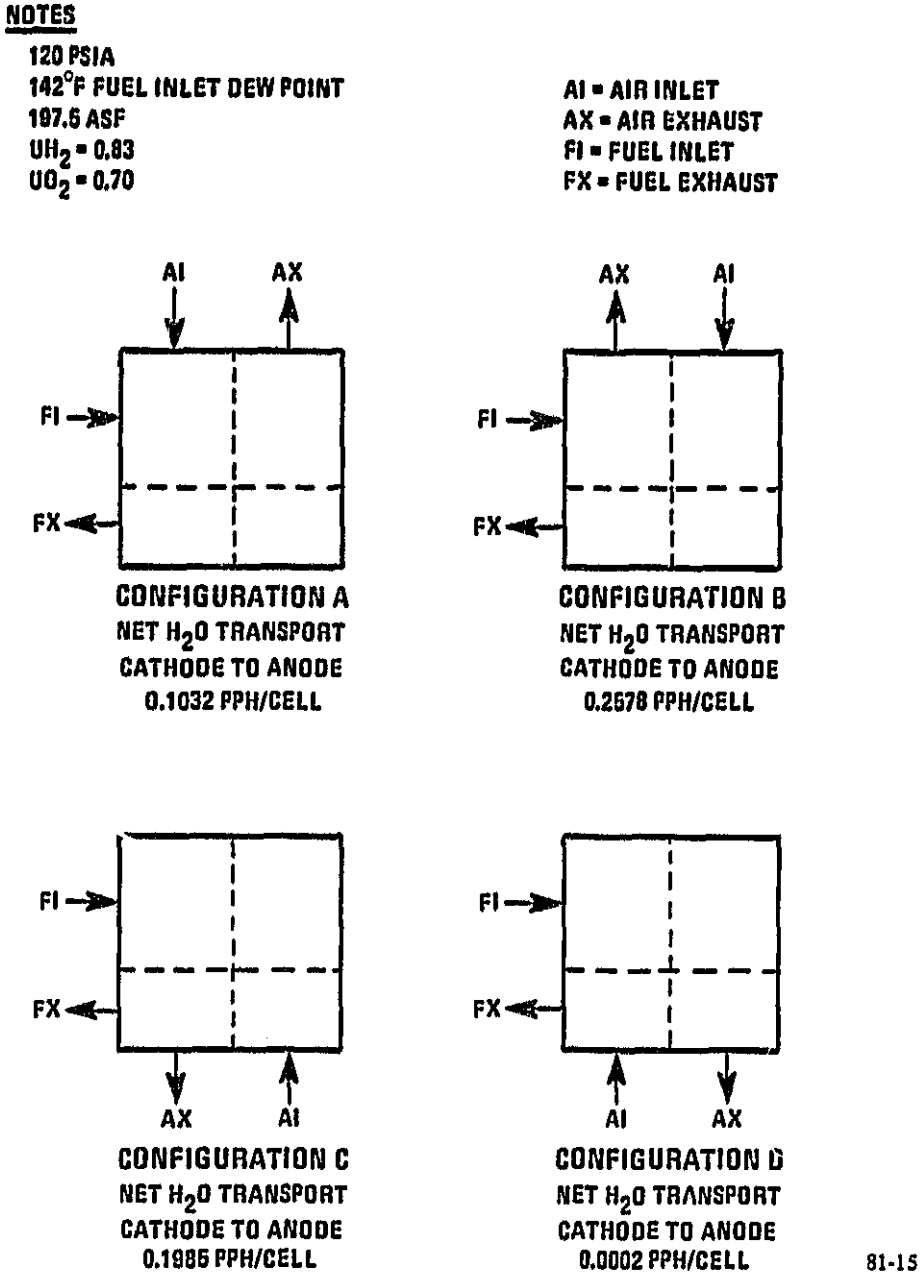

Figure 4-1. Results of Water Transport Study

Shipping Constraints - Truck transportation constraints were reviewed relative to impact on cell stack size and weight for this conceptual design study. An overall load height of 13 ft. 6 in. is the limit for interstate roadways. Two basic pallet configurations were considered: one is designed to be carried on a flat bed trailer, which allows an overall pallet height of 11 ft. 6 in.; the second is designed for low-boy trailer transportation with an overall pallet height of 12 ft. 8 in. Pallet weight limits for shipping these configurations are 70,000 and 80,000 lb, respectively, based on truck shipping weight limits. Another approach considered was to not palletize the CSA but to ship it as a separate 11 ft. 10 in. containment vessel. A specific palletizing and shipping approach had not been finalized at the end of this conceptual design study.

System Constraints - System studies indicate that total cell area should be approximately 85,000-88,000 ft^2, with at least 2916, but not more than 3750 cells in series, to meet inverter input voltage requirements. The resulting maximum number of cells per stack for various cell areas is shown in Figure 4-2. Design studies show that these requirements can be met with any of the combinations listed in Table 4-1 at five cells/cooler.

TABLE 4-1. RESULTS OF DESIGN STUDIES

Cell Area, ft^2	Number of Stacks	Number of Cells/Stack	Number of Stacks Per Pallet	Height
9.75	18	490	6	12' 8"
11.5	18	415	9	11' 6"
11.5	16	460	8	12' 8"
10.6	18	460	Non-Palletized	11' 10" Vessel

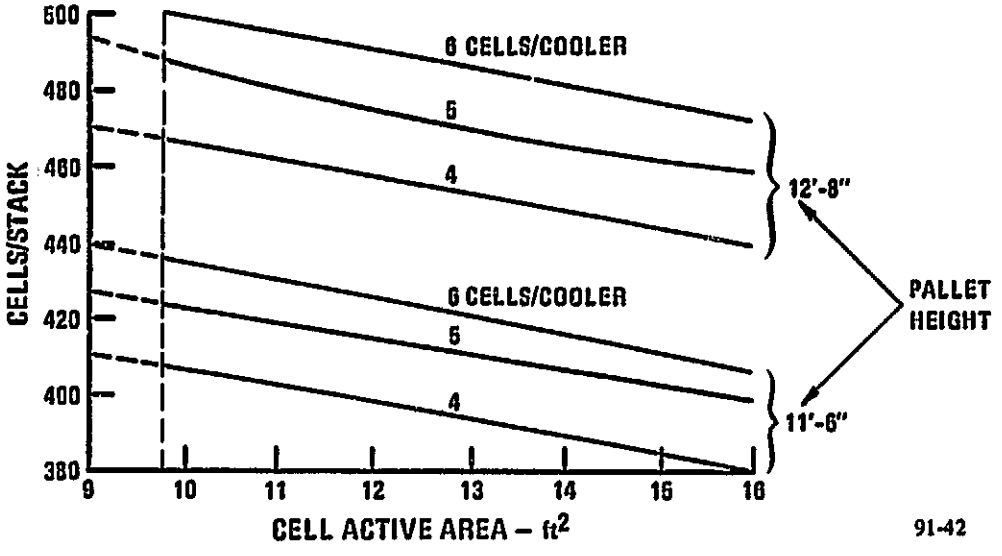

Figure 4-2. Number of Cells in a Stack

Design Studies - An initial assessment of cell temperatures as a function of cells per cooler has been conducted. For the baseline cooler with 1/8-in. diameter Teflon-coated tubes, calculations show that at five cells per cooler, the maximum expected cell temperature is 418°F. At six cells per cooler, the temperature increases to 430°F. These values were determined for a coolant exit temperature of 375°F. For this conceptual design study, the maximum practical cell temperature has been established at 425°F. Subsequent development activity following this conceptual design ability showed that it is feasible to increase the cells per cooler by increasing the diameter of the cooler tube.

A structural analysis of a cell stack pressure plate was completed. A 3-in. thick plate is acceptable for a 10-ft^2 stack with a square planform. Maximum plate deflection is an acceptable 0.018-in. and load variation is an acceptable 10%. These studies also showed that the thickness could be reduced to 1.5 in. at the corners. This provides more clearance between the nuts on the tie-rods and the containment vessel.

SECTION 5

PRELIMINARY POWER PLANT PALLETIZATION

This task of Contract DEN3-191 was directed at a study of the conceptual component arrangement of the pallets of the dc module. The approach was to consider the advantages and disadvantages of such design criteria as maintainability, minimum footprint, preliminary checkout at the factory and site versus factory assembly. Considering only one of the above criteria would result in very different pallet arrangements. The most compatible arrangement featuring selected advantages from the alternative arrangements was evolved, producing a final conceptual arrangement of the dc module components and pallets.

Objective

The objective of this task was to study a conceptual power plant dc module component arrangement by pallet with primary emphasis on ease of fabrication and maintenance.

Summary

Preliminary process and instrumentation diagram and component design requirements were reviewed. All dc module components were selected or sized and assigned to designated pallets. A conceptual component arrangement on each pallet was defined, as well as the arrangement of pallets and interconnecting piping for the entire dc module. Selected features are the result of reviews completed in conjunction with comments provided by potential pallet fabricators and potential utility customers. Comparative cost estimates showed that the total installed dc module pallet cost, including foundations, was within 5% for all four of the pallet arrangement alternatives which were studied.

Discussion

To achieve the goals envisioned for a multimegawatt fuel cell power plant, an early task was to conduct conceptual palletization layout design studies. The basis for

this conceptual design was a preliminary process and instrumentation diagram and component design requirements. Under this task preliminary component sizing was used to define component arrangements by pallet. The approach employed was to generate four alternative pallet arrangements for the studies. A pallet fabricator with previous experience with fuel cell pallet assembly was selected to assist with palletization studies. Potential pallet fabricators and utility customers assisted by critiquing the pallet arrangements. Specific consideration was given to various design features and their impact on maintainability; shop assembly and checkout; site interfacing, fabrication/erection and checkout; and impact on manufactured and installation cost differences.

Arrangement Alternatives Study - In order to provide a basis for dc module arrangement review, United conceived four configurations with different emphasis in each:

Alternative Arrangement	Emphasis
1	Maintainability
2	Reduced site area
3	Alternative clustering of fuel processing components for checkout
4	Alternative factory/site assembly mix

The key design features of each alternative arrangement are listed in Table 5-1.

United provided a description of each of the above dc module arrangements to a pallet fabricator who had previous experience with fuel cell pallet assembly in the 4.8-MW Demonstrator program. Also provided were dc module preliminary process and instrumentation diagrams, component design requirements, component definition and description, electrical systems definition and description, maintenance and overhaul requirements, applicable codes and standards, site mechanical and electrical systems definition and design requirements, shipping and handling requirements and site installation requirements.

The initial effort by the pallet vendor was to assess and develop an understanding of cost differences between performing tasks in the fabricator's shop and performing the tasks at the site.

Review of the four alternative dc module pallet arrangement configurations by the pallet vendor was completed. Comparative cost estimates showed that the total installed dc module pallet cost including foundations was within 5% for all four alternatives. Configuration assessments were made in each of the following areas: (1) pallet shop fabrication and assembly, (2) pallet field installation, (3) power section field installation, (4) instrumentation and electrical checkout, and (5) pallet vendor field installation project management.

DC Module Conceptual Configuration - A dc module configuration/feature selection was made. The selected features are a result of reviews with potential pallet fabricators and comments from potential utility customers. Table 5-2 provides a summary of the dc module feature alternatives, selection, and reasons for selecting the features.

The selected conceptual design arrangement of the dc module is shown in Figure 5-1. Equipment located includes:

Power Section

- 18 cell stack assemblies with manifolding and interconnecting piping.

Process Section

- Nine truck-transportable pallets including two stacked pallets (steam separator and deaerator) with components on each.
- Six fuel processing system vessels (including the reformer) mounted directly onto the concrete slab.
- Interconnecting piping.
- Optional location of air coolers.

TABLE 5-1. ARRANGEMENT ALTERNATIVES STUDY

Alternative	Emphasis	Design Features
1	Maintainability	Horizontal heat exchangers with tube bundle pull space Power section interior access aisles and string isolation Access to system pallets from internal aisle Elevated central system pipe racks Palletized subsystems for checkout
2	Reduced Site Area	Vertical heat exchangers Elimination of power section interior access aisles Smaller shell and tube heat exchangers Regrouped hydrodesulfurizer, high temperature and low temperatures shift converter pallets
3	Alternative Clustering of Fuel Processing Components for Checkout	Same as 1, except: . No power section access aisles . Smaller heat exchangers . Repackage fuel processing subsystem for checkout through heatup at vendor
4	Alternative Factory/Site Assembly Mix	Power section same as 2 & 3 above Palletize only controls and rotating components Erect all pressure vessels and heat exchangers at site

TABLE 5-2. DC MODULE CONFIGURATION/FEATURE SELECTION SUMMARY

General Features	Alternatives	Selection	Reason
DC Module Arrangement			
o General Equipment Arrangement	Alt. 1, 2, 3 or 4	Alt. 3	Minimum Interconnecting Piping
Heat Exchanger			
o Orientation Where Optional	Horizontal vs. Vertical	Horizontal	Reduced Field Erection and Structure
o Maintenance	Space for Tube Bundle Removal or Not	Space for Tube Bundle Removal	Utility Practice, No Footprint Penalty with Selected Arrangement
o Packaging	Palletize vs. Field Install	Palletize	Lower Cost Approach for Production
Fuel Process Vessels			
o Packaging	Palletize vs. Field Install	Field Install	Avoid Double Handling Large Vessels and Extra Structure
o Isolation Provision	Valves vs. Line Blinds vs. None	Line Blinds	Need Demonstrated - Lower Cost Approach
Power Section			
o Packaging	Palletize vs. Field Install	Field Install	Stacks too high (12') to Palletize
o Removal of Center String Stacks	Adjacent Aisle vs. Crane Lift	Adjacent Aisle	Reduce Height for Crane Lift
o String Fluid Isolation	Line Blinds, Valves, No Provision	No Provision	Offer as Optional Extra
o Power Connection Bus Duct	Low Pressure vs. Process Pressure	Process Pressure	Eliminate Vessel Penetrators - Higher Reliability
Air Cooler			
o General Location	Above DC Module Pipe Rack vs. Ground Installation	Site Optional	Dictated by Local Constraints of Footprint, Aesthetics and Noise
o Type Units	Custom Induced Draft Commercial Forced Draft vs. Commercial Induced Draft	Commercial Forced Draft Where 60 dBA Acceptable	Lower Cost Approach and Freeze Protection
Process and Control Test Provision			
o Power Section Bypass Piping	Permanent vs. Temporary	Permanent	Reduce Field Labor
o Changeover	Line Blinds vs. Valves	Line Blinds for Gases; Valves for Water	Compromise of Cost and Convenience

TABLE 5-2. DC MODULE CONFIGURATION/FEATURE SELECTION SUMMARY (CONT'D)

General Features	Alternatives	Selection	Reason
Thermal Insulation Installation			
o Pallets	Shop vs. Field	Shop	Lower Cost Approach for Production
o Vessels	Shop vs. Field	Shop	Lower Cost Approach for Production
o Piping Between Pallets	Shop vs. Field	Field	Difficulty in Handling Offsets Lower Cost Approach
Interconnecting Piping Assemblies			
o Power Section o System Section	Shop Made Assemblies vs. Field Erected Spools	Shop Fabricated Spools Field Erected	Extra Structure for Assembly Offsets Labor Saving
Electrical Junction Boxes			
o Auxiliary Power	Each Pallet vs.	One for DC Module (Wire to Loads)	Standard Practice
o Instrumentation and Controls	DC Module Common	Each Pallet Pin Connectors (T/C's and Controls Separate Boxes)	Minimize Site Wiring
DC Module Maintenance Weather Enclosure			
o Power Section o System Area	Full Enclosure vs. Partial Enclosure vs. None	Site Optional (Weather Conditions)	Utility Preference Varies
DC Module Concrete Foundation	Full Slab vs. Section Slabs	Section Slabs	No Settlement Requirement for Full Slab, Lower Cost Approach
Pallet Structural Skid	Platform vs. Box Structure	Combination Platform and Box	Lower Cost Approach for Lift and Racking Capability

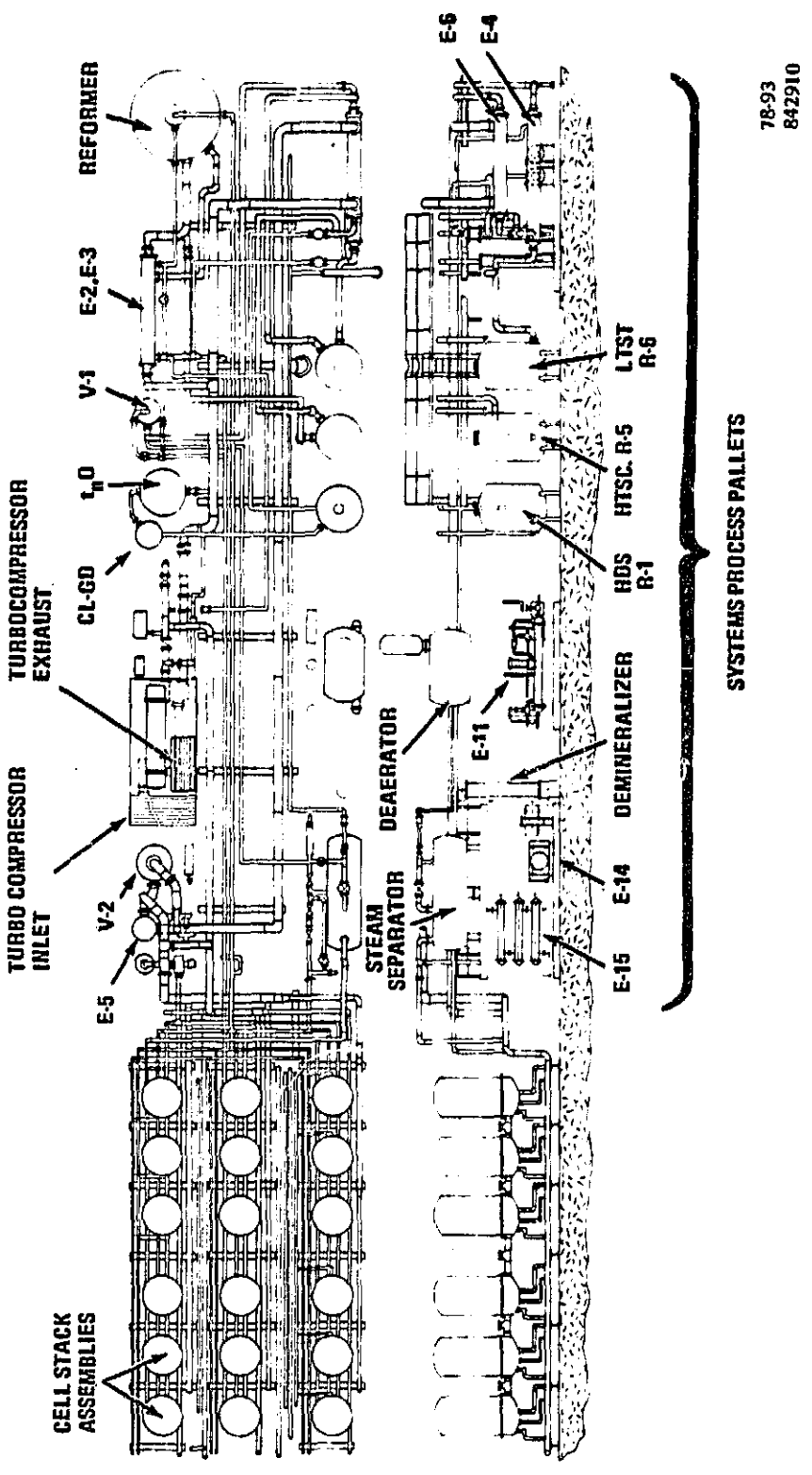

Figure 5-1. DC Module - Arrangement Selection